

**CLASS IA PI3K ISOFORMS LEAD TO DIFFERENTIAL  
SIGNALING DOWNSTREAM OF PKB/AKT**

A THESIS SUBMITTED TO  
THE GRADUATE SCHOOL OF ENGINEERING AND SCIENCE  
OF BILKENT UNIVERSITY  
IN PARTIAL FULFILLMENT OF THE REQUIREMENTS FOR  
THE DEGREE OF  
MASTER OF SCIENCE  
IN  
MOLECULAR BIOLOGY AND GENETICS

By

Hazal Beril ÇATALAK

December 2020

**CLASS IA PI3K ISOFORMS LEAD TO DIFFERENTIAL SIGNALING  
DOWNSTREAM OF PKB/AKT**

By Hazal Beril ÇATALAK

Fall 2020

We certify that we have read this thesis and that in our opinion it is fully adequate, in scope and in quality, as a thesis for the degree of Master of Science.

---

Onur ÇİZMECİOĞLU (Advisor)

---

Işık G. YULUĞ

---

Ayşe Elif ERSON BENSAN

Approved for the Graduate School of Engineering and Science:

---

Ezhan Karaşan

Director of the Graduate School of Engineering and Science

## **Abstract**

### **CLASS IA PI3K ISOFORMS LEAD TO DIFFERENTIAL SIGNALING DOWNSTREAM OF PKB/AKT**

Hazal Beril ÇATALAK

M.Sc. in Molecular Biology and Genetics

Advisor: Onur ÇİZMECİOĞLU

Fall 2020

PI3K pathway has been deregulated in one third of human cancers. All Class IA PI3Ks, which are composed of catalytic and regulatory subunits, catalyze conversion of PIP2 to PIP3 on plasma membrane. The catalytic subunits of Class IA – p110 $\alpha$ , p110 $\beta$ , and p110 $\delta$  –, are found to be mutated/amplified in cancers. As inhibiting all Class IA catalytic isoforms lead to widespread toxicity, identification of isoform specific targets of especially p110 $\alpha$  and p110 $\beta$  have the potential to transform targeted therapy for PI3K deregulated cancers.

In our studies, isogenic mouse embryonic fibroblasts (MEFs) were used as they constitute a genuine model for signaling experiments with their genetically stable, and non-transformed phenotype. MEFs were engineered to have their first exons of PIK3CA and PIK3CB floxed, enabling double knock out of p110 $\alpha$  and  $\beta$  in a temporally regulated manner, which allowed us to study their isoform specific targets. Myristoylation (Myr), a lipidation signal anchoring proteins to the plasma membrane, leads to constitutive activation of kinases. We tagged p110s with Myr signal and transfected MEFs with them to study their novel as well as redundant targets. Proliferation assays, pharmacological inhibition, Western Blots are used to elucidate the unique targets of p110 isoforms.

Myristoylated p110s result in activation of unique as well as common Akt substrates. These unique targets were highlighted in proliferation experiments where MEFs were treated either with Doxorubicin or Cisplatin, chemotherapeutic agents to induce apoptosis. Cell cycle analysis of double knock-out overexpression constructs generated in MEFs have shown that p110 $\alpha$  and p110 $\beta$  downstream signaling lead to different cell

cycle kinetics. mTORC1 inhibition by Rapamycin, mTORC1 inhibition by Everolimus, and Rac1 inhibition by EHT1864 translate differentially to the corresponding downstream targets in p110s. We also tested a potential scaffold function p110 $\beta$  together with Rac1 to phosphorylate mTOR by using docking simulations.

This study suggests differential regulation of translation, metabolism as well as survival signalling downstream of unique class IA p110 isoforms.

**Key words:** Phosphoinositide 3-kinase, Protein Kinase B, Mammalian Target of Rapamycin, Ras-related Botulinum Toxin Substrate 1

## Özet

### SINIF IA PI3K İZOFORMLARININ SİNYAL İLETİMİNDEKİ ÖZGÜN HEDEFLERİ

Hazal Beril ÇATALAK

Moleküler Biyoloji ve Genetik, Yüksek Lisans

Tez Danışmanı: Onur ÇİZMECİOĞLU

Güz 2020

PI3K sinyal yolağı kanserde sıklıkla etkinleşen yolaklardan birisidir. Bütün Sınıf IA PI3K'ler, katalitik ve düzenleyici altbirimlerden oluşmakta, ve plazma membranındaki PIP2 moleküllerini PIP3'e fosforile etmektedir. Sınıf IA katalitik altbirimleri – p110 $\alpha$ , p110 $\beta$ , ve p110 $\delta$  –, kanserde mutasyona ya da amplifikasyona uğrar. Bütün Sınıf IA katalitik izoformlarının topyekün inhibisyonu yaygın bir toksisiteye yol açtığından, özellikle p110 $\alpha$  ve p110 $\beta$ 'nin izoforma özel hedeflerinin belirlenmesi, PI3K mutant kanserlerde hedeflere yönelik terapinin gelişmesine büyük katkı sağlayacaktır.

İzogenik fare embriyonik fibroblastları (MEFler), genetik olarak stabil ve transforme olmamış fenotiplerinden yararlanılarak hücre içi sinyalizasyon deneylerinde, özgün modeller olarak kullanılmıştır. MEFler, p110 $\alpha$  ve p110 $\beta$ 'yi kodlayan PIK3CA ve PIK3CB'nin ilk ekzonlarına LoxP bölgeleri yerleştirilecek şekilde geliştirilmiştir. Bu şekilde, p110 $\alpha$  ve p110 $\beta$ 'nin genomdan silinmesi kontrollü, ve izoform spesifik hedeflerin çalışılmasına olanak sağlanacak biçimde gerçekleştirilebilir. Bir lipidasyon modifikasyonu olan Miristoilasyon (Myr), proteinlerin plazma membranına bağlanmasını sağlamakla beraber belli kinazların sürekli aktivasyonunu tetikler. Bu çalışmada, MEFler 5'-uçlarında Myr sinyali bulunan sınıf IA p110'larla transfekte edilip izoforma özel hedefler çalışılmıştır. Proliferasyon deneyleri, farmakolojik inhibisyonlar, ve fosfospesifik antikolar ile bağışık immünoblotlar, izoformlara özel hedeflerin bulunmasında kullanılan yöntemlerdir.

Miristoile olmuş p110lar hem ortak hem de izoformlara özgü Akt substratlarını fosforile etmişlerdir. Bahsedilen spesifik hedeflerin varlığı Doksorubisin ve Sisplatin kullanılarak belirlenmiştir. p110 $\alpha$  ve p110 $\beta$  fazladan ifade yapıları kullanılarak transfekte edilmiş olan

MEFlerin hücre döngüsü analizi, p110lerin devamındaki sinyal yolağının farklılıklarını göstermiştir. Rapamisin'le mTORC1 ve mTORC2, Everolimus'la mTORC1, EHT1864'le Rac1 inhibisyonu aktif PI3K izoformlarının, farklı sinyalizasyon bileşenleri kullandıklarına yönelik bulguları güçlendirmiştir. p110 $\beta$ 'nın, Rac1 ve mTOR ile yapması olası bir komplekste bir iskele görevi görüp göremeyeceği moleküler yerleştirme simülasyonlarıyla test edilmiştir.

Bu çalışma, sınıf 1A PI3K izoformlarının özgün aşağı akım sinyal bileşenlerini kontrol ettiğini, ve translasyonel regülasyonu, metabolizma ve hatta sağkalımda birbirinden farklı rollerinin olduğunu göstermektedir.

Anahtar Sözcükler: Fosfoinsitid 3-kinaz, Protein Kinaz B, mTOR, Rac1

**To my family...**

**Aileme...**

## **Acknowledgements**

First and foremost, I'd like to share my deepest gratitude for my scientific advisor, Asst. Prof. Dr. Onur Çizmeciođlu, whom I'll always be looking up; on how to become a role model for their graduate and undergraduate students. I feel upmost lucky for having worked under his precious guidance, which is the watershed of my career. His indirect personal teaching on how to become a true scientist and direct scientific teaching are the main reasons that enable me to continue my quest on science.

I'd like to thank Mahnoor Sulaiman, who has been there for me when I need a second hand with my experiments, and for her warm friendship. I'd like to express my gratitude for Ođuzhan Tarman, who has provided me different scientific points of view, helped me with lab related software, and for his heartfelt companionship in lab and life related problems. I'd like to thank Beste Uygur, for her selfless help in experiments and caring friendship, Melike Dinççelik Aslan, for her generous and loyal friendship, Marzana Ishraq, for her positive energy and sweet companionship, and Javaid Jabbar, for his alternative points-of-view and funny companionship.

I'd like to thank to my colleagues in OC Lab for their support. I'd like to share my gratitude for EpiStem Lab in METU for their generous help.

I'd like to thank to our undergraduate students; Nil Kirişçiođlu, Ceylin Zeybek, and Sefa Berkay Çayır for their help in experiments and sympathetic energy.

I'd like to share my gratitude for our lab managers; Pelin Makas, Seda Birkan and our lab technician Okan Erşahan for their help and patience in my reagent related problems.

Last but not least, to my husband Utku Yılmaz; with whom we have started to climb this mountain as valentines, and become lifelong partners in these three years. He is my main propeller to carry on, and to go beyond. I'd like to share my gratitude to my mom, who is my first role model to have a profession in biology and for her never-ending support and love, and to my dad, who is always there for me, to my grandmother, for her unending support and love, to my mother- and father-in-law, for their love and acceptance, and Kekik, for her lovely companionship.

Hazal Beril Çatalak is supported by a scholarship from TÜBİTAK grant 118Z976.

## Teşekkürler

Öncelikle danışman hocam Dr. Onur Çizmeicoğlu'na en derin şükranlarımı sunarım. Kendisi benim için lisans ve yüksek lisans/doktora öğrencilerine nasıl bir rol model olunacağı konusunda her zaman örnek alacağım figür olacaktır. Kendisinin son derece kıymetli rehberliğinde çalışmış olduğum için çok şanslı hissediyorum, ve bunun kariyerimde bir dönüm noktası olduğunun farkındayım. Kariyerimin devamını getirebilmemdeki en büyük yardımcılarından biri, kendisinin nasıl gerçek bir bilim insanı olmak üzerine olan indirekt, ve bilim üzerine olan direkt öğretileridir.

Mahnoor Sulaiman'a deneylerimde yardımcı olduğu ve sıcak arkadaşlığı için teşekkürlerimi sunarım. Oğuzhan Tarman'a farklı bilimsel bakışaçıları sunduğu, bilimsel yazılım kullanımındaki yardımları, ve lab ve hayatla ilgili problemlerdeki sıcakkanlı yoldaşlığı için teşekkürlerimi sunarım. Beste Uygur'a özverili yardımları ve şefkatli arkadaşlığı, Melike Dinççelik Aslan'a cömert yardımları ve vefakar arkadaşlığı, Marzana Ishraq'a pozitif enerjisi ve sevgi dolu arkadaşlığı, ve Javaid Jabbar'a alternatif bakış açısı ve eğlenceli arkadaşlığı için teşekkürlerimi sunarım.

OC Lab'daki çalışma arkadaşlarıma destekleri için teşekkürlerimi sunarım. ODTÜ EpiStem Lab'ına eliaçık yardımları için teşekkür ederim.

Lisans öğrencilerimizden Nil Kirişçioğlu, Ceylin Zeybek, ve Sefa Berkay Çayır'a deneylerdeki yardımları ve sempatik enerjileri için teşekkür ederim.

Lab sorumlularımız Pelin Makas ve Seda Birkan'a, teknisyenimiz Okan Erşahan'a materyal konusundaki yardımları ve sabırları için teşekkür ederim.

Sonuncu ancak en önemlilerinden biri olarak, eşim Utku Yılmaz'a teşekkürlerimi sunarım. Bu zorlu sürece sevgili olarak başlayıp, üç yılın sonunda ömür boyu sürececek bir partnerliğe imza attık. O, benim için devam etmek ve bilimde daha da ötesini görebilmek için en büyük desteğim. Anneme, biyoloji alanında bir meslek seçmemin en büyük faktörü olduğu, sonsuz desteği ve sevgisi için, babama, her zaman yanımda olduğu için, anneanneme, bitmeyen desteği ve şefkati için, ve eşimin anne ve babasına sevgi ve destekleri için, ve tabi ki arkadaşlığı için Kekik'e teşekkürlerimi sunarım.

Hazal Beril Çatalak bir TÜBİTAK Proje No: 118Z976 bursiyeridir.

## Table of Contents

Abstract.....	ii
Özet.....	iv
Acknowledgements.....	vii
Teşekkürler .....	viii
Table of Contents.....	ix
Table of Figures .....	xii
List of Tables .....	xiv
Abbreviations.....	xv
1. Introduction.....	1
Cancer .....	1
Cellular Signaling .....	2
PI3K.....	4
<b>1.1.1. PI3K Class IA Catalytic Isoforms</b> .....	8
<b>1.1.2. PI3K Signaling</b> .....	10
2. Aim of the Study.....	21
3. Materials and Methods.....	24
3.1 Materials .....	24
3.2 Media and Solutions .....	24
3.3 Methods .....	30
<b>3.3.1 Thawing Cells From Cryovials</b> .....	30
<b>3.3.2 Passaging/Splitting Cells</b> .....	30
<b>3.3.3 Freezing Cells</b> .....	31
<b>3.3.4 2D Growth Assay</b> .....	31

<b>3.3.5 Fixation for Crystal Violet Staining</b> .....	34
<b>3.3.6 Crystal Violet Staining</b> .....	34
<b>3.3.7 Destaining Crystal Violet Stained Samples</b> .....	34
<b>3.3.8 Quantifying Crystal Violet Stain</b> .....	34
<b>3.3.9. Retroviral Transfection</b> .....	35
<b>3.3.10 Harvesting Cells for SDS – PAGE</b> .....	37
<b>3.3.11 Lysing Cells for SDS – PAGE</b> .....	38
<b>3.3.12 BCA Assay</b> .....	39
<b>3.3.13 SDS – PAGE</b> .....	40
<b>3.3.14 Western Blot</b> .....	41
<b>3.3.15 Wound Healing Assay (Scratch Assay)</b> .....	43
<b>3.3.16 Cell Cycle Analysis by PI Staining</b> .....	44
4. Results.....	45
4.1 Generation of MEF Cell Lines Expressing Unique Constitutively Activated Class IA PI3K Catalytic Isoforms .....	45
4.2 Activated p110 Isoforms Show Differential Akt Activity.....	48
4.3 Phosphorylated Tyrosine Levels of Constitutively Activated p110 Isoforms in MEFs.....	53
4.4 Docking Simulations by HADDOCK.....	58
4.5 Genotoxic Stress Sensitivity .....	70
<b>4.5.1 Doxorubicin – Induced Genotoxic Stress</b> .....	71
<b>4.5.2 Cisplatin – Induced Genotoxic Stress</b> .....	72
4.6 Cell Cycle Analysis of MEFs Overexpressing p110s.....	74
4.7 Investigation of Non-Canonical Functions of p110 $\beta$ .....	75
4.8 Migration Kinetics of Activated p110s.....	79
5. Discussion.....	82

6. Conclusion and Future Perspectives .....	87
Appendices.....	88
Appendix A - Doxorubicin – Induced Genotoxic Stress .....	88
Appendix B - Cisplatin – Induced Genotoxic Stress .....	91
Appendix C – Copyright Permissions .....	93
Bibliography .....	96

## Table of Figures

Figure 1.1 Map depicting cancer as a cause of death in people younger than 70. ....	1
Figure 1.2 Phosphatidylinositols and their phosphatases .....	6
Figure 1.3 Membrane lipids and protein domains that can attach to them. ....	7
Figure 1.4 Schematic representation of different activation modes of p110 $\alpha$ , p110 $\beta$ , and p110 $\delta$ upon p85 $\alpha$ interaction with phospho-tyrosine residues of RTKs. ....	9
Figure 1.5 mTORC1 activation status and catabolic processes. ....	14
Figure 1.6 MAPK/ERK pathway regulation of PI3K pathway. ....	18
Figure 2.1 cBioPortal data on PIK3CA, PIK3CB, and PIK3CD alteration frequencies in cancer from their curated set of non-redundant studies, derived on 12.11.2020. ....	22
Figure 4.1 Investigation of generated MEF lines on their dependence on ectopically expressed activated p110 isoforms. ....	47
Figure 4.2 Myristoylated p110 expressing cell lines have different phospho – Akt Ser 473 levels. ....	48
Figure 4.3 Levels of Phosphorylated Akt substrate levels differ among myristoylated p110 expressing cell lines. ....	50
Figure 4.4 Biochemical pathway analysis of MEFs expressing constitutively active p110 $\alpha$ and p110 $\beta$ . ....	52
Figure 4.5 Biochemical analysis of phosphotyrosine signature of activated p110 expressing cells. ....	54
Figure 4.6 Phospho-Src levels of WT MEFs, MEFs overexpressing p110 $\alpha$ , and p110 $\beta$ . ....	55
Figure 4.7 Phospho-STAT3 levels of MEFs that are WT or ectopically expressing activated p110 isoforms or Akt1. ....	56
Figure 4.8 Functional interaction networks obtained by STRING Database. ....	58
Figure 4.9 Schematic representations of each docking run. ....	65
Figure 4.10 The successful docking runs predicted a possible scaffold function of p110 $\beta$ . ....	67
Figure 4.11 The successful docking runs predicted a possible scaffold function of p110 $\alpha$ . ....	69

<b>Figure 4.12 Doxorubicin sensitivities of WT MEFs and MEFs expressing activated p110s exogenously.</b> .....	71
<b>Figure 4.13 Cisplatin sensitivity of WT MEFs and MEFs expressing activated p110s ectopically.</b> .....	73
<b>Figure 4.14 Cell cycle analysis of HA Alpha and HA Beta MEFs exhibits different cell cycle kinetics.</b> .....	74
<b>Figure 4.15 Biochemical investigation of scaffold function of activated p110<math>\beta</math>.</b> .....	76
<b>Figure 4.16 Scaffolding function of p110<math>\beta</math> on mTORC2 activity is tuned by Rac1.</b> 78	
<b>Figure 4.17 Migration kinetics of WT and constitutively activated p110<math>\alpha</math> and <math>\beta</math> MEFs.</b> .....	81
<b>Figure 5.1 A schematic representation of PI3K pathway and used inhibitors.</b> .....	86

## List of Tables

<b>Table 3.1 Routinely used chemicals list</b> .....	24
<b>Table 3.2 Routinely used tissue culture reagents list</b> .....	25
<b>Table 3.3 List of used inhibitors</b> .....	25
<b>Table 3.4 Cell cycle analysis reagents</b> .....	26
<b>Table 3.5 In-house prepared buffer recipe list</b> .....	26
<b>Table 3.6 Materials and reagents used to perform Western Blot.</b> .....	27
<b>Table 3.7 Antibodies used in this study</b> .....	28
<b>Table 4.1 Used molecular models from PDB.</b> .....	60
<b>Table 4.2 HADDOCK Scores of performed dockings by p110s, p85<math>\alpha</math>, Rac1, and KRAS.</b> .....	60

## Abbreviations

4EBP	4E – Binding Proteins
AKT/PKB	Akt/Protein Kinase B
AMP	Adenosine Monophosphate
AMPK	AMP – Activated Protein Kinase
ATG13	Autophagy – Related Protein 13
BAD	Bcl2 – Associated Agonist of Cell Death
Bcl	B – Cell Lymphoma
cAMP	Cyclic Adenosine Monophosphate
Cdc42	Cell Division Control Protein 42 Homolog
c-Myc	Cellular Myelocytomatosis
CRKL	Crk – Like Protein
DEPTOR	DEP Domain – Containing mTOR – Interacting Protein
DNA – PK	DNA – dependent protein kinase
Dvl	Disheveled
EGFR	Epidermal Growth Factor Receptor
eIF4B	Eukaryotic Translation Initiation Factor 4B
eIF4E	Eukaryotic Translation Initiation Factor 4E
ERK	Extracellular Signal – Regulated Kinase
ETV7	ETS – Variant 7
FKBP-38	Peptidyl – Prolyl cis – trans Isomerase
FOXO	Forkhead Box O
GAP	GTPase Activating Protein

GEF	Guanine Exchange Factor
GPCR	G Protein – Coupled Receptor
Grb2	Growth Factor Receptor – Bound Protein 2
GSK3	Glycogen Synthase Kinase 3
HIF1 $\alpha$	Hypoxia Inducible Factor 1 $\alpha$
INPP4A	Type I Inositol Polyphosphate 4-Phosphatase
INPP4B	Type II Inositol Polyphosphate 4-Phosphatase
IRS 1/2	Insulin Receptor Substrate 1/2
ITAM	Immunoreceptor Tyrosine – containing Activation Motifs
KSR	Kinase Suppressor of Ras
MAPK	Mitogen-Activated Protein Kinase
MEF	Mouse Embryonic Fibroblast
MEK	Mitogen – Activated Protein Kinase Kinase
mLST8	Mammalian Lethal with SEC13 Protein 8
MP1	MEK1 Scaffolding Protein
mSIN1	Mitogen – Activated Protein Kinase – Associated Protein 1
mTOR	Mammalian/mechanistic Target Of Rapamycin
mTORC1	mTOR Complex 1, Mammalian/mechanistic Target Of Rapamycin in Complex 1
mTORC2	mTOR Complex 2, Mammalian/mechanistic Target Of Rapamycin in Complex 2
p70S6K1	S6 Kinase 1
PDGFR	Platelet – Derived Growth Factor Receptor
PDK1	3 – Phosphoinositide – Dependent Kinase 1
PH	Pleckstrin Homology

PI3K	Phosphatidylinositide 3 – Kinase
PIP2	PtdIns – 3,4 – P2 (Phosphatidylinositol 3,4 biphosphate)
PIP3	PtdIns – 3,4,5 – P3 (Phosphatidylinositol 3,4,5 trisphosphate)
PKA	Protein kinase A
PP1	Protein Phosphatase 1
PP2A	Protein Phosphatase 2A
PPAR $\gamma$	Peroxisome Proliferator – Activated Receptor – $\gamma$
PRAS40	Proline – Rich Akt1 Substrate 1
PROTOR	Protein Observed with RICTOR
PtdIns	Phosphatidylinositol
PTEN	Phosphatase and Tensin Homolog
Rab5	Ras – Related Protein 5
Rac1	Ras-related Botulinum Toxin Substrate 1
Raf	Rapidly Accelerated Fibrosarcoma
Rag	GTPase Ras – Related GTP Binding Protein
RAPTOR	Regulatory – Associated Protein of mTOR
Ras	Rat Sarcoma
Rb	Retinoblastoma
RBD	Rac binding domain
RICTOR	Rapamycin – Insensitive Companion of mTOR
ROS	Reactive Oxygen Species
RSK	Ribosomal S6 Kinase
RTK	Receptor tyrosine kinase
S6K	S6 Kinase
SH2	Src Homology 2

SHIP 1/2	SH2 Domain - Containing Inositol 5-phosphatases 1/2
SOS	Son of Seventhless
SREBP1/2	Streol Regulatory Element Binding Protein 1/2
TSC1	Tuberous Sclerosis Complex 1
TSC2	Tuberous Sclerosis Complex 2
ULK1	unc51 – Like Autophagy – Activating Kinase 1
VDAC	Voltage – Gated Anion Channels

# Chapter 1

## 1. Introduction

### Cancer

Cancer is caused by dysregulations in molecular machinery of cell growth.<sup>1,2</sup> It has been expected to be the major cause of death in 21<sup>st</sup> century worldwide. As cancer is anticipated as the main cause of death, it is considered as the grand obstacle in extending human lifespan. In the map below, figure 1.1, cancer is the first or second main cause of premature death in 91 of 172 countries.<sup>1</sup>

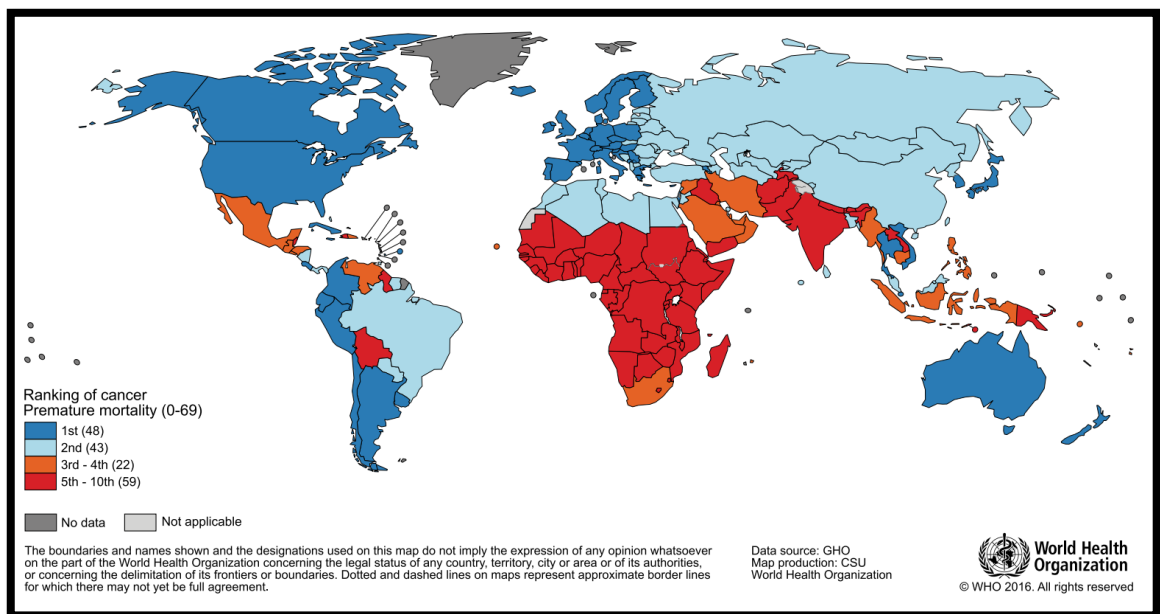


**Figure 1.1 Map depicting cancer as a cause of death in people younger than 70.**

(Reprinted with the permission from Ref. [1], John Wiley and Sons)

Cancer is a neoplastic disease where cells have accumulated variable mutations because of genetic instability benefiting them with selective advantage over time. These advantages comprise continued proliferative signals, escape from growth suppressors and cell death, inhibition of replicative senescence, trigger angiogenesis, and initiating invasion and metastasis. In addition, cancer cells have been reported to modulate their metabolism according to their needs and to hide from immune cells. Another factor that increases the complexity of the disease is that normal cells that are recruited to the vicinity

of the tumor where they serve for the cancer cells by producing molecules required by cancer cells. These healthy cells serving for cancer cells are called tumor stroma. All of these hallmarks that contribute to cancer cells to be selected over healthy cells are serving for their need to proliferate in an uncontrolled manner and to evade immune system attacks.<sup>3</sup>

There are different options to treat cancer; radiotherapy, chemotherapy, and targeted therapy, and these options are used sometimes in combination.<sup>2,4</sup> As the molecular machinery that is responsible for proliferation is overly activated, one of the most reasonable ways to keep the proliferation machinery in check is targeting growth promoting signaling components with inhibitors.<sup>2</sup> Different types of targets have been suggested. Cancer stem cells, tumor microenvironment, protein kinases, and different effector pathways that are downstream of an overly activated kinase have been proposed as targets to be inhibited.<sup>2</sup> Proteins with gain – of – function mutations that take part in proliferative pathways have been used as targets in targeted therapies. Inhibiting the enzymes with gain – of – function mutations in proliferative pathways are shown to be slowing the proliferation rate down. Targeted therapy and chemotherapy principle is based on the fact that cancer cells proliferate faster in comparison to healthy cells. Since cancer cells amplify faster in number, the inhibitor hits the cancer cells better.<sup>5</sup> The difference between chemotherapy and targeted therapy is that chemotherapy targets the whole cellular amplification machinery, e.g DNA damaging agents, and targeted therapy is specific to the molecule/s.<sup>6</sup> One exception to this case is familial cancers, where the mutations are occurred in germline cells. The therapy will not be effective as all of the cells have the same mutation throughout the body. Since targeted therapy don't target growing cells all together, they don't cause adverse effects like chemotherapeutics. On the other hand, monotherapy with these inhibitors almost always lead to drug resistance during treatment.<sup>5</sup>

### **Cellular Signaling**

Cells consist of different molecular machineries that serves for different processes. In cancer, the molecular machineries responsible for growth, proliferation, metabolism, and even mobility of the cell are disrupted. Cells sense environmental cues via signaling cascades.<sup>6</sup> Signaling is a chemical way that the cells communicate, and most of the time

the communication takes place between proteins.<sup>6</sup> Signaling consists of a receiver (sometimes the cell itself), a transmitter, and ligands that induce or block the signaling. There are different modes of signaling. The classification of different modes of signaling depend on the distance between the cells, ligand and receptor relationship, and receptor. Receptors are specific type of proteins that detect ligands.<sup>7</sup> Receptors can be soluble ((nuclear receptors), like estrogen receptor<sup>7</sup>) or cell surface receptor (like EGFR<sup>7</sup>). Membrane – bound receptors can have autophosphorylation activity or they undergo conformational changes that enable downstream enzymes to bind them when bound by their ligands (like cytokine receptors<sup>7</sup>)<sup>7</sup>.

Enzymes that work through adding or removing a phosphoryl group are named as kinases and phosphatases, respectively.<sup>8</sup> These kinases and phosphatases are the most important actors in cellular signal transduction, and their deregulation is implicated in cancer.<sup>9</sup> So far identified, human genome encodes for 520 kinases and 130 phosphatases. Both groups can be divided on the amino acid that they act upon: tyrosine, serine/threonine, or acting upon both serine/threonine and tyrosine, called dual specificity proteins.<sup>8</sup> The signal is detected by receptors, and transmitted to downstream messengers, like G proteins or kinases. While stepping down, the signal volume, that is the effect of the signal, increases exponentially, as there are more secondary messengers than the upstream elements. Respond to a signal can be transcription of a target gene, translation of proteins, change in the direction of metabolism, apoptosis, recycling proteins, and so on.<sup>7</sup>

Most of the receptors that have autophosphorylation/transphosphorylation activity that phosphorylates their tyrosine residues. These receptors are called receptor tyrosine kinases (RTKs). RTKs regulate different and essential molecular processes. These processes include proliferation, metabolism, differentiation, and survival<sup>7</sup>. RTKs have three parts; extracellular domain, transmembrane alpha helix, and tyrosine kinase domain on the inside. RTKs work as dimers, and they dimerize upon ligand binding. When dimerized, they transphosphorylate kinase domains and tyrosine residues situated on their intracellular domains.<sup>7</sup> These phosphotyrosine residues are used as anchoring sites by numerous proteins having PTB and SH2 domains.<sup>7</sup> One of the protein families that have SH2 domains belong to phosphatidylinositol – 3 kinases family (PI3K). PI3Ks are a family of lipid kinases that phosphorylate membrane lipids.<sup>7</sup>

GPCRs, G protein coupled receptors, are transmembrane receptors responsible for transmission of different chemical information. <sup>7</sup> GPCRs span the plasma membrane seven times, thus called “serpentine” receptors. These receptors associate with G proteins that have three subunits; G $\alpha$  (has intrinsic GTPase activity), G $\beta$ , and G $\gamma$ . Without ligand, G protein remains attached to the GPCR. Upon ligand binding, conformational changes occur. G $\alpha$  subunit and G $\beta\gamma$  subunit dissociate, as G $\alpha$  is now able to bind GTP, rather than GDP.<sup>6</sup> It has been shown that some members of PI3K family bind to GPCRs in addition to RTKs. <sup>10</sup>

### **PI3K**

Phosphoinositide 3-Kinases are a group of lipid kinases. There are three classes of PI3Ks; Class I, II, and III, and they are classified according to their lipid substrate specificity <sup>11</sup> and their sequence homology. <sup>12</sup> Class I catalyzes phosphorylation of PIP2s (PtdIns-3,4-P2) into PIP3s (PtdIns-3,4,5-P3) on the plasma membrane. In mammals, Class I consists of four catalytic and seven regulatory subunits, separated into two subgroups, namely Class IA and Class IB. <sup>13</sup> Catalytic subunits; p110 $\alpha$ ,  $\beta$ , and  $\delta$  belong to Class IA and p110 $\gamma$  belongs to Class IB. Regulatory subunits; p85 $\alpha/\beta$ , p55 $\alpha/p50\alpha$ , and p55 $\gamma$  belong to Class IA, and p84/p101 belong to Class IB. Although p110 $\alpha$  and p110 $\beta$  are expressed ubiquitously, p110 $\delta$  and p110 $\gamma$  are specific to the immune cells. Each catalytic subunit is found to be bound by regulatory subunits of the same subclass. <sup>13</sup>

PI3K Class I catalytic and regulatory subunits are obligatory couples. <sup>14</sup> Regulatory subunits stabilize and inhibit catalytic subunits.<sup>15</sup> In cancer, deregulation of catalytic as well as regulatory subunits are observed. <sup>14</sup> The binding of the catalytic subunits with their regulatory subunits aid catalytic subunits with their proper cellular localization as well as modulation. <sup>13</sup> Regulatory subunits have SH2 domains which enable them to bind adapters that are bound to receptors or phosphotyrosine residues on receptors. <sup>11</sup>

Regulatory subunits are bound to catalytic subunits through their inter SH2 domains and locate catalytic subunits closer to the plasma membrane where they can catalyze PIP2 to PIP3 phosphorylation. There are two proposed modes for phosphorylating PIP2 on the plasma membrane. The first one is the fact that catalytic subunits are in close proximity

to the membrane when bound by their regulatory subunits, where their lipid substrates are located. The second one is stated as regulatory subunits are bound to lipids and proteins close to the membrane, they undergo conformational change, and cause relieving of p110s from themselves.<sup>16</sup> Released catalytic subunits can phosphorylate PIP2s to PIP3s, where PIP3s become secondary messengers of the signaling cascade.<sup>13</sup> Increase in PIP3 molecules on the plasma membrane is related to oncogenicity.<sup>14</sup>

Different lipid moieties on the membrane signals differently, and generation of those lipid moieties depend on both PI3K and lipid phosphatases.<sup>17</sup> There are two different options to downregulate PI3K activity on the lipids. In the canonical pathway, PTEN (Phosphatase and Tensin Homolog) is active. PTEN is firstly defined as a protein phosphatase that can remove phosphate groups from serine, threonine, and tyrosine residues. PTEN also has lipid phosphatase activity. Because it counteracts PI3K signaling by decreasing PIP3 levels on the plasma membrane, it is considered as a tumor suppressor.<sup>18</sup> PTEN dephosphorylates 3'-phosphate of PtdIns - 3,4,5 - P3.<sup>13</sup> In noncanonical pathway which dephosphorylates membrane lipids, SHIP 1/2 (SH2 Domain - Containing Inositol 5-phosphatases 1/2 ) and INPP4B work. SHIP1 and INPP4B are considered as tumor suppressors, although there are controversial reports on resulting cellular states of SHIP2 activity.<sup>14, 19, 20, 21</sup> SHIP1/2 dephosphorylates 5'-phosphate of PtdIns - 3,4,5 - P3, resulting in Ptd Ins - 3,4 - P2. INPP4A/B has been shown to dephosphorylate Ptd Ins - 3,4 - P2 to Ptd Ins - 3 - P.<sup>17</sup> Schematic representation of phosphatases acting on different 3 - phosphatidylinositols and their cellular localization can be found in figure 1.2. PTEN deletion is a common occurrence in cancer.<sup>22</sup> Interestingly, downregulation of phosphatases are observed with upregulation of specific PI3K Class IA catalytic subunits. It has been documented that when PTEN is deleted, p110 $\beta$  becomes the prominent PI3K isoform supporting cellular growth and proliferation.<sup>10</sup>

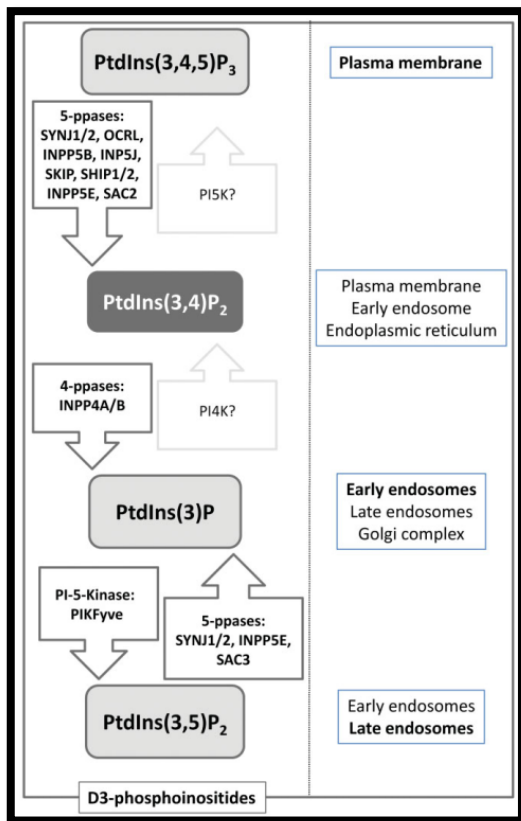


**Figure 1.2 Phosphatidylinositols and their phosphatases**

(Reprinted with the permission from Ref. [17], John Wiley and Sons)

PIP3 molecules act as anchors for proteins with PH domains.<sup>16</sup> Protein families with PH domains that are taking advantage of PIP3 anchors include AGC kinases having serine/threonine kinase activity, TEC family kinases with tyrosine kinase activity, GAPs (GTPase Activating Proteins), GEFs (Guanine Exchange Factors)<sup>13</sup>, and key signaling molecules such as PDK1, AKT, mTOR, Rac1, and Ras.<sup>23</sup> A schematic representation could be found in figure 1.3.

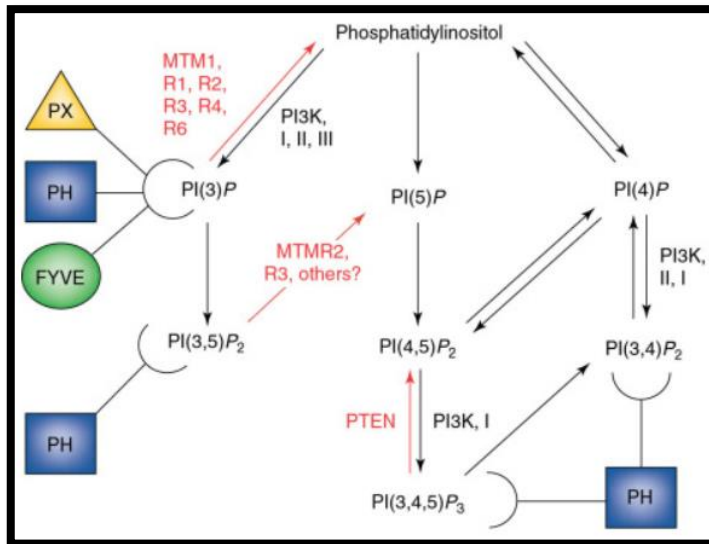


**Figure 1.3 Membrane lipids and protein domains that can attach to them.**

(Reprinted with the permission from Ref. [24], Elsevier)

After PI3Ks produce PIP3s on the plasma membrane, downstream molecules containing PH domain are located on those lipid moieties. Firstly, PDK1 and Akt are localized to membrane via PIP3 and PH domain interactions. PDK1 phosphorylates AKT on its Thr 308 site.<sup>25</sup> Downstream of AKT, mainly two complexes of mammalian / mechanistic target of rapamycin (mTOR) transduce the signaling. mTOR, one of the most important downstream effectors in PI3K pathway, takes part in two complexes; mTOR Complex 1 (mTORC1) and mTOR Complex 2 (mTORC2) in most of the eukaryotes, and mTOR Complex 3 (mTORC3) in humans.<sup>26</sup> The two main and classical complexes, mTORC1 and mTORC2, are differentiated on their short term sensitivity to rapamycin. mTORC2 is activated upon PI3K pathway activation, and mTORC1 is activated upon different stimuli, e.g growth factors, hypoxia, and low energy levels, amino acids.<sup>27</sup> Phosphorylation of AKT at T308 poises it to be ready for phosphorylation by mTORC2. mTORC2 phosphorylates Akt on Ser473, which results in fully activated AKT. Followed by fully activation of AKT, subsequent downstream effectors of mTOR complexes are activated. Some of the important downstream effectors are 4E-BP, S6K, S6, SGK, and Grb10. Results of the signaling are cell survival, protein translation, ribosome generation, autophagy and lipid metabolism regulation.<sup>27</sup>

### 1.1.1. PI3K Class IA Catalytic Isoforms

Plasma membrane acts as a platform for various signaling mechanisms. This platform is arranged into different domains, and these domains help actuating the cellular signal as well as regulating the strength of the signal. These domains are defined laterally by different composition of different lipids and proteins, thus they compartmentalize the membrane. One of these subcompartments, called lipid rafts, are composed of high amounts of sphingolipids and cholesterol.<sup>10</sup> Lipid rafts have been shown to be vital in different signaling processes, e.g EGFR signaling.<sup>10,28</sup> These rafts have been observed to attract Akt to dock after enriched with PIP3 for activation. In addition, PTEN is proposed to be localized to the nonraft areas.<sup>10</sup>

Lateral compartmentalization of the plasma membrane can modulate the specificity of Class IA PI3K signaling as well. For p110 $\alpha$  and p110 $\beta$  catalytic subunits, it is clearly demonstrated that p110 $\alpha$  localizes mostly to nonraft regions, where it can be activated downstream of RTKs. On the other hand, p110 $\beta$  selectively localizes to lipid raft regions.,<sup>10</sup> p110 $\delta$  has been depicted as a catalytic isoform similar to both p110 $\alpha$  and p110 $\beta$ , as p110 $\delta$  has been shown to be signaling through both GPCRs and RTKs in immune cells.<sup>29</sup>

To obtain constitutive activation of wild type p110s lipidation tags were used. The lipidation signal that has been used in this study is myristoylation tag. The tag sequence has been obtained from N – terminal of Lyn kinase. The myristoylation tag enables p110s transfer to plasma membrane, and these p110s remain attached to the membrane continuously.<sup>30</sup> Myristoylation signal does not have a preference over lipid rafts or nonraft regions.<sup>10</sup>

Although p110 $\alpha$  and  $\beta$  are expressed ubiquitously, they have different roles. p110 $\alpha$  has shown to be signaling downstream of RTKs, on the other hand, p110 $\beta$  has been observed to signal downstream of GPCRs. They also interact with different small GTPases. p110 $\alpha$  interacts with Ras, while p110 $\beta$  interacts with Rac1. It is also pointed out that p110 $\beta$  is located mainly to the membrane raft regions through Rac1 and p85 binding, on the contrary, p110 $\alpha$  seems to be located mostly to the nonraft regions where it can interact with RTKs through Ras and p85.<sup>10</sup>

In addition to the fact that p110s serve under different receptors, they bind p85 molecules in different fashion. p110 $\alpha$  binds nSH2 domain of p85, however, p110 $\beta$  and  $\delta$  binds nSH2 and cSH2 domains of p85.<sup>31</sup> Although both p110 $\alpha$  and  $\beta$  are inhibited by nSH2 domain of p85, p110 $\alpha$  is inhibited by iSH2 and p110 $\beta$  is inhibited by cSH2 domains as well.<sup>32</sup> These differences in mode of binding and inhibition cause different upregulation patterns in cancer. While p110 $\alpha$  upregulations are mostly hotspot mutations, p110 $\beta$  requires to other means to be constitutively activated so that it would be able to escape from p85 inhibition.<sup>14</sup>

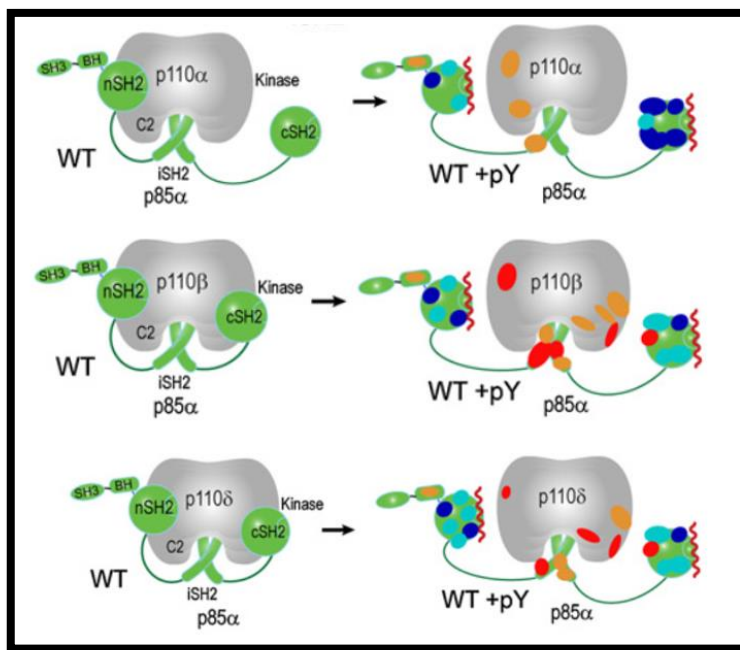


**Figure 1.4 Schematic representation of different activation modes of p110 $\alpha$ , p110 $\beta$ , and p110 $\delta$  upon p85 $\alpha$  interaction with phospho-tyrosine residues of RTKs.**

(Reprinted with the permission from Ref. [31], Elsevier)

In addition to the differential association with p85, each p110 isoform has specific interaction partners. One of the most striking evidence for that is their preference to bind Rac1 or Ras. It has been shown that p110 $\alpha$  and  $\delta$  interacts with Ras, and p110 $\beta$  interacts with Rac1 and Cdc42, independent of p85.<sup>33</sup>

Different nanodomains produced by different Ras proteins (H-Ras, K-Ras, and N-Ras) have been suggested to explain signaling specificity downstream of RTKs. As an example, clathrin nanodomains are found to be essential in epidermal growth factor

receptor (EGFR) – PI3K – Akt signaling only when ErbB2 is lacking.<sup>34</sup> Distinct nanodomains preference of different G-proteins can explain why and how p110 $\alpha$  interacts with different substrates.

p110 $\alpha$  has been depicted as the main isoform signaling downstream of insulin receptors, where p110 $\beta$  activity is observed to be minimum. The most striking difference between p110 $\alpha$  and p110 $\beta$  in insulin signaling is that p110 $\alpha$  has been preferred over p110 $\beta$  to interact with Insulin Receptor Substrate 1/2 (IRS1/2).<sup>35</sup>

PI3K Class IA isoforms and the main negative regulator of the pathway, the tumor suppressor PTEN, have been found to be deregulated in many cancers. PIK3CA and PIK3CB genes coding for p110 $\alpha$  and p110 $\beta$ , respectively, have been reported to be mutated or amplified in cancer, especially p110 $\alpha$ , being the main driver of the pathway. The most frequent mutations that PIK3CA undergoes are E545K and H1047R. These missense mutations correspond to helical (E545K) and catalytic (H1047R) domains of p110 $\alpha$ . Both of these mutations constitutively activate the pathway. In some cancer subtypes, p110 $\alpha$  amplifications have also been observed.<sup>14</sup> p110 $\beta$  is upregulated through amplification in PTEN null cells, either through loss of heterozygosity or mutations, as PTEN deficient cancers depend on p110 $\beta$ .<sup>36,37,38</sup>

### **1.1.2. PI3K Signaling**

p110 $\alpha$  has been shown to be activated mostly downstream of RTK signaling. To be activated, RTKs need to detect ligands on the extracellular space.<sup>34</sup> After detection of ligand, RTKs dimerize and undergo conformational change leading to their tyrosine residues and kinase domains to be transphosphorylated. The phosphorylated residues act as anchors for proteins with SH2 and PTB. One of the key proteins with SH2 domains that are recruited to the site is growth factor receptor – bound protein 2 (Grb2). Grb2 brings son of seventhless (SOS) protein through its SH3 domains. SOS, being a guanine nucleotide exchange factor (GEF), activates Ras.<sup>7</sup> Activated Ras transmits the signal to Raf – MEK – ERK pathway. Independent of Raf – MEK – ERK signaling, by forming nanodomains on the plasma membrane, Ras has been shown to induce PI3K signaling by interaction with p110 $\alpha$ . Interaction between p110 $\alpha$  and Ras is formed by phosphorylated

S191 residue on K-Ras. S191 – phosphorylated K-Ras nanoclusters have been depicted as different than nonphosphorylated nanoclusters because of p110 $\alpha$  interactions.<sup>34</sup>

p110 $\beta$  has been observed acting mostly downstream of GPCRs. The activation is mediated through Rac Binding Domain (RBD) of p110 $\beta$ . Another form of interaction with GPCR has been depicted through G $\beta\gamma$  and p110 $\beta$ . In addition, it needs to be addressed whether both of these interactions can fully activate p110 $\beta$ , negating p85 mediated inhibition. Other distinct forms of activation of p110 $\beta$  have been suggested to take place under different conditions. In leukocytes, p110 $\beta$  requires dual input from RTKs and GPCRs to be fully activated. A similar condition is proposed for thrombocytes. In thrombocytes, it has been shown that integrins, Immunoreceptor Tyrosine – containing Activation Motif (ITAM) – bearing receptors, and GPCRs are required to fully activate p110 $\beta$ . In mouse embryonic fibroblasts (MEFs), p110 $\beta$  is proposed to be activated through two different arms under Rac/Cell division control protein 42 homolog (Cdc42). One arm requires Dock180/Elmo1 interaction with G $\beta\gamma$  and Rac, while the other arm states G $\beta\gamma$  interaction with p110 $\beta$ . It is unclear whether these two interactions can occur under same GPCR, and other Rac protein interactions. It needs to be further investigated whether Dock180/Elmo1 involvement is direct.<sup>33</sup>

AKT is activated downstream of RTKs, and its activation requires membrane localization via PtdIns – 3,4 – P2 or PIP3. Akt has three isoforms: Akt1, Akt2, and Akt3. These isoforms contain N – terminal pleckstrin homology (PH) domain, an internal domain with kinase responsibility, and a regulatory domain at C – terminus. Isolated PH domain of these three isoforms has been shown to have affinity for both PtdIns – 3,4 – P2 and PIP3. On the other hand, when full length Akt isoforms are investigated, Akt1 and Akt3 have been observed to have higher tendencies to bind PIP3, and Akt2 to PtdIns – 3,4 – P2. The produced PtdIns – 3,4 – P2 and PIP3 molecules on the plasma membrane attract 3 – phosphoinositide – dependent kinase 1 (PDK1) as well. Likewise Akt, PDK1 is bound to those lipids through its PH domain. When in proximity, PDK1 phosphorylates Akt on its Threonine 308 residue. To be fully activated, Akt requires an additional phosphorylation. mTORC2 (Mammalian/mechanistic target of rapamycin in complex 2) phosphorylates Akt on its Serine 473 residue. DNA – dependent protein kinase (DNA – PK) has been shown to phosphorylate Akt on S473 under different conditions.<sup>34</sup>

AKT isoforms have redundant as well as unique substrates. Since there are isoform specific substrates, the isoforms perform non - overlapping functions, which makes them characteristic actors for different physiological conditions and requirements. To illustrate, actin – bundling protein palladin has been shown to be phosphorylated by Akt1, and not Akt2. It has been proposed that Akt1 induces breast tumors, on the contrary, Akt2 promotes metastasis.<sup>34</sup>

mTOR, belonging to PI3K – related kinase family (PIKK), forms different complexes.<sup>39</sup> There are two different complexes of mTOR, namely mTORC1 and mTORC2, in majority of eukaryotic organisms. mTORC3 is specific to humans.<sup>26</sup> These complexes are differentiated on their auxiliary subunits, as well as their short term responds to rapamycin.<sup>40</sup> The main subunits of mTORC1 are mTOR, RAPTOR, mLST8, DEPTOR, PRAS40, FKBP-38.<sup>26, 39</sup> mTORC2 consists of mTOR, RICTOR, mLST8, mSIN1, PROTOR.<sup>39</sup> mTORC3, on the other hand, has been shown to contain mTOR, ETV7, and p4EBP1.<sup>26</sup>

mTOR complexes are distinguished by their different roles in cells. mTORC1 is responsible for initiation of protein synthesis, anabolism and cellular energy balance, as well as inhibition of catabolism.<sup>40</sup> mTORC2 regulates cytoskeleton, migration, lipogenesis, apoptosis, and glucose metabolism.<sup>40,41</sup> There has been different feedback regulations between two complexes, which will be discussed further.<sup>40</sup>

mTORC1 regulates protein synthesis by phosphorylating; inhibiting 4E-Binding Proteins (4E-BPs), and activating S6 Kinase 1 (p70S6K1). Eukaryotic translation initiation factor 4E (eIF4E) is bound by unphosphorylated 4E-BPs. Phosphorylated 4E-BPs release eIF4E, and as eIF4Es are responsible for 5' cap-dependent translation of mRNAs, mRNA translation rate increases. Secondly, mTORC1 phosphorylates S6K1 in addition to phosphorylation by PDK1. When phosphorylated, S6K1 becomes activated and phosphorylates ribosomal protein S6. It has been suggested that phosphorylated S6 could be increasing transcription of ribosome biogenesis related genes. rRNA transcription has been observed to be elevated by S6K1 and mTORC1. S6K1 has been observed to induce protein synthesis through eIF4B activation and downregulation of programmed cell death 4, a negative regulator of 4E-BP1, as well.<sup>40</sup>

In addition to enhancing protein synthesis, mTORC1 responds to growth factor stimulations. Tuberous sclerosis complex (TSC) mediates inputs of growth factor signaling and cellular stress. TSC is a GTPase-activating protein (GAP) of Rheb. As Rheb activates mTORC1, TSC becomes a negative regulator of mTORC1. In addition, insulin or insulin-like growth factor-1 (IGF-1) stimulation phosphorylates TSC element TSC2 via PI3K activated AKT1. When phosphorylated, TSC2 becomes released from lysosome and Rheb. Other arms of signaling that phosphorylates TSC are Wingless and Int-1 (WNT) and Ras pathways. One of the subunits of mTORC1, PRAS40, is phosphorylated by AKT1.<sup>39</sup> When phosphorylated, PRAS40 is released from mTORC1 and enables RAPTOR to bind its substrates 4E-BP1 and S6K1.<sup>39,42</sup>

In addition to promoting translation initiation, mTORC1 in mammals regulates lipid biosynthesis as well. It induces lipid production via two arms of transcriptional regulation: sterol regulatory element binding protein 1/2 (SREBP1/2) and peroxisome proliferator-activated receptor- $\gamma$  (PPAR $\gamma$ ). SREBPs are translocated to nucleus to drive transcription of mRNAs that induce de novo lipid synthesis. mTORC1 takes part in this regulation by inhibiting lipin-1 through leading its translocation from nucleus to cytosol. Lipin-1, when excluded from nucleus, no longer inhibits SREBPs. On the PPAR $\gamma$  arm of regulation, it has been shown that lipid homeostasis genes under regulation of PPAR $\gamma$  has been downregulated when mTORC1 is inhibited.<sup>40</sup>

To supply for the need of nucleotides in a proliferating cell, mTORC1 regulates processes that promote biosynthesis of one-carbon units. As proliferating cells are in need of high energy and glucose, mTORC1 also upregulates hypoxia inducible factor 1 $\alpha$  (HIF1 $\alpha$ ), leading to production of building blocks for different anabolic processes.<sup>40, 43</sup>

To keep the newly synthesized biomolecules, mTORC1 inhibits catabolism by suppressing autophagy via two major autophagy inducers, unc-51-like autophagy-activating kinase 1 (ULK1) and autophagy-related protein 13 (ATG13). Phosphorylation by mTORC1 of ULK1 and ATG13 inhibits formation of autophagosome.<sup>40</sup> In addition, AMPK has been shown to be regulating ULK1 activity. Phosphorylation of several Ser/Thr residues of ULK1 by AMPK induces ULK1 activation. On the other hand, mTORC1 phosphorylates Ser757 of ULK1, leading to blunting ULK1 activity by suppressing ULK1 and AMPK interaction.<sup>44</sup> Suppression of autophagosome leads

accumulation of proteins and organelles that can be unwanted or damaged. mTORC1 also suppresses maturation process of autophagosomes by inhibiting the switch that works through endosomes to lysosomes.<sup>40</sup>

When catabolism is favoured, mTORC1 is activated on lysosome surface by Rheb – GTP. This is a two – step process requiring activation of mTORC1 and Rheb. mTORC1 needs to be translocated to the surface of lysosome by Rags and nutrients. Rheb is a GTPase and located at lysosome surface as it is farnesylated. A heterotrimeric complex consisting of TSC1, TSC2, and TBC1D7 works as GTPase – Activating Protein (GAP) of Rheb. This trimeric complex is also located on lysosomes. Under growth factor stimulation, Akt is activated and it inhibits TSC by phosphorylating it. Inhibited TSC releases inhibition on Rheb, rendering it active. It is not known where Akt performs this phosphorylation clearly, as Akt is activated when bound to PIP3 molecules on the plasma membrane by PDK1.<sup>41</sup> In figure 1.5, a schematic model of mTORC1 and catabolism could be found.

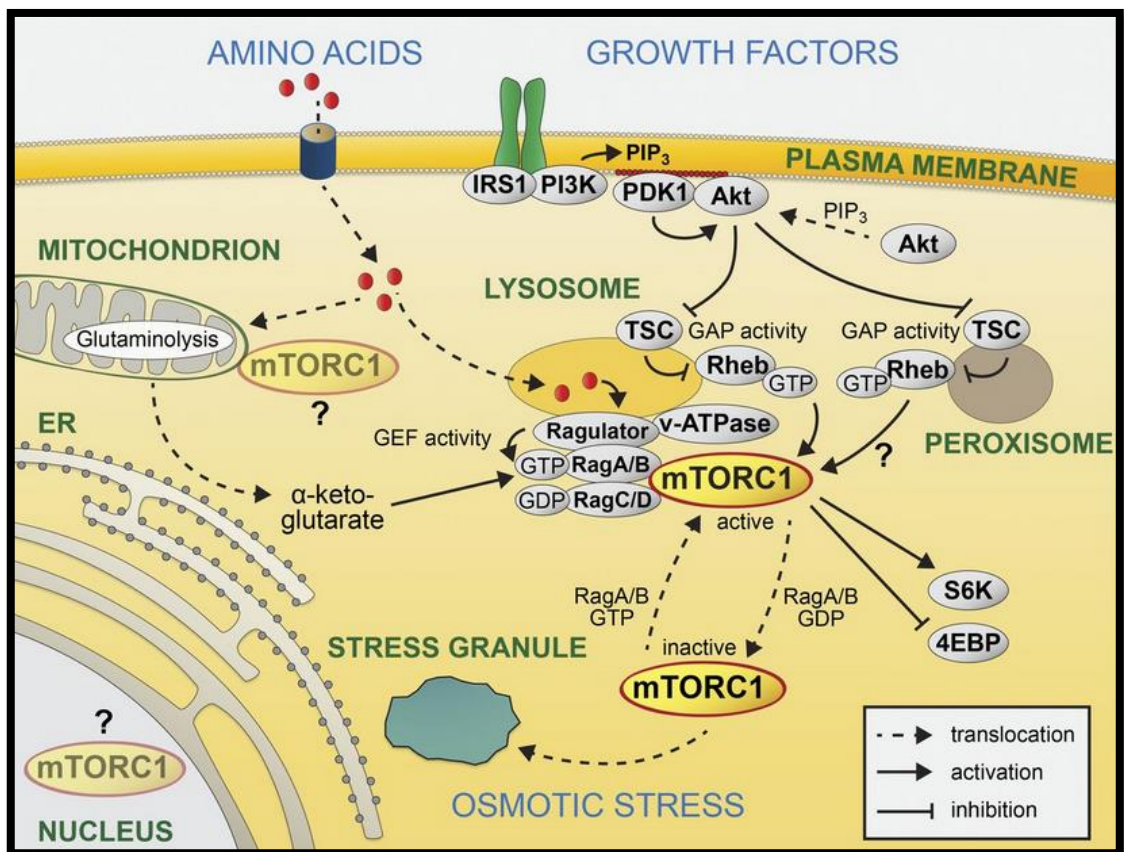


**Figure 1.5 mTORC1 activation status and catabolic processes.**

(Reprinted with the permission from Ref. [41], Rockefeller University Press)

The decision on whether favouring catabolism or anabolism is made by regulation of mTORC1 by AMPK. If cellular energy levels are low, AMPK phosphorylates Raptor on Ser722 and Ser792, or it activates TSC2. Both Raptor phosphorylations as well as TSC2 activation result in blockage of mTORC1 activity. It has been proposed that both mTORC1 and AMPK were under regulation of lysosomal v-ATPase-Ragulator complex. AMPK has been observed to localize to lysosomes by its interaction with AXIN subunit of LAMTOR1. If energy is low, AXIN has been observed to localize to lysosomal membrane. There, AXIN interacts with previously described v-ATPase-Ragulator complex as well as AMPK which is bound by AMP. By being translocated to the lysosomal surface, AXIN activates AMPK and removes mTORC1 from lysosome. When removed, mTORC1 cannot perform its anabolic work, and catabolism is favoured.<sup>44</sup>

The cornerstone marker for mTORC1 inhibition is phosphorylation of PRAS40.<sup>39</sup> Another inhibitory regulation of mTORC1 has been shown to be facilitated by GPCR signaling. GPCRs that are coupled G $\alpha$ s have shown increased cAMP levels and mTORC1 activity and protein synthesis inhibition, which could be explained by cells having decreased energy levels, thus catabolism is overcoming anabolism. The authors have suggested that this inhibition was downstream of either Rag GTPases or Arf1, as forced elevation of cAMP levels in cells (both Rag GTPase deficient and proficient MEFs) have inhibited mTORC1 activation by amino acids. Because increased cAMP levels activate PKA, it has been hypothesized that the inhibition could be through PKA activity. Activated PKA has been shown not to be interfering with localization of mTORC1 on the lysosomes. Rather, PKA has been shown to phosphorylate Raptor on Ser 791, as a result, mTORC1 activity is blunted.<sup>45</sup>

In addition to its critical involvement in activation of AKT, mTORC2 regulates cytoskeleton as well. Because of its vital role in cytoskeleton rearrangement, mTORC2 induces mobility of cancer cells, and metastasis.<sup>40</sup>

High expression of Rictor was observed in mouse embryos. In addition, rictor null embryos were smaller in comparison to WT embryos at E9.5, and died at E11.5. In rictor

null cells, cellular degeneration has been observed. Nuclear swelling and vacuole formation have been shown to occur in rictor null cells. Like rictor, mSin1 knockout in mice is lethal.<sup>46</sup>

Like its mTORC1 counterpart Raptor, phosphorylation of Rictor inhibits mTORC2.<sup>45</sup> Rictor has been shown to be phosphorylated by immediate downstream of mTORC1, S6K1. S6K1 phosphorylates Rictor at Thr1135. This phosphorylation has been indicated as growth factor induced, rapamycin sensitive, and inhibitory of mTORC2 activity.<sup>47</sup>

AKT phosphorylation on Ser473 residue has been considered as the major phosphorylation site of mTORC2. Akt T308 phosphorylation did not vanish when mTORC2 is downregulated. Other proteins have been found out to phosphorylate S473 to a lesser extent. These proteins include DNA-PK.<sup>46</sup>

Recently, a new complex of mTOR has been discovered in human, and it has been identified on its absolute resistance to rapamycin. It has been shown that mTOR forms another complex with ETV7, a transcription factor whose transcription levels are elevated in cancer patients, and p4EBP1. Interestingly, the complex did not show any interactions with main subunits of mTORC1 and 2: RAPTOR, RICTOR, SIN1, mLST8. mTORC3 has been shown in-vitro kinase activity on p70S6K1. The complex is said to be in size of MDa range, which points out the existence of other unidentified proteins in the complex, or mTORC3 could be forming oligomers with itself, or both. However, the complex is sensitive to second generation mTOR inhibitors, like the major mTOR complexes. In mice models of embryonal rhabdomyosarcoma, ETV7 expression has been shown to decrease percent survival in comparison to controls.<sup>26</sup> There is not any investigation published on functional mechanism of mTORC3 yet.

mTORC1 and mTORC2 have been shown to regulate each other at different levels. At transcriptional level, Forkhead box O transcription factor 1 (FoxO1) has been identified as one of the main actors of this regulation.<sup>48,49</sup> FoxO1 induces transcription of Sestrin3 and RICTOR, which inhibits mTORC1 and facilitates mTORC2 activity in TSC2 +/+ cells. In TSC2 null cells, mTORC2 formation has been induced by RICTOR transcription. As there are limited number of shared mTOR complex subunits like mTOR, mTORC1 assembly suffers, thus mTORC1 activity decreases.<sup>49</sup>

### 1.3.2.1. Regulation of PI3K Pathway

In MEFs, Rac1 and Cdc42 have been suggested to regulate p110 $\beta$  activity downstream of GPCRs for basal activity.<sup>33</sup>

### MAPK / ERK Pathway Crosstalk

Ras – ERK and PI3K – mTOR pathways regulate each other with feedforward and feedback loops. Crossinhibition of the pathways involve an adapter protein called Grb2 – associated – binding protein 1(Gab1).<sup>50</sup> Gab1 has been observed to bind many important proteins, e.g PLC $\gamma$ , p85, Grb2, CRKL, and MAP3K3.<sup>51 52 53</sup> It has been shown that ERK phosphorylation of GAB1 has inhibitory effect on PI3K signaling since those phosphosites are proposed as SHP2 binding sites. SHP2 binding to GAB1 dephosphorylates the sites where Ras can bind, thus, anchors for Ras binding will be lost. Another inhibition is shown between Akt and Raf when cell is stimulated with insulin – like growth factor 1 (IGF1) strongly. Akt inhibits ERK activity by phosphorylating N – terminus residues of Raf. The same residues are phosphorylated by protein kinase A (PKA) if cAMP concentration in the cell is increased. Phosphorylated Raf is inhibited by 14-3-3 dimers bound to the phosphorylated sites. These dimers sequester Raf. These crossinhibitions on Akt and Raf are resolved by dephosphorylations. Dephosphorylations are performed by protein phosphatase 1 (PP1) and/or PP2A.<sup>50</sup>

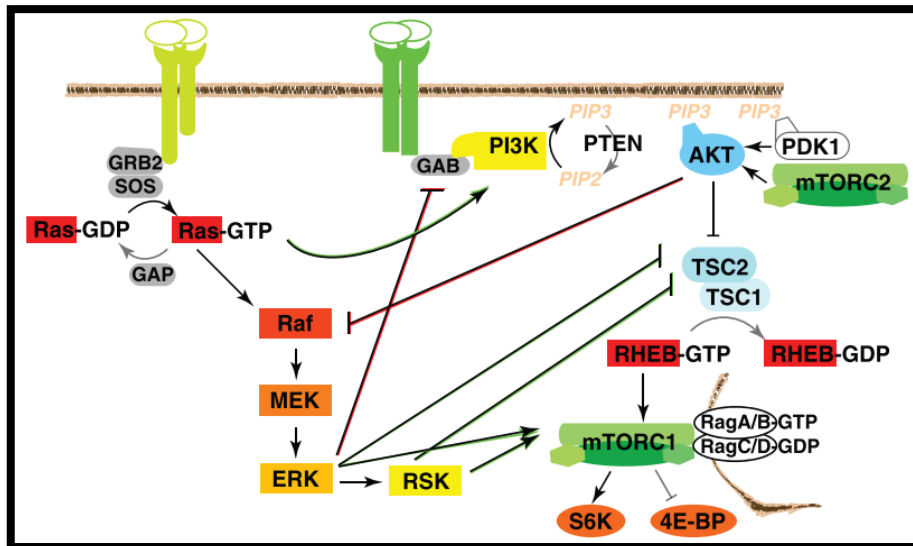


**Figure 1.6 MAPK/ERK pathway regulation of PI3K pathway.**

(Reprinted with permission from Ref. [50], Elsevier)

Crossactivation of the pathways occurs through regulation of PI3K, tuberous sclerosis complex 2 (TSC2), and mTORC1 by Ras – Erk pathway. As stated before, Ras binds and activates p110 $\alpha$  isoform of PI3K. When Ras – Erk pathway is highly activated, mTORC1 can also be activated, since under these conditions, Erk and ribosomal S6 Kinase (Rsk) inhibit TSC complexes. Inhibition of TSC complexes result in activation of mTORC1. Different molecules and conditions in which Ras is constitutively active lead to phosphorylation of TSC2 by Erk and Rsk. In addition, mTORC1 component RAPTOR is phosphorylated directly by Erk and Rsk under similar conditions.<sup>50</sup> Figure 1.6 represents the regulatory loops involving MAPK/ERK pathway.

mTORC1 has been shown to be regulated by MAPK scaffolds, e.g MEK1 scaffolding protein (MP1). MP1 acts at late endosomes where it facilitates MEK and ERK localization and ERK activity. In addition, Rag GTPases are localized to lysosomes by MP1 as well. All in all, MP1 has been proposed to be one of the crosstalk facilitators between MAPK – Erk and PI3K – mTORC1. Another node of crosstalk is kinase suppressor of Ras (KSR) MAPK scaffold. KSR has been depicted as interacting with PI3K pathway elements; mTOR, RAPTOR, RICTOR, AMPK, GSK3. It needs to be noted that AMP – activated protein kinase (AMPK) and glycogen synthase kinase 3 (GSK3) also activates TSC2 by phosphorylation. KSRs are stated to be localized to

membrane upon growth factor stimulation. On membrane, KSRs scaffold RAF, MEK, and ERK, and they are required for ERK activation. It needs further research that whether KSRs can regulate AMPKs, in turn, mTORC1.<sup>50</sup>

Both MAPK – Erk and PI3K – mTOR pathways regulate the same cellular events, so in addition to crossactivation and crossinhibition regulations, they converge. Cell survival, proliferation, motility, and metabolism are regulated by ERK, RSK, AKT, and S6 kinase (S6K). These proteins act on the same transcription factors, that are forkhead box O (FOXO) and c-Myc. In addition to these transcription factors, Bcl2-associated agonist of cell death (BAD) and GSK3. FOXO proteins are responsible for apoptotic protein expression and cell cycle suppression. FOXO3A is phosphorylated by ERK on multiple residues. These phosphorylations poises FOXO3A to be degraded by proteasomes. FOXO1 and FOXO3A are phosphorylated by AKT and SGK as well. These phosphosites are masked by 14-3-3 and blocks nuclear translocation of FOXO proteins. FOXO proteins that are sequestered in cytosol by 14-3-3 cannot induce apoptosis.<sup>50</sup>

### **Feedback Mechanisms Involving AKT and mTOR Complexes**

In the downstream of insulin and insulin – like growth factor signaling, AKT and mTOR complexes are activated, and p70S6K1 activity balances mTOR complex activities and overall pathway activity. Activated mTORC1 phosphorylates p70S6K1, and p70S6K1 phosphorylates insulin receptor substrate (IRS) to prevent overactivation of the pathway. It has been reported that mTORC1 and mTORC2 activities as well as abundances are inversely correlated with each other. Another feedback regulation that mTORC1 activity exerts is that p70S6K1 phosphorylation on Rictor, which inhibits mTORC2 activity.<sup>54</sup>

Another step that involves intervention of p70S6K1 as feedback regulation is glycogen synthase 3 $\beta$  (GSK3 $\beta$ ). p70S6K1 inhibits GSK3 $\beta$ , which is one of the substrates of AKT. GSK3 $\beta$  inhibits Rictor through phosphorylation. Involving in diverse reactions, GSK3 $\beta$  is one of the key signaling proteins in Wnt pathway. One of the roles of GSK3 $\beta$  involves voltage-gated anion channels (VDAC) on mitochondria. GSK3 $\beta$  has been shown to phosphorylate VDAC, thus inhibiting apoptosis and regulation mitochondrial metabolite transport.

54,55

## **Cell Cycle Is Regulated by Wnt and PI3K Pathway Interactions**

Wnt pathway has been reported as one of the main regulators of cell cycle. When activated, Wnt signaling induces activation of many actors like c-Myc and Cyclin D. The pathway downregulates p53 and P16ink4A (ARF). Cyclin D binds to cyclin – dependent kinase 4/6 and forms a complex. This complex inhibits retinoblastoma (Rb) activity, and initiates cell cycle by passing through G<sub>0</sub> to G<sub>1</sub>. As Rb is not phosphorylated, E2F becomes free to transcribe cyclin E. Cyclin E forms a complex with Cdk2, and they facilitate the cell passing through G<sub>1</sub>/S point.<sup>54</sup>

Autophagy is inhibited by mTORC1 mediated ULK1 phosphorylation. Disheveled (Dvl), being the major actor in Wnt pathway, has been reported to be degraded upon autophagy. When autophagy is inhibited by mTORC1 activity, Dvl is rescued. Wnt signaling has been shown to be downregulated upon autophagy inhibition – mediated Dvl release. Thus, Dvl becomes the key factor binding Wnt and PI3K / Akt / mTOR pathways, as well as MAPK pathway on cell proliferation upon autophagy inhibition.<sup>54</sup>

FoxO has been reported to be activated upon metabolic reprogramming in cancer cells, where p53 inhibition promotes glycolysis and pentose phosphate pathway. In addition, glutamine metabolism and production of reactive oxygen species (ROS) is elevated. These metabolic changes with increment in ROS production activates FoxO.<sup>54</sup>

Activated FoxO induces transcription of different genes. One of its targets is Rictor, a key component of mTORC2. Aside from being the main unique component of mTORC2, Rictor promotes ubiquitilation of c-Myc and cyclin E, leading to their degradation and G<sub>1</sub> arrest. On the other hand, Rictor activates RhoA, which is critical for G<sub>1</sub>/S phase transition. Thus, Rictor has been suggested to be considered as facilitating G<sub>1</sub>/S phase transition, rather than arresting cells at G<sub>1</sub>. Another group of target genes of FoxO consists of Sestrins. Sestrins are antioxidant genes that inhibit mitochondrial metabolism as well as mTORC1 activity. mTORC1 inhibition and autophagy initiation and cyclin A activation has been shown to be linked on basis of their timing.<sup>54</sup>

## Chapter 2

### 2. Aim of the Study

Cancer is expected to be the first cause of premature death in 21<sup>st</sup> century. <sup>1</sup> As PI3K pathway regulates growth and proliferation of the cells, the Class IA p110 $\alpha$  and p110 $\beta$  catalytic isoforms are considered to be oncogenic when mutated. <sup>56,57</sup> When pooled, all three catalytic isoform genetic alterations have been observed to occur in more than 50% of endometrial carcinoma, and more than 30% in esophageal squamous cell carcinoma, breast cancer, and head and neck cancer (Figure 2.1). So, it is important to identify the consequences of their activated forms to understand the redundant and unique outcomes to manipulate them in cancer.

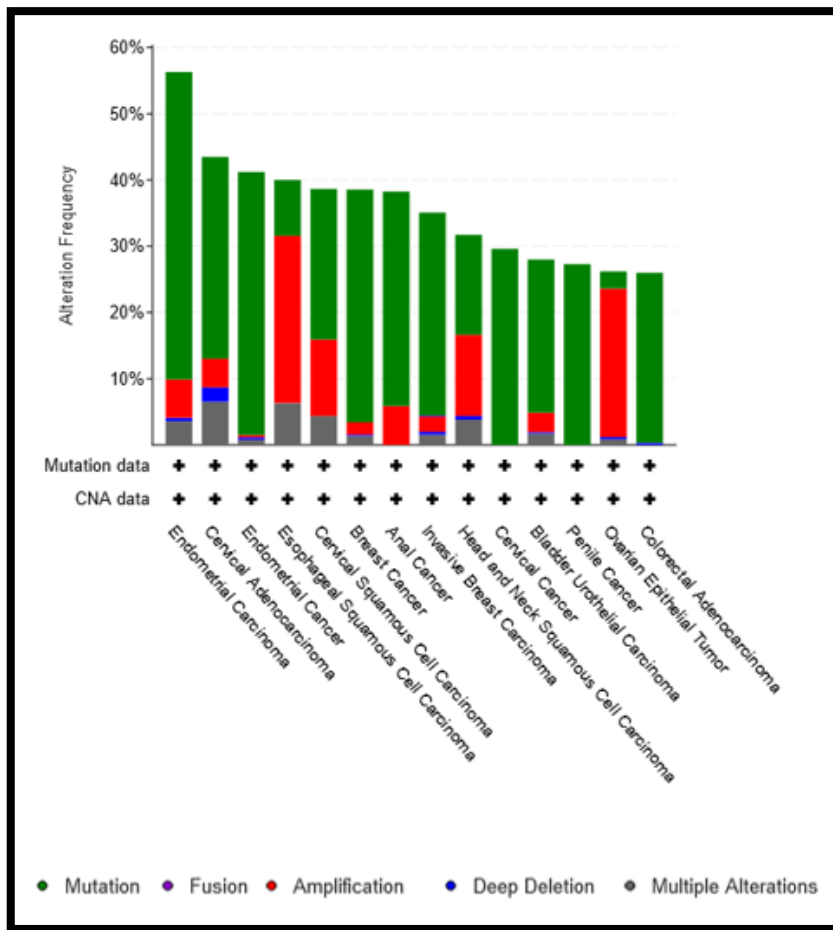


**Figure 2.1 cBioPortal data on PIK3CA, PIK3CB, and PIK3CD alteration frequencies in cancer from their curated set of non-redundant studies, derived on 12.11.2020.**

Class IA PI3K catalytic subunits p110 $\alpha$  and p110 $\beta$  are ubiquitously expressed, although both isoforms catalyze the same reaction on inner leaflet of the cytosolic membrane.<sup>10</sup> The main question of this study is why the body requires two isoforms to perform the same reaction. Previous studies have demonstrated that p110 $\alpha$  and p110 $\beta$  have different interaction partners thus they localize to different nanodomains on the membrane.<sup>10</sup> The consequences of such specificity are needed to be investigated as they have enormous potential to bring new and better treatments in cancer, as pan-PI3K inhibition has been shown to cause severe toxicities in clinical trials.<sup>58</sup>

To investigate the isoform specific functions of Class IA PI3K catalytic isoforms, the following hypotheses have been answered:

- Is Akt differentially regulated by distinct class IA isoforms?
- As Akt regulates survival, are cells ectopically expressing activated p110 isoforms have different sensitivities to genotoxic stress?
- Can PI3K catalytic isoforms exist in differential signaling complexes associated with different small G-proteins and mTOR complexes?
- Can the different sensitivities for genotoxic stress be explained by differential regulation of cell cycle?

## Chapter 3

### 3. Materials and Methods

#### 3.1 Materials

Routinely used chemicals could be found in the table below.

**Table 3.1 Routinely used chemicals list**

Name	Catalog Number	Supplier Company
di - Sodium hydrogen phosphate dihydrate	1.06580.1000	Millipore
Potassium chloride	1.04936.1000	Millipore
Sodium chloride	31434-1KG-R	Sigma-Aldrich
Ethanol	32221-2.5L	Sigma-Aldrich
Acetic Acid	27222-2.5L-R	Sigma-Aldrich
Crystal Violet	131762.1608	AppliChem
Trizma-Base	T1503-1KG	Sigma-Aldrich
Potassium phosphate monobasic	04243-1KG	Sigma-Aldrich
Potassium chloride	1.04936.1000	Millipore
Glycine	1154KG001	BioFroxx

#### 3.2 Media and Solutions

Routinely used cell culture media and solutions can be found in the table below.

**Table 3.2 Routinely used tissue culture reagents list**

Name	Catalog Number	Supplier Company
High Glucose DMEM	L0103-500	Biowest
RPMI 1640	L0496-500	Biowest
FBS	10500-056	Gibco
Pen/Strep	15140-122	Gibco
Trypsin 0.25% - EDTA 0.02% in HBSS	L0932-100	Biowest
G-418	47995.01	Serva
Lipofectamine 2000	11668-027	Invitrogen
Puromycin	A11138-03	Gibco

List of used inhibitors could be found below.

**Table 3.3 List of used inhibitors**

Name	Catalog Number	Supplier Company
BYL719	S2814	SelleckChem
KIN193	S1462	SelleckChem
CAL101	S2226	SelleckChem
Rapamycin	S1039	SelleckChem
Everolimus	S1120	SelleckChem
EHT1864	S7482	SelleckChem
Cisplatin	L01XA01	Koçak Farma İlaç ve Kimya Sanayi A.Ş.
Doxorubicin	L01DB01	Deva Holding A.Ş.

Chemicals used in cell cycle analysis could be found below.

**Table 3.4 Cell cycle analysis reagents**

Name	Catalog Number	Supplier Company
Propidium iodide	P4170-10MG	Sigma-Aldrich
RNaseA	R6513-10MG	Sigma-Aldrich

Recipes for buffers prepared in-house could be found below.

**Table 3.5 In-house prepared buffer recipe list**

Stacking Gel Buffer	15.125 g Tris-Base, in 250 ml ddH <sub>2</sub> O, Adjust pH to 6.8
Resolving Gel Buffer	46.75 g Tris-Base, in 250 ml ddH <sub>2</sub> O, Adjust pH to 8.8
SDS - PAGE Running Buffer, 10X	30 g Tris-Base, 144 g Glycine, 10 g SDS
PBS, 10X	80 g NaCl, 7.64 g Na <sub>2</sub> HPO <sub>4</sub> , 2 g KCl, 2 g KH <sub>2</sub> PO <sub>4</sub> , in 1 L ddH <sub>2</sub> O
TBS, 10X	80 g NaCl, 2 g KCl, 30 g Tris-Base, in 1 L ddH <sub>2</sub> O, Adjust pH to 7.4
Western Blot Transfer Buffer, 10X	144.1 g Glycine, 30.3 g Tris-Base, in 1 L dH <sub>2</sub> O
Crystal Violet Stain	50 ml Ethanol, 1 g Crystal Violet, 200 ml dH <sub>2</sub> O
Destaining Solution	100 ml acetic acid, 900 ml dH <sub>2</sub> O
Fixation Solution	100 ml acetic acid, 100 ml ethanol, 900 ml dH <sub>2</sub> O

Materials used in lysing cells, SDS – PAGE, and Western Blot could be found below.

**Table 3.6 Materials and reagents used to perform Western Blot.**

Name	Catalog Number	Supplier Company
RIPA Buffer	RIPA-100	EcoTech
Protease Inhibitor Coctail	12910500	Roche
Membrane Stripping Solution	2502	Millipore
4x Laemmli Buffer	1610747	BioRad
Phosphatase Inhibitor Coctail	39055.01	Serva
SDS	8.22050.100	Millipore
2-propanol	24137-2.5L-R	Sigma-Aldrich
Methanol	24229-2.5L-R	Sigma-Aldrich
TEMED	1.107.320.100	Millipore
HCl	30721-2.5L	Sigma-Aldrich
Whatman Gel Blot Paper	10426890	GE Healthcare Life Sciences
Nitrocellulose Membrane	10600003	GE Healthcare Life Sciences
ECL	34075	ThermoScientific
Acrylamide/Bis Solution 37.5:1	10688.01	Serva
Protein Ladder	1610373	BioRad
Sodium Orthovanadate	P0758S	NEB

2-Mercaptoethanol	M3148- 250ML	Sigma-Aldrich
PonceauS Solution	P7170-1L	Sigma-Aldrich
Ammonium persulphate	A2941,0500	AppliChem
Tween20	39796.51	Serva
Bovine Serum Albumin	11930.02	Serva

Antibody list could be found below.

**Table 3.7 Antibodies used in this study**

Name	Catalog Number	Supplier Company
Phospho-Akt1 (Ser473) (D7F10) XP	9018P	Cell Signaling Technology
Phospho-PRAS40 (Thr246) (C77D7)	2997S	Cell Signaling Technology
Akt	9272S	Cell Signaling Technology
Phospho-Akt Substrate (RXXS*/T*) (110B7E)	9614S	Cell Signaling Technology
Phospho-Akt (Thr308) (D25E6) XP	13038S	Cell Signaling Technology
S6 Ribosomal Protein (54D2)	2317S	Cell Signaling Technology
PI3 Kinase p110 $\alpha$ (C73F8)	4249S	Cell Signaling Technology

PI3 Kinase p110 $\beta$ (C33D4)	3011S	Cell Technology	Signaling
Phospho-mTOR (Ser2481)	2974T	Cell Technology	Signaling
Phospho-S6 Ribosomal Protein (Ser240/244)	2215S	Cell Technology	Signaling
HA-Tag (6E2)	2367S	Cell Technology	Signaling
Phospho-Stat3 (Tyr705)	9131S	Cell Technology	Signaling
Phospho-Akt (Ser473)	9271S	Cell Technology	Signaling
GAPDH (14C10)	2118S	Cell Technology	Signaling
PI 3-kinase p110 $\beta$	sc-376641	SantaCruz Biotechnology	
PI 3-kinase p110 $\delta$	sc-55589	SantaCruz Biotechnology	
Phospho-mTOR (Ser2448)	5536	Cell Technology	Signaling
mTOR	2972	Cell Technology	Signaling
PRAS40	2691	Cell Technology	Signaling
Anti-rabbit IgG, HRP-linked	7074S	Cell Technology	Signaling

Anti-mouse IgG, HRP-linked	7076S	Cell Signaling Technology
----------------------------	-------	------------------------------

### 3.3 Methods

#### 3.3.1 Thawing Cells From Cryovials

Cells were previously stored in cryovials at either -80°C or liquid nitrogen.

1. Cryovials are thawed in waterbath at 30°C until no soluble frozen particles can be observed.
2. In sterile 15 ml falcons, relative choice of media for thawed cells are added in 8 ml. In this media, FBS is required in relative percentage according to the cell line. The media should be free of Pen/Strep. Label the falcons accordingly.
3. Thawed cells from cryovials are transferred to falcons by a 1000 µl pipette.
4. Centrifuge the falcons at 1300 rpm at room temperature for 5 minutes.
5. Remove the supernatant and obtain harvested cells.
6. Upon the falcons, add 5 ml of relative choice of media and FBS percentage of cell lines. Resuspend the cell harvest by pipetting up and down gently.
7. Plate the cell resuspension in a 6 cm cell culture plate.

#### 3.3.2 Passaging/Splitting Cells

Cells previously thawed are cultured as below.

1. Remove the medium over the cells.
2. Add;
  - a. 5 ml sterile PBS if cells were seeded into a 6 cm plate,
  - b. 10 ml sterile PBS if cells were seeded into 10 cm plate.
3. Swirl the plate gently to wash the cells for a couple of times.
4. Remove the PBS.
5. Add;
  - a. 1 ml Trypsin if cells were seeded into a 6 cm plate,
  - b. 2 ml Trypsin if cells were seeded into a 10 cm plate.
6. Swirl gently to spread Trypsin evenly over the cells.
7. Place the plate into incubator for minimum 3 minutes, maximum 5 minutes.

8. Check the cells under a light microscope to understand whether they are detached. If not, swirl the plate or gently tap on the side of the plate. Check to observe the cells under the microscope. If they are started lifting, continue with the next step.
9. Add 10 ml medium in which FBS and Pen/Strep is present. Resuspend the cells by pipetting up and down until there is no visible cell clumps present.
10. The amount of passaged resuspended cell volume should be minimum 1/12, maximum 1/2 under regular conditions. Take the amount required and seed it to a new cell culture plate.
11. Add required amount of medium with FBS and Pen/Strep over the newly seeded cells. Add required specific antibiotics if any.
12. Label the plate accordingly. Increase passage number by 1.

### **3.3.3 Freezing Cells**

1. Passage the cells as in 3.3.2 until step 9.
2. Transfer the cell resuspension to 15 ml sterile falcon.
3. Centrifuge the cell resuspension at 1300 rpm for 5 minutes at room temperature.
4. Remove the supernatant to obtain cell harvest.
5. Add;
  - a. 1 ml freezing medium if the plate was 6 cm,
  - b. 3 ml freezing medium if the plate was 10 cm.Freezing medium consists of 50% medium, 40% FBS, and 10% DMSO in volume.
6. Resuspend the cells in the freezing medium until there is no observable cell clump present.
7. Pipette each 1 ml cell resuspension to one cryovial by 1000  $\mu$ l pipette.
8. Label the cryovial accordingly. Increase the passage number by 1.
9. Store the cryovial at -20°C for one or two days.
10. Transfer the cryovial to -80°C after checking the vial is frozen.

### **3.3.4 2D Growth Assay**

12 well plates were used for growth assays in this study, so 3.3.4, 3.3.5, 3.3.6, and 3.3.7 are optimized for 12 wells. For each well, 4000 cells/well were seeded, if not stated otherwise. Each well is considered to take 1 ml maximum.

A triplicate of wells were left unseeded. They were used in quantifying how much the wells retain stain by staining these empty wells and destaining them. These empty / blank wells are important in following calculations.

1. Passage the cells as in 3.3.2 until step 9.
2. Transfer 10  $\mu\text{l}$  of cell resuspension on a haemocytometer and cover it with a glass cover. This resuspension will be called as stock resuspension further on.
3. By using light microscope, count the cells in each  $1\text{mm}^2$  squares. Minimum of 3 squares needed to be counted.
4. Calculate the following to find out the seeding volume:

$n_{\text{Avg}}$  : Average number of cells

$n_{\text{Counted}}$  : Number of counted cells

$n_{\text{Sqr}}$  : Number of squares counted

$$n_{\text{Avg}} = n_{\text{Counted}} / n_{\text{Sqr}}$$

$V_{\text{well}}$  : Volume of stock resuspension to be seeded in  $\mu\text{l}$

$n_{\text{well}}$  : Number of cells to be seeded into one well

$$V_{\text{well}} = n_{\text{well}} / ( (\text{Dilution ratio} = 10) * n_{\text{Avg}} )$$

For the ease of pipetting and decreasing the pipetting errors, the volume of resuspended cells to be seeded in  $\mu\text{l}$  is equalized to 1000  $\mu\text{l}$  in order to seed them with a pipetteboy. To do that, cell resuspension (stock resuspension) needs to be diluted.

$n_{\text{FD}}$  = Fold dilution number from stock resuspension

$$n_{\text{FD}} = 1000 \mu\text{l} / V_{\text{well}}$$

Find the closest volume of diluted stock. E.g, if 12 wells x 2 plates are required, it is better to use the final dilution volume as 30 ml, instead of 24 ml. It is

recommended to leave some volume extra for pipetting errors.

$V_{\text{Stock}} = \text{Total volume of required cells from stock resuspension}$

$V_{\text{Final}} = \text{Final volume of cells after dilution}$

$$V_{\text{Stock}} = V_{\text{Final}} / n_{\text{FD}}$$

Finally, total volume of required cells from stock is transferred to an empty falcon to be diluted. The cell resuspension is filled up to final dilution volume with culturing medium.

5. By using a pipetteboy, the diluted cell resuspension is seeded to 12 well plates. Each well is seeded with 1 ml cell resuspension.
6. Label the plate(s) and grow them in the incubator. After minimum of 5 hours, the cells will be attached. Preferably, overnight incubation is performed.
7. Following day, the cells are treated. To treat the cells, following calculations are performed.
  - a. Calculate the volume of inhibitor required in a total volume of final dilution volume of cells, as explained in step 4. E.g, if 3 wells x 4 plates will be used, consider final dilution volume as 15 ml instead of 12 ml, if enough inhibitor is present. Simply,  $M_1 * V_1 = M_2 * V_2$  formula can be used as the added volume of inhibitor is negligible.
  - b. Prepare the medium with halved amount of FBS of culturing conditions. Add Pen/Strep as well. Label the falcons accordingly.
  - c. Add calculated amount of inhibitor over the media.
8. Aspirate media over the wells. Be careful not to detach any cell. Tilt the plate and remove the pooled medium.
9. Gently add inhibitor treated media over the wells 1ml each, without lifting any attached cell, by tilting the plate, as described in step 8. Label the plates.
10. Incubate the cells until DMSO treatments reach 90-100% confluency. Check the DMSO wells each day after 3 days.

### **3.3.5 Fixation for Crystal Violet Staining**

1. Remove the media over the wells.
2. Add minimum 2 ml of fixation solution, freshly prepared.
3. Store the plates at room temperature, preferably in a closed container or a cupboard, minimum 3 days prior to staining procedure to allow fully fixation.

### **3.3.6 Crystal Violet Staining**

1. Remove fixation solution gently.
2. Wash each well with 1 ml nonsterile PBS gently by tilting the plates.
3. Remove PBS carefully.
4. Add 1 ml crystal violet stain to each well without lifting the cells.
5. Incubate the plates at room temperature, in dark, for minimum 1 hour.
6. Collect the stain back gently.
7. Wash each well with 1 ml single distilled water. Before removing the water, make sure that the excess dye is dissolved by shaking gently. Wash once more with single distilled water and check whether the excess dye is dissolved.
8. Leave plates overnight to dry. In order to get the most damp out of the plates, place them tilted on their covers, on paper towels.
9. If destaining is not going to be performed the following day, the dried plates must be stored in somewhere dark. At least, their photos need to be taken that day. It is the best if photographing the plates and destaining them are performed the following day, so that the intensity of stain is the least harmed.

### **3.3.7 Destaining Crystal Violet Stained Samples**

1. Add 1 ml of destaining solution to each well.
2. Incubate at room temperature, in dark, for minimum 20 minutes.
3. Read the values with a spectrometer at 592 nm. 200  $\mu$ l from each well can be transferred to each well of a 96-well plate and reading can be obtained.

### **3.3.8 Quantifying Crystal Violet Stain**

After obtaining results in a spreadsheet, the following calculations are performed.

1. Take average of blank / empty well triplicate read.

2. Subtract the blank / empty well triplicate read from each well read. These values correspond the growth of the cells.  
It is recommended to switch to GraphPad Prism software at this step.
3. Copy and paste the growth values to an empty grouped data sheet in GraphPad to obtain graph with proper error bars.
4. Return back to the spreadsheet file. For each treatment well, perform the following to obtain percent inhibition.

$OD_{\text{Treatment}} = \text{Read obtained from treatment}$

$OD_{\text{DMSO}} = \text{Read obtained from DMSO control}$

$i = \text{Percent inhibition}$

$$i = 100 - (( OD_{\text{Treatment}} / OD_{\text{DMSO}} ) * 100)$$

The order of well replicate number is the same in both treatment and DMSO read for ease. E.g, if the first well of a treatment is going to be calculated, the first well of DMSO is selected.

5. After obtaining these results, copy them to a grouped data sheet in GraphPad to obtain graph with proper error bars.
6.  $IC_{50}$  of the treatment can be calculated by this graph after obtaining the equation of fitted line.

### **3.3.9. Retroviral Transfection**

Day 1

1. Seed HEK293T cells so that they will reach a confluency around 30 – 40% when fully attached and obtained their morphology. Preferentially, after observing their growth rate in a couple of passages, mostly they grow faster than MEFs, seed them around 10% confluency to the wells of 6 – well plate as required. Leave them to grow overnight in the incubator.

Day 2

2. Take two eppendorves and add 250  $\mu\text{l}$  DMEM to each.

3. Label two eppendorves for the following;
  - a. DNA Eppendorf: 1  $\mu$ g pCMV (vsv.g) plasmid, 1  $\mu$ g gag/pol plasmid, 2  $\mu$ g plasmid of choice
  - b. Lipofectamine Eppendorf: 5  $\mu$ l Lipofectamine
4. Add plasmids to DNA tube. Mix thoroughly.
5. Add Lipofectamine to Lipofectamine tube. Mix thoroughly. Incubate at room temperature for 5 minutes.
6. Transfer DNA tube contents over Lipofectamine tube. This mix will be called transfection complex. Mix thoroughly. Incubate at room temperature for 15 minutes.
7. Take the plate out of the incubator and aspirate the well(s).
8. Add 1.5 ml DMEM with 8% FBS and 1% Pen/Strep each well.
9. Add slowly dropwise 500  $\mu$ l transfection complex over the cells.

#### Day 3

10. It is recommended to seed the cells into to be infected with the viral packages between these days into another 6 well plate, according to their proliferation rate. Cells are needed to be in 50 – 70% confluency when infected, and this rate should be adjusted to their durability against viral complex and polybrene.
11. After 24 hours of transfection, remove the transfection complex over HEK293T cells. Add 2 – 3 ml 8%FBS 1%Pen/Strep DMEM.

#### Day 4

12. Collect the medium into 15 ml falcon. Cover the falcon with aluminum foil as viral particles are sensitive to light. Store them at +4°C.
13. Add 2 – 3 ml 8%FBS 1%Pen/Strep DMEM over the cells.

#### Day 5

14. Collect the medium over previously collected falcons.
15. To get rid of remaining viral particles, add bleach over HEK293T cells. Incubate at room temperature to disseminate.
16. Filter the viral particles with 0.45  $\mu$ m filter into a clean 15 ml falcon.

17. Add 8  $\mu\text{g/ml}$  polybrene to filtered viral particles in 1:1000 ratio of volume. Mix the falcon by inverting.
18. Aspirate the wells of cells to be infected if the confluency of cells is 30 – 50%. Add 2 ml filtrate over each well.
19. Store the cells back to the incubator.

### **3.3.10 Harvesting Cells for SDS – PAGE**

1. Check the cells under a light microscope. If they are observed healthy and in enough confluency, continue with the next step.
2. Prepare two ice buckets. First, fill one bucket with ice, fully. Place nonsterile PBS bottle into the second bucket, and fill it with the ice. Label 15 ml falcons according to the experiments, and place them around the PBS bottle into ice. Fill the other bucket with ice as well. It is recommended to prepare a slightly tilted surface of ice to ease the process.
3. Remove plate(s) from incubator and place them on the bench. Remove the medium over the cells and wash them with 5 ml PBS very gently after placing them on the ice.
4. Remove the PBS on the lower side of the plate without removing any cells from the plate. Add 6 ml PBS over the cells and scrape them with a scraper. Scrape each area minimum twice without splashing any cell resuspension. Collect the resuspension on the tilted side of the plate by pooling all of the liquid by wiping the plate with the scraper.
5. Collect the resuspension into relatively labelled falcon and place it back into the ice.
6. Centrifuge all of the falcons at  $+4^{\circ}\text{C}$  at 1500 rpm for 8 minutes to collect the whole cell pellet.
7. Remove the supernatant by decanting the falcon and remove the remaining PBS with a micropipette without disrupting the pellet.
8. Snap – freeze the falcons in liquid nitrogen and store them at  $-80^{\circ}\text{C}$ .

### 3.3.11 Lysing Cells for SDS – PAGE

1. Predict the volume of cell pellets collected by eyeballing. 70-80% confluent MEFs produce 20 - 30  $\mu$ l pellet. According to required final lysate concentration, adjust the total lysis buffer to be prepared. Adjust the lysis buffer ratio between 1:1 to 1:3. It is not recommended to use a ratio outside of this interval, because it will either result in low concentrations that cannot be used in SDS – PAGE followed by Western Blot, or it won't be able to fully lyse the pellet. E.g HMECs do not produce that much of protein than MEFs so it is recommended to use 1:1 volumes.
2. After deciding on the volume of the lysis buffer to be used, prepare the lysis buffer on ice by using the recipe below:  
200  $\mu$ l 1x RIPA buffer  
4  $\mu$ l 50x Protease Inhibitor Cocktail  
2  $\mu$ l 100x Phosphatase Inhibitor Cocktail  
2  $\mu$ l Sodium Orthovanadate  
0.5  $\mu$ l DTT
3. Add the required amount of lysis buffer over falcons on ice. Bury the falcons back to ice and flick the bottom of falcons gently each 10 minutes until pellet is totally lysed.
4. Transfer the lysates to eppendorves after labelling the eppendorves accordingly. Centrifuge the eppendorves at 13000 rpm at +4°C for 15 minutes. To obtain better separation, 20 minutes of centrifuge is recommended. Another way to obtain a better separation, collect the supernatant to another clean eppendorf and centrifuge it once more at 13000 rpm at +4°C for another 15 minutes.
5. Collect the supernatant from the eppendorves after labeling them as it contains proteins, and pellet is cell debris.
6. Store the eppendorves for further use at -80°C after snap – freezing them. If it is possible to continue BCA without losing any time, it is recommended to continue to BCA, and then snap – freezing the samples.

### 3.3.12 BCA Assay

This protocol is a modified version of Microplate procedure of Pierce™ BCA Protein Assay kit (#23225).

1. Calculate the volume of working reagent (WR) mixture needed by using the formula below:

$$V_{WR} = (n_{Standards} + n_{Unknowns}) * (n_{Replicates} = 3) * (V_{WR \text{ per Sample}} = 200)$$

Floor the  $V_{WR}$  as following ( $V_{WR} = (50 V = V_A) + (1 V = V_B)$ ):

$$V_{WR} / 51 = V_B$$

Floor the value of  $V_B$  to tolerate the pipetting errors.

$$V_A = 50 * V_B$$

After preparing the WR, cover it with aluminum foil since it is light sensitive.

2. Use the following table to prepare the required standards according to the experiment with the standards provided with the kit:

<b>Standards</b>	<b>Volume of the Standard (2 µg / µl)</b>	<b>RNase/Dnase - Free Water Volume to be Added into Wells</b>
0 µg	0 µl	10 µl
1 µg	0.5 µl	9.5 µl
2 µg	1 µl	9 µl
3 µg	1.5 µl	8.5 µl
5 µg	2.5 µl	7.5 µl
7 µg	3.5 µl	6.5 µl
10 µg	5 µl	5 µl
15 µg	7.5 µl	2.5 µl
20 µg	10 µl	0 µl

3. Add 1  $\mu\text{l}$  of unknown samples to the labelled wells accordingly.
4. Add 9  $\mu\text{l}$  RNase/Dnase – Free water over the unknown wells.
5. Add 200  $\mu\text{l}$  WR over each well.
6. Immediately cover the plate with aluminum foil.
7. Shake the plate on an orbital shaker harshly for 30 seconds.
8. Place the plate into a bacterial incubator at 37°C for 30 minutes.
9. Read the plate with a spectrometer, and obtain the OD<sub>562 nm</sub>.
10. Draw the standard curve in a spreadsheet software as following;
  - a. Calculate the average of each data point.
  - b. Normalize each data point by subtracting blank wells from each data point.
  - c. Generate a linear trendline graph from standards. Make the line go through the origin by setting the intercept. Obtain R<sup>2</sup> and equation of the line.
11. After obtaining the equation in  $y = mx$  form, input read values to  $y$  and find the concentrations by solving for  $x$ .
12. Calculate how much of volume from each sample is required to load to SDS – PAGE. For this study, SDS – PAGE experiments were always followed with a Western Blot, so final concentrations after Laemmli Buffer addition are needed to be adjusted according to the material of the membrane. If nitrocellulose membrane is used, recommended interval is 30 – 50 nM. If PVDF membrane is used, minimum concentration of samples could be 15 nM.

### **3.3.13 SDS – PAGE**

Prepare Laemmli Buffer – treated protein lysates according to the supplier of Laemmli Buffer. Note whether  $\beta$ -mercaptoethanol is needed, and if needed, how much  $\beta$ -mercaptoethanol should be added to each sample. After adding Laemmli Buffer (and  $\beta$ -mercaptoethanol) boil samples in a heatblock at 95°C for 5 minutes.

If low molecular proteins (<40 kDa) are targets for Western Blotting, chill the running buffer at +4°C, preferably minimum overnight.

## 1. Gel Preparation

According to the number of gels to be run, adjust given recipe for one gel. It is recommended to add the ingredients in the same order, and mix by inverting the falcon:

**10% Resolving Gel – 10 mL:** 4.1 mL d/ddH<sub>2</sub>O, 2.5 mL resolving gel buffer (pH=8.8), 3.3 mL 30% acrylamide/bisacrylamide commercial mix, 5 µl TEMED, 50 µl APS (1g in 100 ml ddH<sub>2</sub>O)

Pour resolving gel mix between glass slides by using 1000 µl pipette. Leaving approximately 2 – 3 cm for stacking gel, add 1 ml 99% isopropanol over the poured gel mix to even the surface. When solidified, remove isopropanol and continue with stacking gel. It is recommended to follow the ingredient order to prepare stacking gel and inverting the falcon to mix as well.

**4% stacking gel – 5 mL:** 3 mL d/ddH<sub>2</sub>O, 1.26 mL stacking buffer (pH=6.8), 0.66 mL 30% acrylamide/bisacrylamide commercial mix, 5 µl TEMED, 25 µl APS (1 g in 100 ml)

Pour stacking gel mix over solidified resolving gel by a 1000 µl pipette. Fill the space between the glass slides fully. Insert comb and wait for the gel to solidify.

1. Place glass slides carefully to a cassette, and insert it into a tank.
2. Fill the space inside the cassette with running buffer.
3. Load protein ladder and samples by noting their order on the gel.
4. Fill the tank with running buffer.
5. Place the tank into a larger styrofoam box and fill it with ice to keep it cool.
6. Run the gel(s) at 100 V until samples reach to the end of the gel (around 2 hours).

### 3.3.14 Western Blot

1. Place two sponges, four whatman papers into a large box to soak them with the chilled transfer buffer. Preferably, take another large box to soak the membrane(s) if they are nitrocellulose. If they are PVDF membranes and require activation, continue with their

activation and place them into 99% methanol. Let PVDF membranes to be activated by letting them sit in methanol for a couple of minutes, if not stated otherwise.

2. Take the gel(s) out of cassette(s) and remove stacking gel. Place the gel attached with the glass slide over the box with sponges and Wattmann Papers. Gently remove the gel into transfer buffer and let it sit to be equilibrated for a couple minutes.

3. Prepare the transfer sandwich. Take plastic transfer slides and start assembling the sandwich from black (negative pole) side. Place one sponge over the black slide. Place two Wattmann Papers on the sponge. Place the equilibrated gel on Wattmann Papers in mirror image (the left of the gel should be placed on the right of the sandwich and vice versa) without turning the gel upside down. This will enable blotting of gel in the same order of loading. Place carefully the membrane with forceps. Make sure there is no remaining bubble between the gel and the membrane by sliding forceps gently on the membrane or pouring some transfer buffer. On membrane, place the remaining two Wattmann Papers. Slide a clean falcon over the sandwich to remove any bubbles. Place the remaining sponge on the sandwich and close the plastic slide.

4. Place the sandwich into transfer cassette.

5. Place a small cool – pack into the tank. Fill the remaining space with transfer buffer.

6. Place the tank into a larger styrofoam box and fill it with ice, and cool – packs.

7. Perform the transfer at 250 mA for;

a. If the gel is 1 mm thick, 120 minutes.

b. If the gel is 1.5 mm thick, 180 minutes.

8. Control the transfer efficiency by dipping the membrane into Ponceau S stain.

9. If transfer is complete, cut the membrane in desired molecular weighted pieces with a scalpel. Soak the membrane pieces into small boxes filled with TBS-T to store them and remove the excess stain.

10. Block the membranes with 5% BSA in TBS-T, if probing is planned against a phosphosite. Otherwise, use 5% milk in TBS-T. Soak the membranes in blocking

solutions and shake them on an orbital shaker for 30 minutes at room temperature, or 1 hour at +4°C.

11. Probe the membranes with antibody aliquotes prepared. Place the membrane boxes on an orbital shaker at +4°C, minimum overnight. Increase the probing period if required.

12. Collect the antibody aliquot and wash the membranes with TBS-T four times on an orbital shaker. Each wash holds 5 minutes at room temperature, 10 minutes at +4°C. If required, the membranes could be stored in TBS-T at +4°C overnight, and these washing steps would be considered done.

13. Probe the membranes with relative secondary antibodies. Probing membranes at room temperature holds 1 hour, and if the target protein requires, 2 hours, on an orbital shaker. If the process will be performed at +4°C, it will take minimum 2 hours.

14. Wash the membranes with TBS-T for three times at room temperature, or they can be stored, as on step 12. Wash the membranes one last time with dH<sub>2</sub>O or TBS. Condition of the last wash is the same as on step 12.

### **3.3.15 Wound Healing Assay (Scratch Assay)**

Day 1

Seed the cells as 200 000/well of 12-well plate in their regular culturing medium.

Day 2

1. By using a 200p pipette tip and the lid of the multiwell plate, scratch the cells. It is recommended to perform the scratches in a plus configuration for the ease of calculations. It is important not to scratch them so hard as coating of the wells could be removed, which leads to false results.
2. Shake the plate a little bit to move the precipitated cells.
3. Remove the media from the wells.
4. Wash the wells twice with PBS by shaking the plate as vigorous as possible, but be careful not to damage the attached cells.
5. Add 1% FBS 1% Pen/strep medium with the inhibitor at required concentration.
6. Immediately take a photo of the wells. This will be recored as 0 hour time point.
7. Repeat the process until all of the wells are treated.

8. Take photos of the wells at 6 hours, 12 hours, 24 hours, 36 hours, and 48 hours of time points.
9. By using TScratch tool, quantify the open area. Normalize open area to DMSO wells.

### **3.3.16 Cell Cycle Analysis by PI Staining**

Collect underconfluent cells by trypsinizing them. It is recommended to pool more than one plate, if possible three, of 10 cm plates as cells get lost in washing steps.

1. Remove the supernatant and resuspend the cells in 500  $\mu$ l ice – cold PBS.
2. Centrifuge them at 2000 rpm at +4°C.
3. Remove the supernatant and resuspend them in 500  $\mu$ l ice – cold PBS once more.
4. Centrifuge them at 2000 rpm at +4°C.
5. Remove the supernatant and resuspend the cells in 50  $\mu$ l ice – cold PBS.
6. Aliquot 450  $\mu$ l ice – cold 70% EtOH.
7. Pipette the cell resuspension into 70% EtOH eppendorf by drawing circles with pipette, gently and slowly.
8. Fix the cells by burying the eppendorfs in ice for minimum of 2 hours.
9. After fixation, add 400  $\mu$ l ice – cold PBS and resuspend the cells.
10. Centrifuge them at 2000 rpm for 5 mins.
11. Wash the cells twice more by resuspend them in 300  $\mu$ l ice – cold PBS and centrifuge them at 2000 rpm.
12. Resuspend the cells in 50  $\mu$ l 100  $\mu$ g/ml RNase A for one 10 cm plate.
13. Incubate the cells at 37°C for 15 mins.
14. Add 200  $\mu$ l 50  $\mu$ g/ml PI per one 10 cm plate and pipette up and down.
15. Incubate on ice for 1 hour in dark.
16. Use a strainer to remove cell clumps. Count and gate the cells in a cell sorter.

## Chapter 4

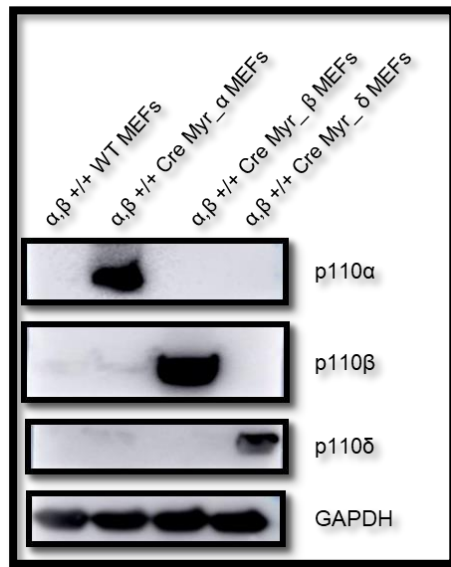
### 4. Results

#### 4.1 Generation of MEF Cell Lines Expressing Unique Constitutively Activated Class IA PI3K Catalytic Isoforms

Mouse embryonic fibroblasts (MEFs) used in this study were previously described.<sup>10</sup> To simultaneously target both ubiquitous class IA p110 isoform, the first exons of genes encoding p110 $\alpha$  and p110 $\beta$  were floxed, and untreated MEFs in this study will be designated as either  $\alpha$ ,  $\beta$  +/+ WT MEFs or WT MEFs from now on. The activated p110 ectopic expressions were facilitated by retroviral transduction of N – terminal myristoylation tagged p110 isoform genes. Because p110 isoforms have N – terminal myristoylation tag, they don't require stimulation with growth factors to be translocated to the plasma membrane. The cells that have ectopic and activated p110 expressions were treated with AdCre (Adenoviruses that carry a construct with Cre recombinase) to delete the first exons of PIK3CA and PIK3CB, so that endogenic expressions of ubiquitous p110 isoforms were ablated.

In order to check whether the cellular systems are depending on the exogenously expressed activated p110 isoforms only, the cells were tested in a growth assay where each cell line were treated with its related small molecule inhibitors of expressed p110 isoform.

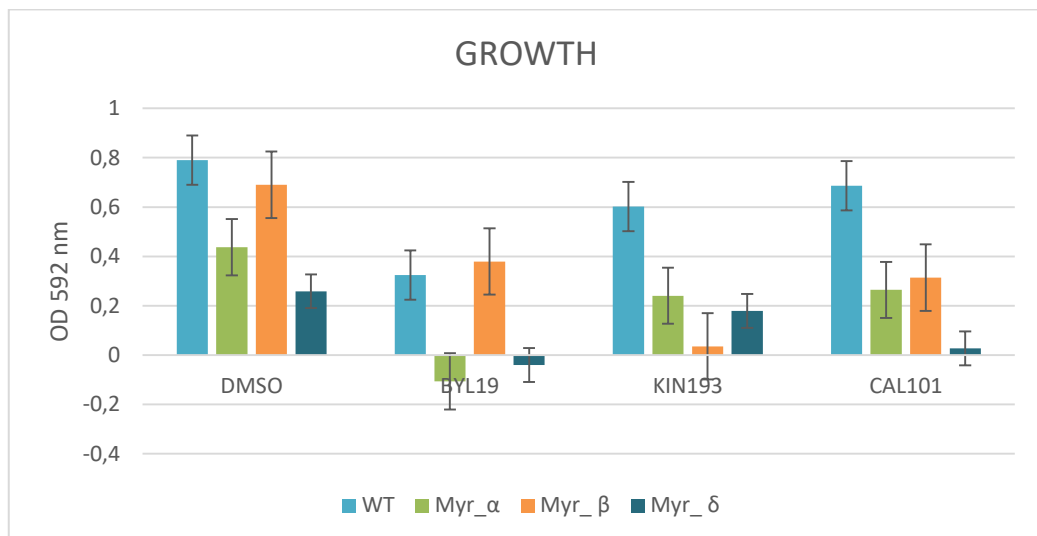
A.



B.

DMSO	300 nM
BYL 719	1 $\mu$ M
KIN 193	1 $\mu$ M
CAL 101	1 $\mu$ M

C.



D.

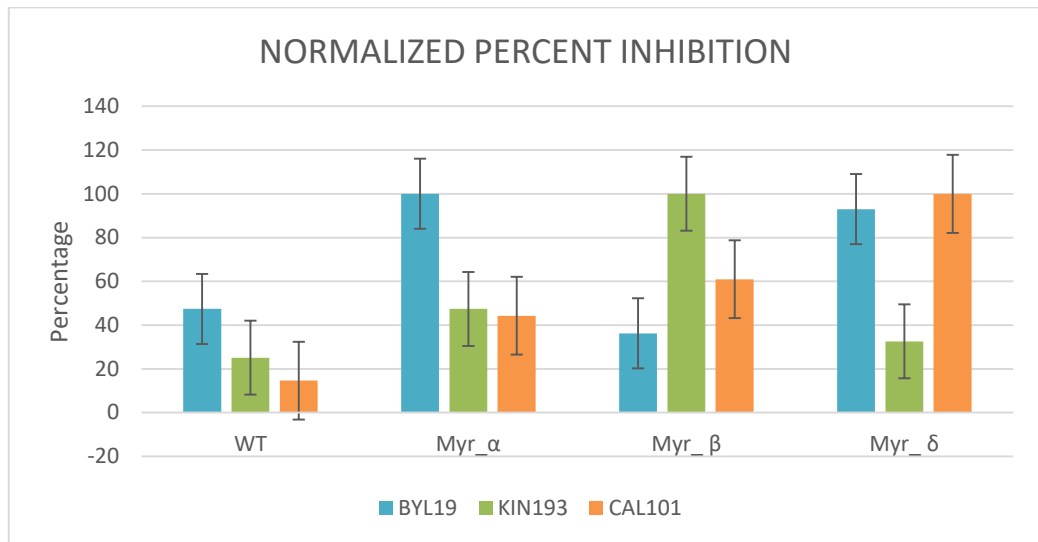


**Figure 4.1 Investigation of generated MEF lines on their dependence on ectopically expressed activated p110 isoforms.**

A. Relative protein levels of myristoylated and WT cell lines. Each well contains 40  $\mu\text{g}$  of protein lysate. B. The concentration of used inhibitors. BYL 719 for p110 $\alpha$ , KIN 193 for p110 $\beta$ , CAL 101 for p110 $\delta$  C. . Crystal violet stained plates were read at OD 592 nm to infer cellular growth. D. The OD measurements that were obtained from B. was used to calculate percent inhibition, then normalized the maximum inhibited condition read in each cell line group to 100%, and calculated the rest accordingly.

Part A of figure 4.1 shows the p110 isoform expression of isoform – specific cell lines. The endogenous expression of p110 $\alpha$  and  $\beta$  have been erased upon Cre treatment, and the only class IA PI3K isoform that regulates their growth is the exogenously expressed isoform. WT MEFs, which are used as control, have their endogenous p110 expressions masked by the overwhelming signals coming from myristoylated cell lines. The growth of MEFs with response to p110 isoform specific inhibitors have been shown in part C. In part C, the cell lines expressing relative p110 isoform has its growth inhibited the most with the relative inhibitor. In other words, we observed the strongest inhibition of each cell line when they are treated with isoform – specific inhibitors; in part D, close to 100% inhibition was obtained when myristoylated p110 $\alpha$  MEFs are treated with 1  $\mu\text{M}$  BYL 719, myristoylated p110 $\beta$  MEFs with 1  $\mu\text{M}$  KIN 193, and myristoylated p110 $\delta$  MEFs

with 1  $\mu$ M CAL 101. WT MEFs, being the control condition, are affected by p110 $\alpha$  inhibition the most, as it is the main isoform among p110s which controls PI3K – related functions, e.g growth.<sup>10</sup>

#### 4.2 Activated p110 Isoforms Show Differential Akt Activity

The first step to investigate the isoform specific consequences of activated p110s is to check the activation levels of their immediate downstream targets. The main downstream target of PI3K pathway is Akt. To obtain phosphorylation status of Akt, the cells were grown under 4% FBS and collected to perform immunoblot analysis.

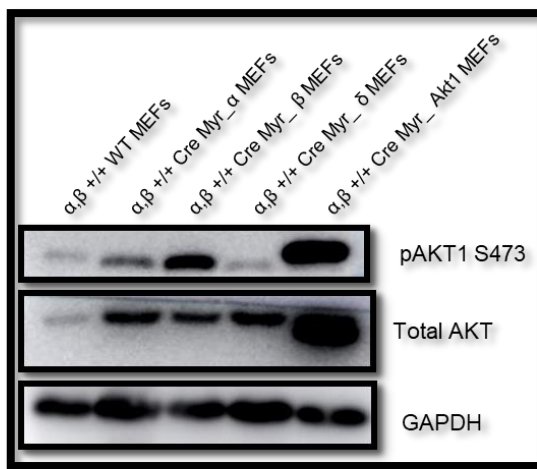


**Figure 4.2 Myristoylated p110 expressing cell lines have different phospho – Akt Ser 473 levels.**

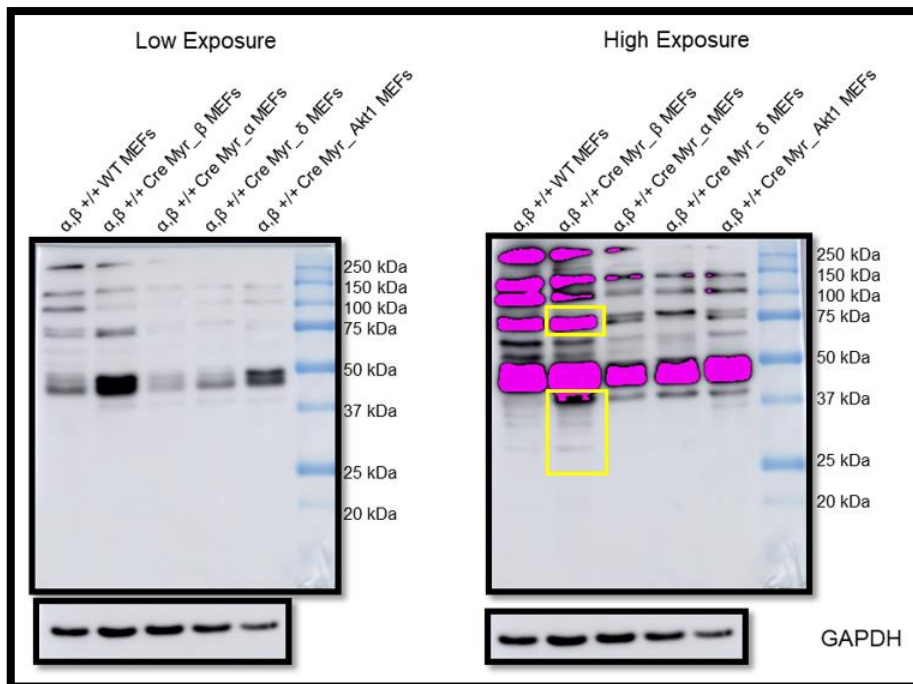
Proteins were harvested from cells grown under 4% FBS. Each well of SDS – PAGE contains 30  $\mu$ g protein lysate. WT MEFs are used as baseline control and myristoylated Akt1 MEFs are used as positive control.

In figure 4.2, MEFs with or without a myristoylated p110 construct have shown different phospho – Akt Ser473 phosphorylations. WT MEFs depict the scenario where both p110 $\alpha$  and p110 $\beta$  isoforms, and to a very lesser extent p110 $\delta$  isoform are expressed. In this cell line, any of the isoforms are not forced to be localized to plasma membrane, thus the functionally dominant PI3K isoform is p110 $\alpha$ .<sup>10</sup> We observed that phosphorylation of Akt on residue Ser 473 is higher in Cre – treated p110 double knock-out myristoylated p110 $\alpha$  MEFs in comparison to WT MEFs, because constitutively activated p110 $\alpha$  MEFs produce

more PIP3 on the membrane and more Akt proteins can translocate there.<sup>59</sup> It is interesting that myristoylated p110 $\beta$  cells exhibit even higher Ser473 phosphorylation, although p110 $\alpha$  and p110 $\beta$  virtually perform the same reaction, and p110 $\alpha$  has been depicted as the major isoform that catalyzes the PIP3 production.<sup>60</sup> Another striking point is myristoylated p110 $\delta$  MEFs have low Ser473 phosphorylation, even lesser than that of WT when normalized to total Akt levels. The last cell line that has been used in this study is myristoylated Akt1 MEFs. These MEFs have the same background with WT MEFs, and the only difference is that these MEFs express a retroviral vector with Akt1 with an N – terminal myristoylation tag. This cell line serves as the positive control in the experiment.

Myristoylated p110 $\beta$  expressing MEFs had the highest phospho-Ser473 signal. As different Akt Ser473 phosphorylations have been obtained, Akt substrate phosphorylations have been checked to understand whether there is a parallel relation between phospho-Akt levels and its substrates, as phospho-Ser 473 levels alone may not signify the activity of Akt.<sup>61</sup> The cells were grown under 4% FBS to be used in immunoblots. By using an antibody against the common phosphorylation motif of Akt substrates, relative levels of Akt activity has been determined.

A.



B.

Target	Size (kDa)	Residue	Outcome of Phosphorylation
Bcl-xL	26,158	S106	Apoptosis inhibition
PRAS40	27,383	T246	Release of inhibition of mTORC1
S6	28,681	S235, S236	Translation
NDRG2	40,789	T348	Apoptosis inhibition
CASP9	46,281	S196	Apoptosis inhibition
GSK3B	46,71	S9	Release of inhibition over glycogen synthase, anabolism is favoured
Bcl-3	47,584	S41	Cell survival
GSK3A	50,981	S21	Release of inhibition over Cyclin D1, cell cycle transition
Cot	52,925	S400	Cell cycle transition
Chk1	54,434	S280	Inhibition of apoptosis, transition of cell cycle through G1/S phase & G2/M phase
Akt1	55,686	T72, S246	Induced enzyme activity, inhibition of apoptosis
EIF4B	68,84	S422	Translation preinitiation complex formation
FOXO1A	69,344	T24, S250, S313, T24, S253, S316, T24, S256, S319	Inhibition of apoptosis

**Figure 4.3 Levels of Phosphorylated Akt substrate levels differ among myristoylated p110 expressing cell lines.**

A. Proteins were harvested from cells grown under 4% FBS. Each well contains 30  $\mu$ g protein lysate. B. Different bands appearing at different kDa sizes were putatively identified using Phosphositeplus database. WT MEFs are used as baseline control and myristoylated Akt1 MEFs are used as positive control.

Myristoylated p110 $\beta$  cells has the highest level of phospho-Ser473 levels. Overall, the same cell line has the strongest bands of phospho-Akt substrates. These suggest that, in

myristoylated p110 $\beta$  cells, the Ser473 phosphorylation is a marker for highly activated Akt.

There are differentially phosphorylated substrates with different sizes in figure 4.3 part A, and the putative identities of those proteins are listed in part B. To identify possible functional outcomes of constitutively activated p110 $\beta$  in myristoylated p110 $\beta$  MEFs, bands with different thickness have been labelled in rectangles. From approximately 25 kDa to 40 kDa, most of the proteins have been phosphorylated the most in myristoylated p110 $\beta$  MEFs. From part B of figure 4.3, we deduced most of the proteins are inhibiting apoptosis or increasing cell survival when phosphorylated. Likewise, around size 70, the phosphorylated protein could be FOXO1A, which is a transcription factor that is regulated by Akt and mTORC1, and it regulates apoptosis.<sup>49, 62</sup> The true identity of these proteins would be addressed in a future phosphoproteomic study.

To investigate whether the differential Akt activity that could be append to isoform dependent kinase activity, phosphorylation levels of different proteins in the pathway were checked in the presence or absence of appropriate small molecule inhibitors. These small molecule inhibitors are BYL 719 and KIN 193, and they inhibit p110 $\alpha$  and p110 $\beta$  dependent catalytic activities, respectively. The cells were grown under 4% FBS and were incubated with the respective inhibitors for two hours. In addition, phosphorylated Rb levels were also investigated to test whether there are differences in cell cycle kinetics between cell lines .

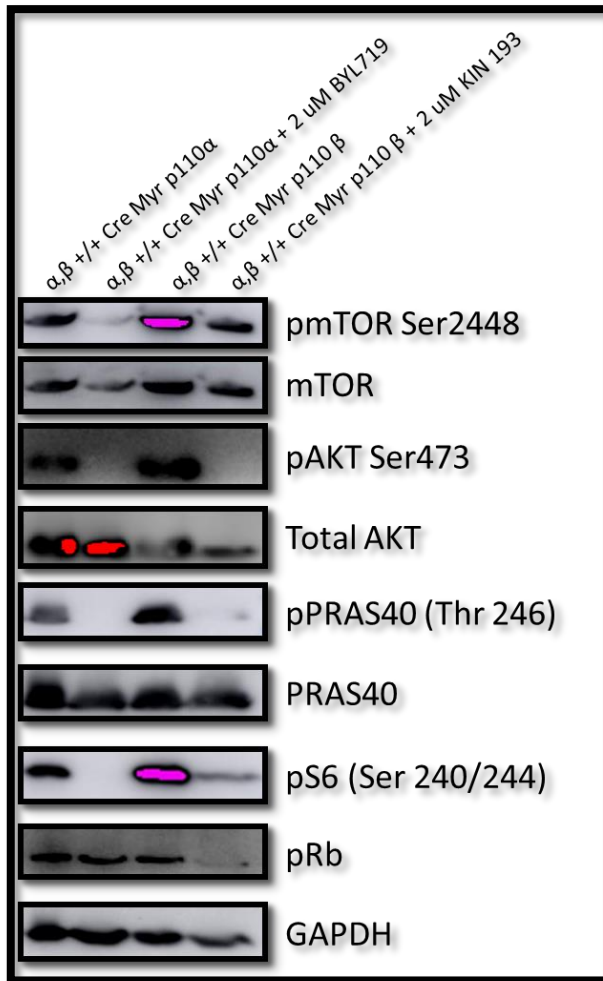


**Figure 4.4 Biochemical pathway analysis of MEFs expressing constitutively active p110 $\alpha$  and p110 $\beta$ .**

The cells were grown in 4% FBS presence and treated with indicated inhibitors two hours before harvest. Each well contains 40  $\mu$ g of protein lysate.

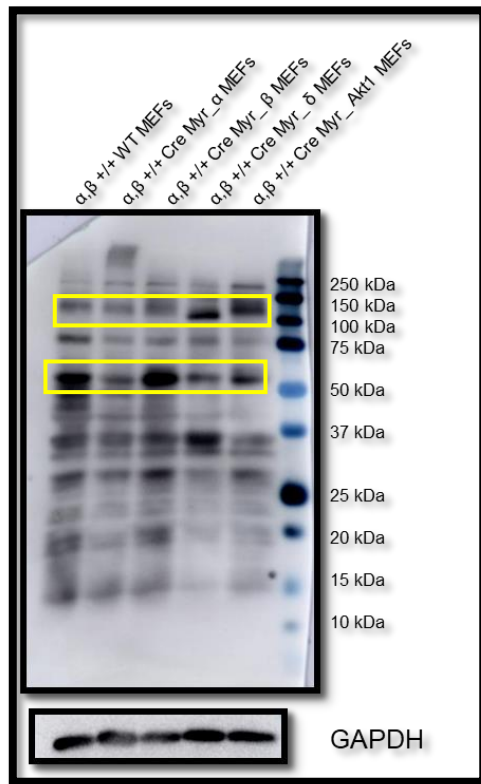
We wanted to identify possible different downstream effectors of constitutively activated p110 $\alpha$  and p110 $\beta$ . In this figure, in myristoylated p110 $\alpha$  cell line, the PI3K pathway activity is dependent on p110 $\alpha$  catalytic activity. The phosphorylations that are observed when myristoylated p110 $\alpha$  cells are treated with 4% FBS are totally erased upon BYL 719 treatment. We consider the phosphorylations that are decreased upon catalytic inhibitor treatments are the functional outcomes of p110 $\alpha$  catalytic activity. The only one exception is phospho-Rb, which does not depend on p110 $\alpha$  activity.

In figure 4.4, phospho-Akt Ser473 levels are higher in 4% FBS stimulated myristoylated p110 $\beta$  cells when normalized to total Akt levels, in comparison to myristoylated p110 $\alpha$  counterpart. We observed PRAS40, an Akt substrate and mTORC1 inhibitor, to be more phosphorylated in 4% FBS stimulated myristoylated p110 $\beta$  cells, comparing to p110 $\alpha$ . This phosphorylation is activatory for mTORC1. S6 is one of the downstream effectors of mTORC1, and it is phosphorylated in 4% FBS stimulated myristoylated p110 $\beta$  cells higher than p110 $\alpha$ . mTOR phosphorylation site Ser 2448 shows pathway activation, and it is the highest when myristoylated p110 $\beta$  cells are treated with 4% FBS. Another interesting point is phospho-Rb levels are ablated only when myristoylated p110 $\beta$  cells are treated with KIN193, suggesting a kinase dependent role of p110 $\beta$  for promoting cell cycle transitions. Most of the phosphorylations (phospho-Akt Ser473, phospho-PRAS40, phospho-Rb) are erased when the myristoylated p110 $\beta$  cells are treated with KIN 193, the catalytic inhibitor of p110 $\beta$  isoform, hence these phosphorylations depend on catalytic activity of p110 $\beta$ . Interestingly, mTOR and S6 phosphorylations are not erased when myristoylated p110 $\beta$  MEFs treated with KIN 193. The persistence of those phospho-mTOR and phospho-S6 signals could implicate involvement of scaffolding function of p110 $\beta$  in mTOR signaling. Kinase – independent functions of p110 $\beta$  have been depicted in the literature previously.<sup>63</sup> Thus, the PI3K pathway related phosphorylations observed in cells depend on the catalytic activity as well as possible scaffolding function of p110 $\beta$ .

### **4.3 Phosphorylated Tyrosine Levels of Constitutively Activated p110 Isoforms in MEFs**

Tyrosine phosphorylations usually depict growth stimulatory signals.<sup>64</sup> WT MEFs and myristoylated p110 and Akt1 MEFs were grown under 4% FBS to be harvested for western blot. We identified putative differential targets of class IA PI3Ks which could promote cell growth by using an antibody that detects common tyrosine phosphorylation motif of growth stimulation.

A.



B.

Protein	Size (kDa)	Residue	Outcome of phosphorylation
Src	59,89	418	Decrease in cell adhesion
JAK2	130,24	570, 613, 913, 1007, 1008	Protein degradation, ubiquitylation

**Figure 4.5 Biochemical analysis of phosphotyrosine signature of activated p110 expressing cells.**

A. Western blot of MEFs that has ectopic expression of activated p110s. The cells were grown under 4% FBS stimulation. Each well contains 30  $\mu$ g of protein lysate. The bands with different intensities were indicated with rectangles. B. Putative proteins belonging to relative sizes of differentially phosphorylated proteins shown in rectangles in part A, curated from Phosphositeplus database.

We wanted to investigate differentially phosphorylated tyrosine signals to identify possible isoform specific roles of constitutively activated p110s in MEFs. We used WT MEFs as basal line phosphorylation control, and myristoylated Akt1 MEFs as negative control to identify Akt – independent phosphorylations in other MEFs, because Akt is a serine/threonine kinase.<sup>61</sup> In part A, the bands that appear with different intensities depicted by the lower rectangle are around 60 kDa of size. One of the main suspects that could be differentially phosphorylated at that size is Src, as it is an abundant tyrosine kinase acting in many different signaling pathways.<sup>65</sup> In addition, Src has been reported to undergo tyrosine phosphorylation through homodimerization in a scaffold where p110 $\beta$  is present.<sup>66</sup> To investigate Src phosphorylation, the cells whose endogenous p110  $\alpha$  and p110 $\beta$  genes deleted and overexpress wild type p110 $\alpha$  or p110 $\beta$  exogenously have been grown under 4% FBS and harvested for immunoblot analysis.

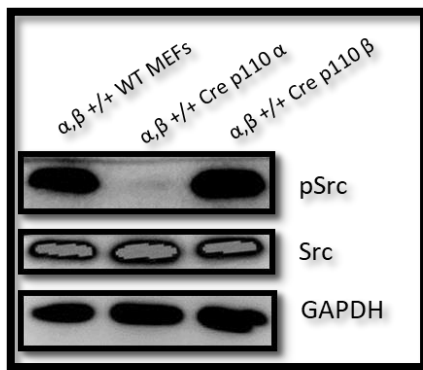


**Figure 4.6 Phospho-Src levels of WT MEFs, MEFs overexpressing p110 $\alpha$ , and p110 $\beta$ .**

The cells were grown under 4% FBS and each well was loaded with 30  $\mu$ g protein lysate. In figure 4.5, part A, the lower rectangle (>50 kDa) shows putative protein(s) with highest phosphorylation signal in WT MEFs and myristoylated p110 $\beta$  MEFs. We checked the possible proteins that could be around 60 kDa, and Src was the main candidate. To confirm the prediction, MEFs that are WT, overexpressing WT p110 $\alpha$ , or p110 $\beta$  were used to produce anti-Src immunoblots in figure 4.6.  $\alpha, \beta +/+$  Cre p110 $\beta$  cell line and WT MEFs had the highest phospho-Src signals, parallel with the observation from figure 4.5 part A.

We suspected JAK proteins to be phosphorylated around >100 kDa in figure 4.5 part A, as the highest phosphorylation intensity was in myristoylated p110 $\delta$  cells. The basis of our suspicion is that fact that p110 $\delta$  is mostly expressed in immunological context, and JAK/STAT pathway has been observed to be activated in immune cell signaling<sup>67</sup>. In addition, activated Myr-p110 $\delta$  cells show very low Akt phosphorylation and downstream activation. Thus, STAT phosphorylations were investigated. To study STAT phosphorylation, the cells were grown under 8% FBS and harvested for immunoblotting.

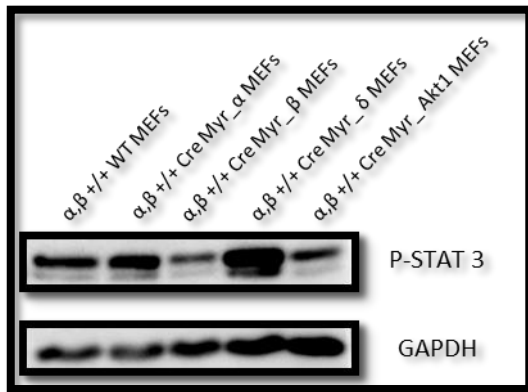


**Figure 4.0.7 Phospho-STAT3 levels of MEFs that are WT or ectopically expressing activated p110 isoforms or Akt1.**

The cells were grown in the presence of 8% FBS and loaded as 30  $\mu$ g per well. WT MEFs are used as baseline control and myristoylated Akt1 MEFs are used as positive control.

STAT3 is observed to be phosphorylated the most in the myristoylated p110 $\delta$  expressing MEF lines, which is expected when figure 5.4 part A is considered. STATs have been depicted to be phosphorylated by JAKs.<sup>68</sup> We used STRING database to understand which isoform it could be.



C. Query: p110 $\delta$  and STAT3, *Mus musculus*

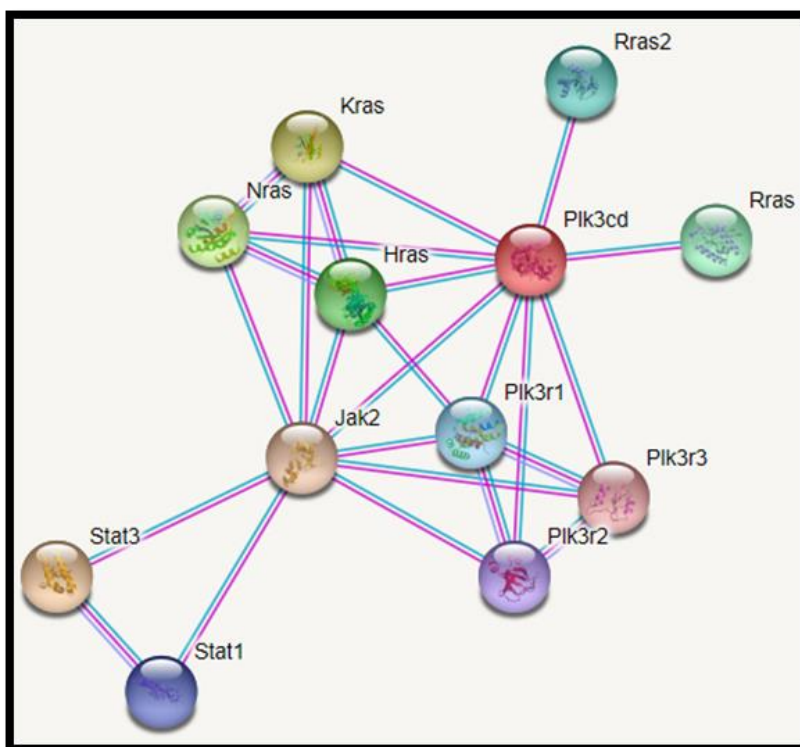


**Figure 4.0.8 Functional interaction networks obtained by STRING Database.**

A. Query is p110 $\alpha$  and STAT3, B. Query is p110 $\beta$  and STAT3, C. Query is p110 $\delta$  and STAT3. For all of the network results, the same filters were used. Those filters are; Network type: full network (functional and physical associations), Meaning of network edges: Evidence, Active interaction sources: Experiments and databases, Minimum required interaction source: Highest confidence (0,900).

We observed that only p110 $\delta$  has STAT3 in the same network, and networks created by other isoforms were excluded from that of STAT3. These results are in line with figure 5.6, which shows the highest phosphorylation level of STAT3 in myristoylated p110 $\delta$  cell line. We also observed that under given conditions, it is highly possible that JAK2 is one of the kinases that interacts with cytokine receptors.

#### **4.4 Docking Simulations by HADDOCK**

HADDOCK (High Ambiguity – Driven Docking) is a web server – based docking simulations platform where molecules up to 20 could be docked. The software can take input information based on NMR, crystallography data, etc. The system gives output in

terms of HADDOCK Score, which is not a true binding affinity, but rather indication of a possible binding in terms of energy. So the more negative the HADDOCK Score, the more possible the binding is.<sup>69</sup>

HADDOCK performs docking in a series of molecular minimizations, called it0 (rigid body minimization), it1 (flexibility is introduced), and itw (solution is refined in an explicit solvent). By using a rather straightforward and simple calculation, HADDOCK Score is generated from those refinement steps.<sup>70</sup>

In this study, we used models obtained from PDB. If the models have unknown residues, they are filled with FASTA sequence obtained from Uniprot.

To investigate whether physiologically relevant results may be obtained from HADDOCK by using PDB models, we simulated p110 isoform specificity on p85 $\alpha$  binding and Rac1/KRAS binding. Used PDB models and HADDOCK Scores of each possible complex could be found in the table below.

Model ID	Used Molecule Part	Organism
4TUU	p110 $\alpha$	Human
2Y3A	p110 $\beta$	Mouse
2WXH	p110 $\delta$	Mouse
4OVU	p85 $\alpha$ niSH2	Human
4OVU	p85 $\alpha$ nSH2	Human
2Y3A	p85 $\alpha$ icSH2	Mouse
2Y3A	p85 $\alpha$ iSH2	Mouse
2Y3A	p85 $\alpha$ cSH2	Mouse
5VQ8	KRAS	Human
2RMK	Rac1	Human
5H64	mTORC1	Human
5ZCS	mTORC2	Human

**Table 4.1 Used molecular models from PDB.**

Luckily, some models include two docked molecules that this study required. Such models were separated into parts and then used as input to HADDOCK.

	Rac1			KRAS		
	p85 $\alpha$ niSH2	p85 $\alpha$ nSH2	p85 $\alpha$ cSH2	p85 $\alpha$ niSH2	p85 $\alpha$ nSH2	p85 $\alpha$ cSH2
p110 $\alpha$	( X )	-108.5 +/- 32.2 , 7	( X )	-116.8 +/- 23.5 , 5		( X )
p110 $\beta$	-167.1 +/- 7.6 , 13		-167.5 +/- 5.4 , 29	-125.7 +/- 15.8 , 9		-180.1 +/- 1.8 , 126
p110 $\delta$	-140.5 +/- 24.0 , 2		-157.8 +/- 14.1 , 5	-127.9 +/- 14.7 , 8		-125.8 +/- 12.3 , 5

**Table 4.2 HADDOCK Scores of performed dockings by p110s, p85 $\alpha$ , Rac1, and KRAS.**

The HADDOCK Scores indicated here belongs to the best solution. ( X ) indicates the unsuccessful docking where triple docking was not possible. The numbers that are separated with a comma indicates the number of models in the best solution cluster.

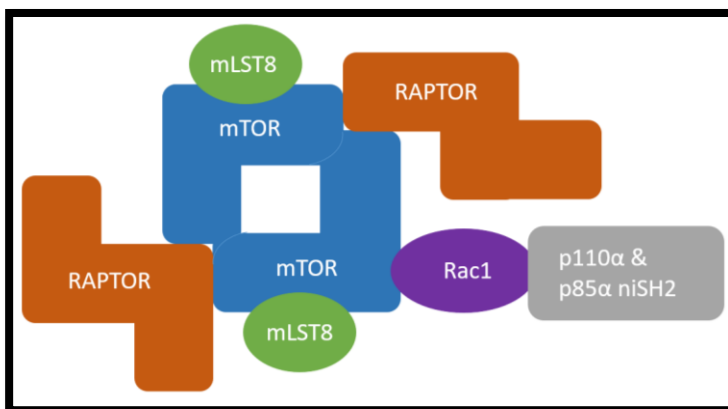
For p110 $\alpha$ , p85 $\alpha$  binding is limited to N – terminal. When the input includes the inter SH2 domain, Rac1 binding fails, but KRAS binding is facilitated. Although physiologically irrelevant, cSH2 domains were also tested, and they also failed. To conclude, KRAS binding is favoured over Rac1 binding in p85 $\alpha$  niSH2 inclusive simulations, which is more physiologically possible than only p85 $\alpha$  N – terminal binding.

For p110 $\beta$ , the binding preference of KRAS seems to be depending on p85 $\alpha$  domains. For KRAS, cSH2 domain seems to be selected over niSH2 domain. On the other hand, Rac1 dockings have similar HADDOCK Scores, indicating that Rac1 binding can be mediated with similar energetics when either part of p85 $\alpha$  is included in the docking simulation.

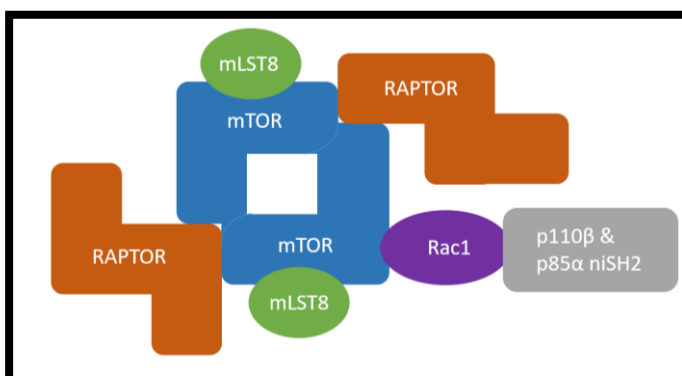
For p110 $\delta$ , KRAS or Rac1 preference is not very pronounced in terms of HADDOCK Scores. This is also physiologically relevant as p110 $\delta$  has been depicted as the isoform that is similar to both p110 $\alpha$  and p110 $\beta$ .<sup>29</sup> On the other hand, p110 $\delta$  functions in immunological signaling pathways, which is unique among class IA PI3K catalytic subunits.<sup>23</sup>

We performed docking simulations in order to address the possibility of a scaffolding function of p110 $\beta$  from figure 4.4. In literature, Rac1 C-Terminus (RKR motif) has been described to be bound by RAPTOR, RICTOR, and mTOR, but there is no information on residues on RAPTOR, RICTOR, and mTOR.<sup>71</sup> Thus, we selected active residues as the whole protein; either RAPTOR, RICTOR, or mTOR. We investigated the question on p110 $\alpha$  and p110 $\beta$ . We also integrated p85 $\alpha$  niSH2 or cSH2 domains in each docking experiment.

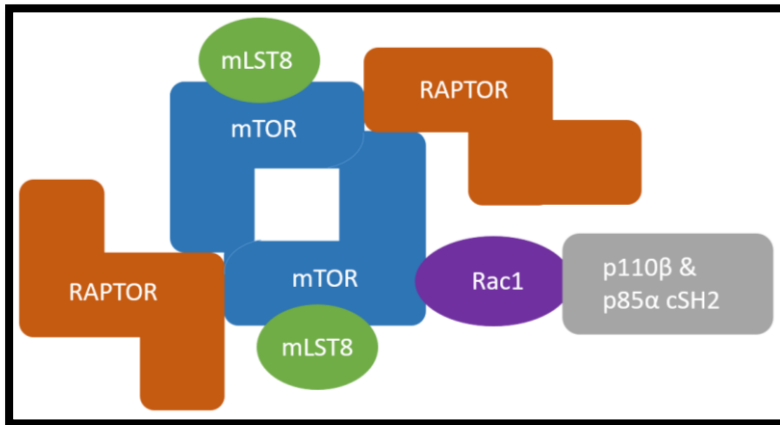
A.



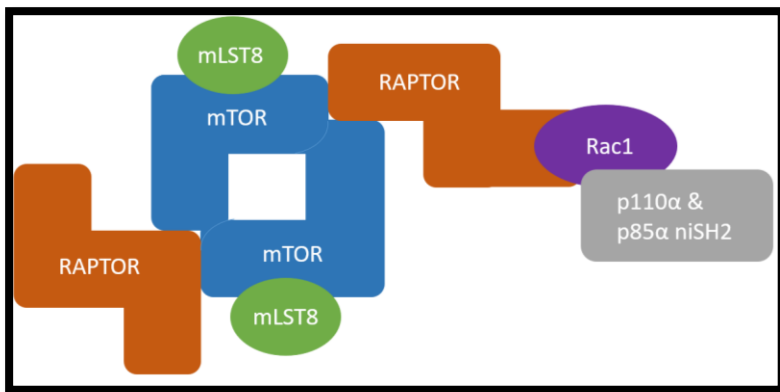
B.



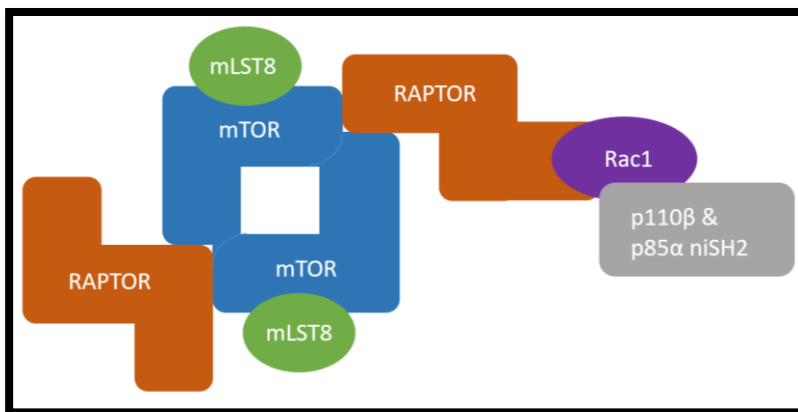
C.



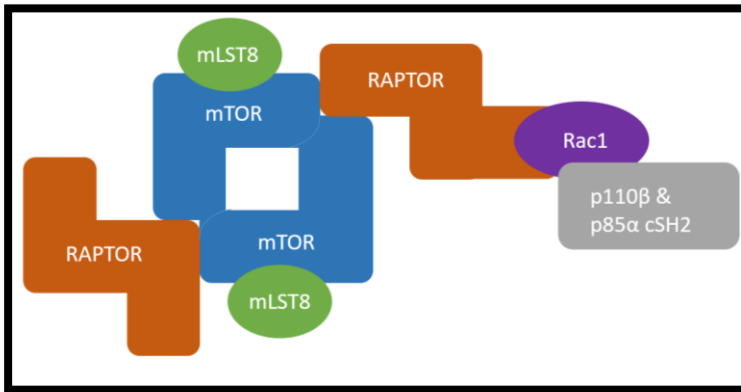
D.



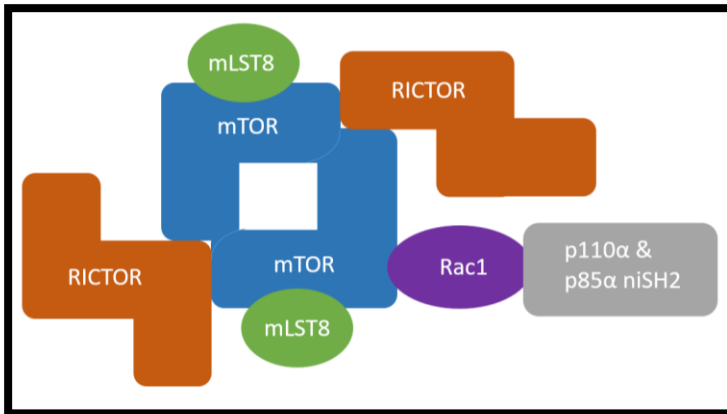
E.



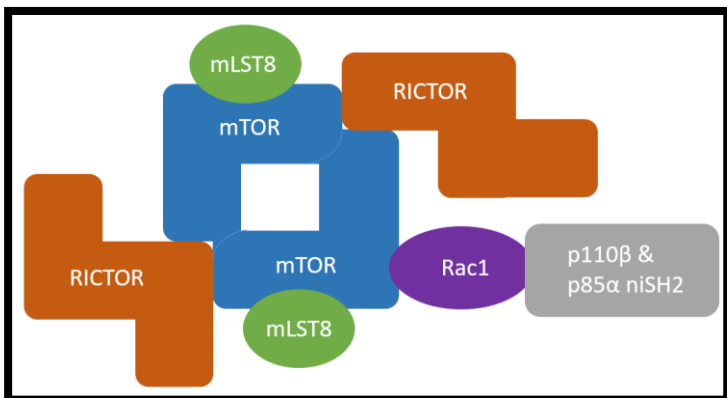
F.



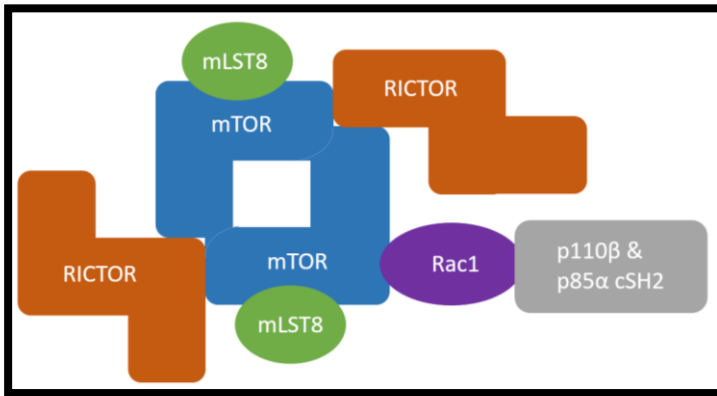
G.



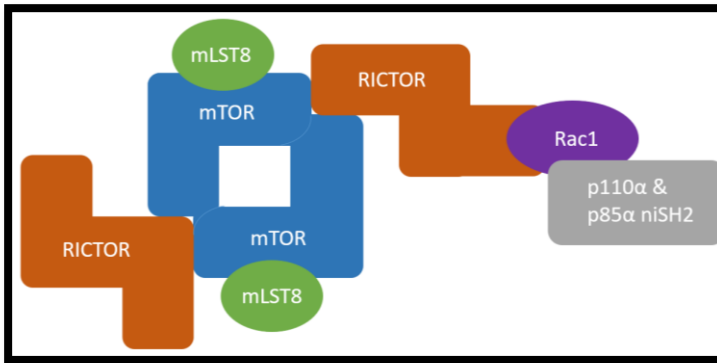
H.



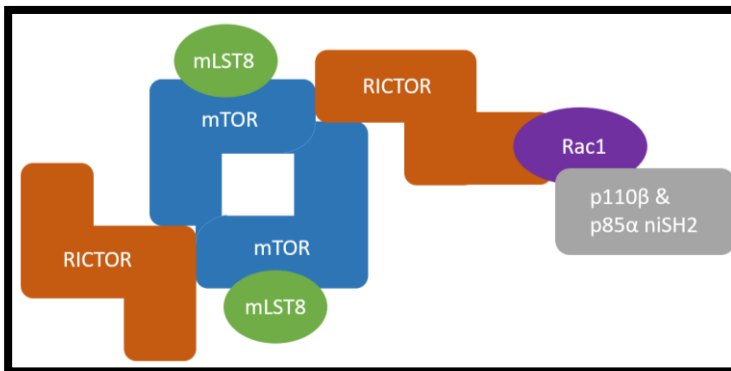
I.



J.



K.



L.

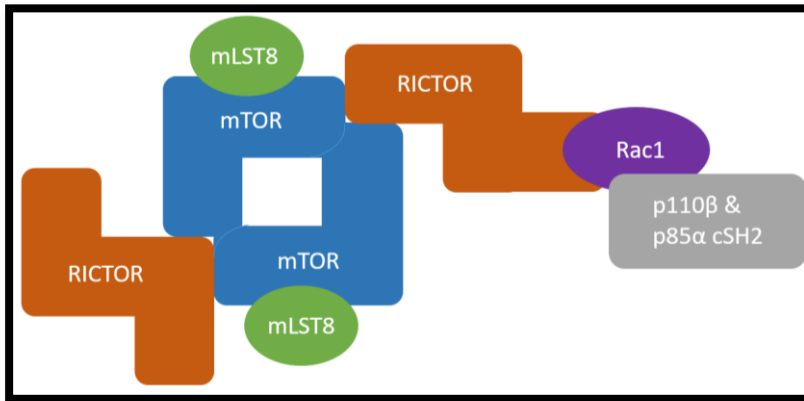
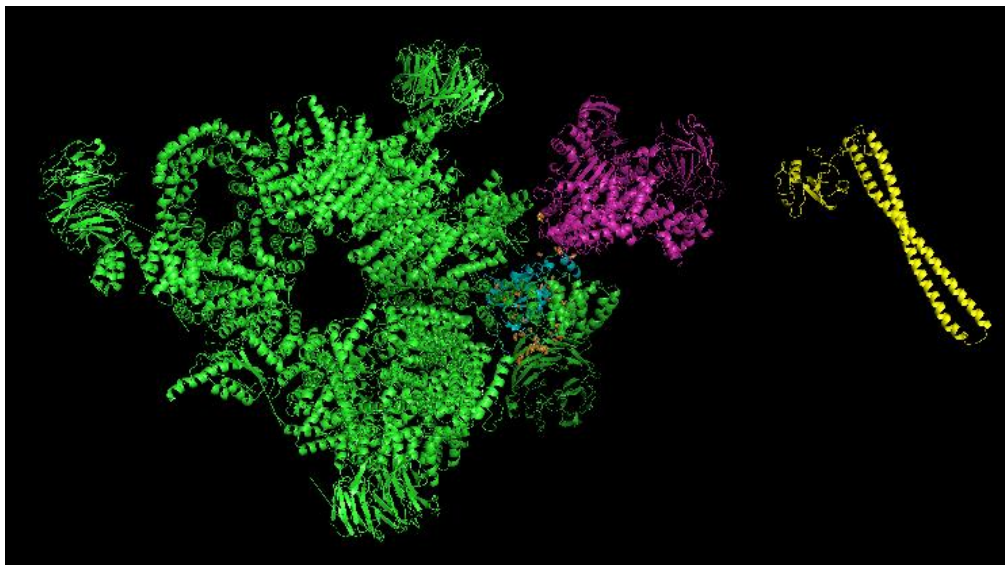


**Figure 4.9 Schematic representations of each docking run.**

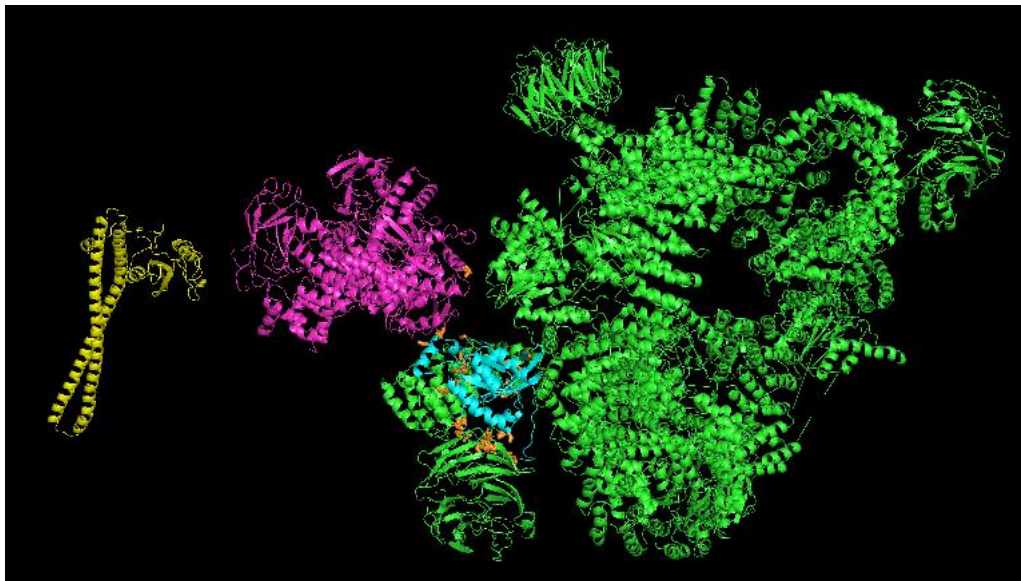
A. – to – F. mTORC1 dockings, G. – to – L. mTORC2 dockings. In parts A., B., C., G., H., and I., the possible interaction is tested on mTOR binding. In parts D., E., and F., the possible contact protein is RAPTOR, and in parts J., K., and L. RICTOR.

A.

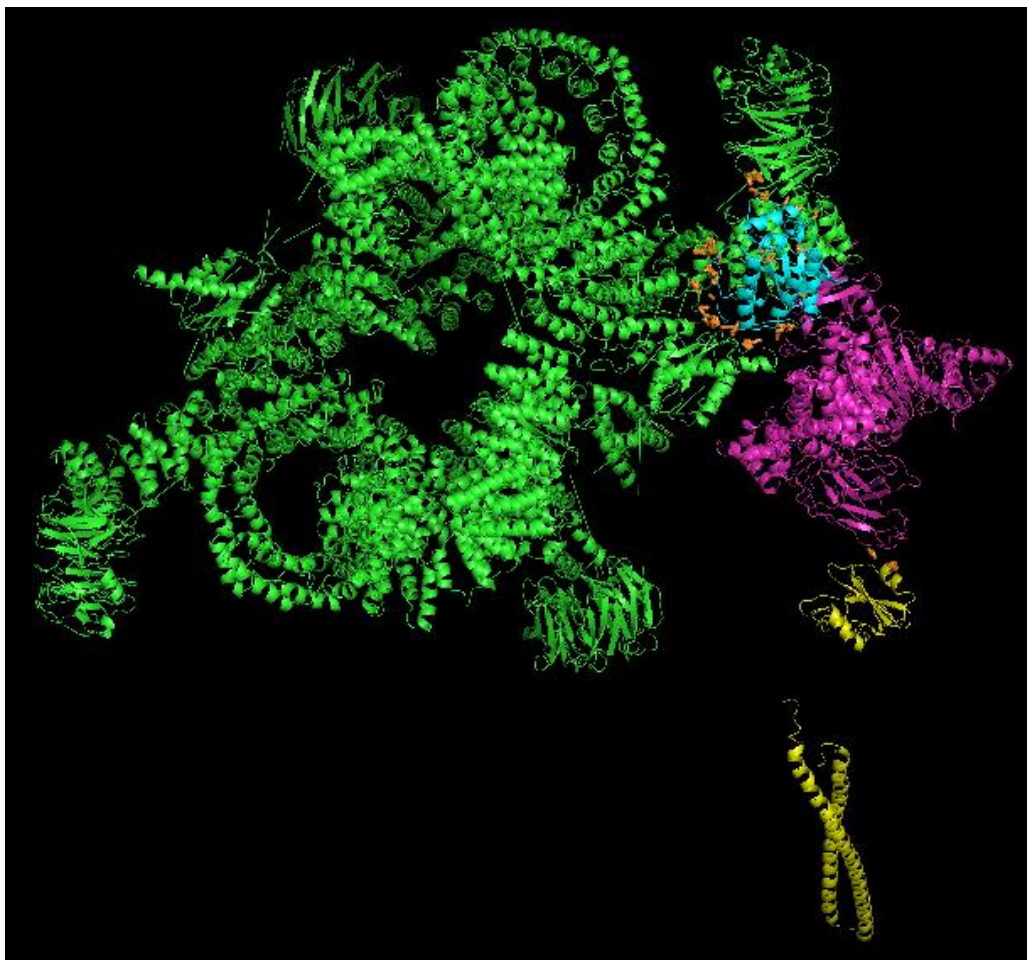


HADDOCK Score: 2037.5 +/- 23.6

B.



C.



HADDOCK Score: 2076.3 +/- 23.5

D.

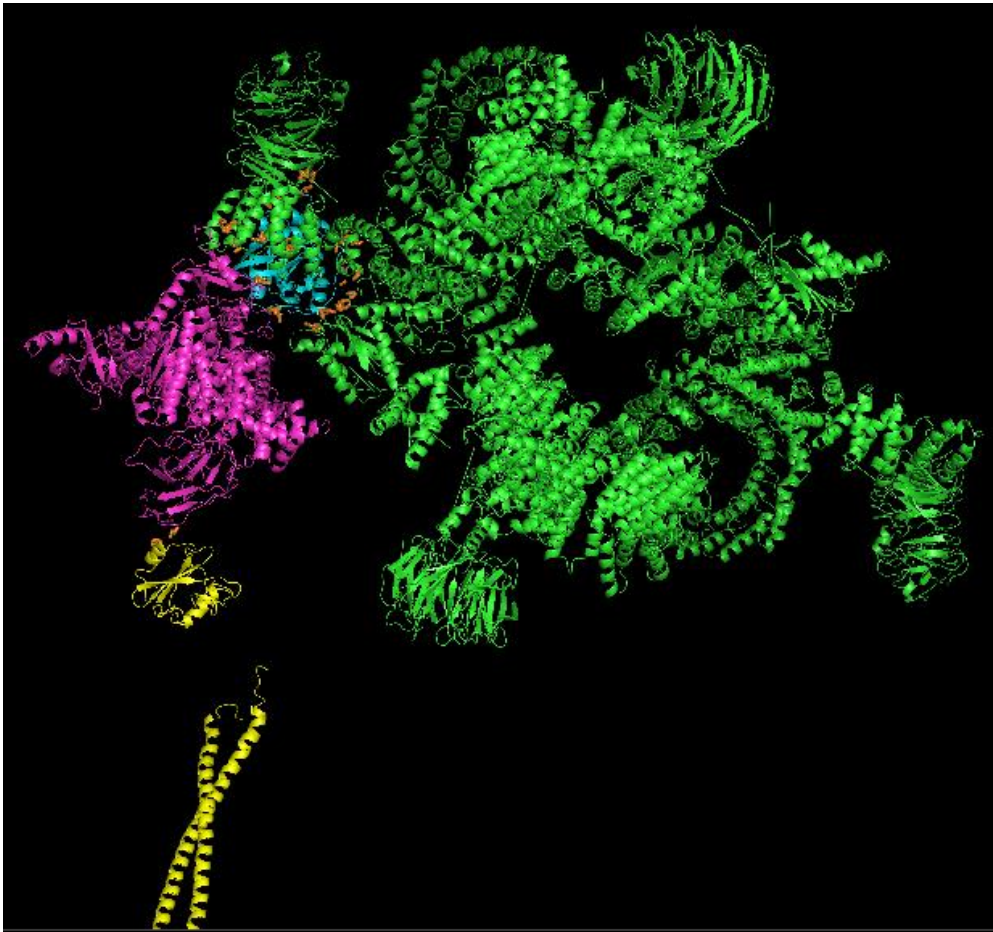
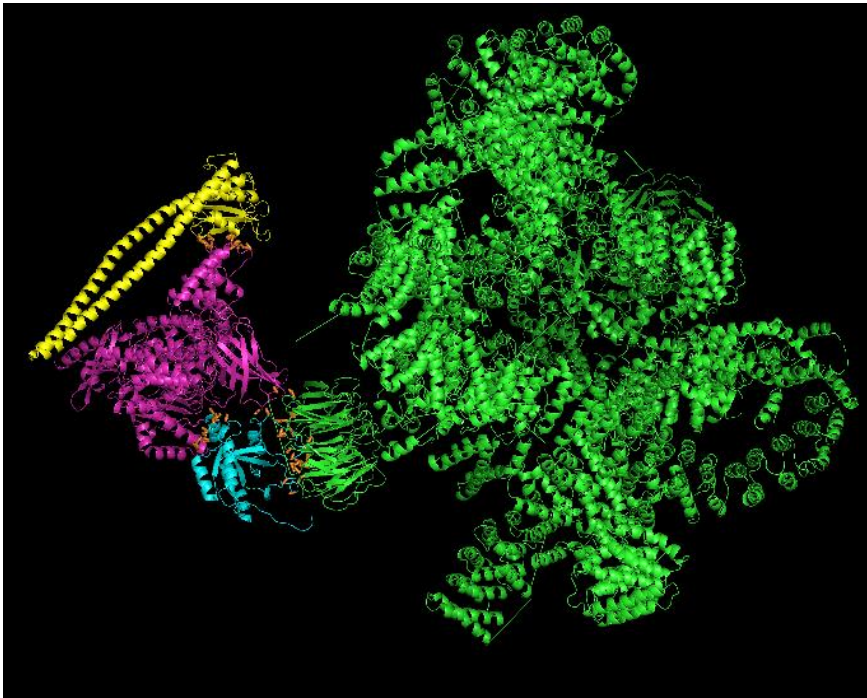


**Figure 4.10** The successful docking runs predicted a possible scaffold function of p110β.

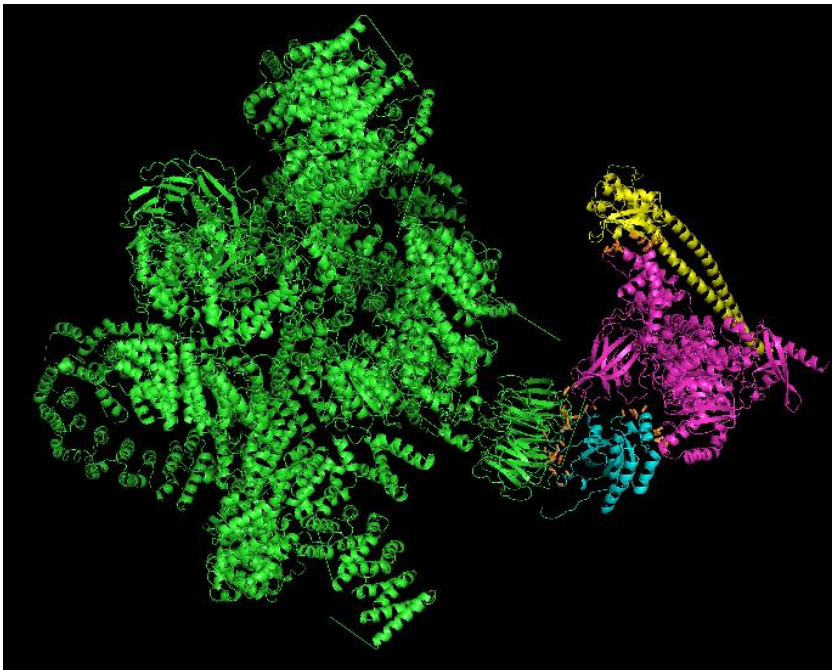
A and B. Green: mTORC1, Blue: Rac1, Pink: p110β, Yellow: niSH2 domain of p85α, Orange: Any contact between chains within 3.0 Å. The binding of p110β and Rac1 is facilitated on mTOR. A and B are the same complex, but turned 180° around y axis, showing the back of the same complex. C and D. Green: mTORC1, Blue: Rac1, Pink: p110β, Yellow: ciSH2 domain of p85α, Orange: Any contact between chains within 3.0 Å. The binding of p110β and Rac1 is facilitated on mTOR. C and D are the same complex, but turned 180° around y axis, showing the back of the same complex. The images were generated in PyMOL.

A.

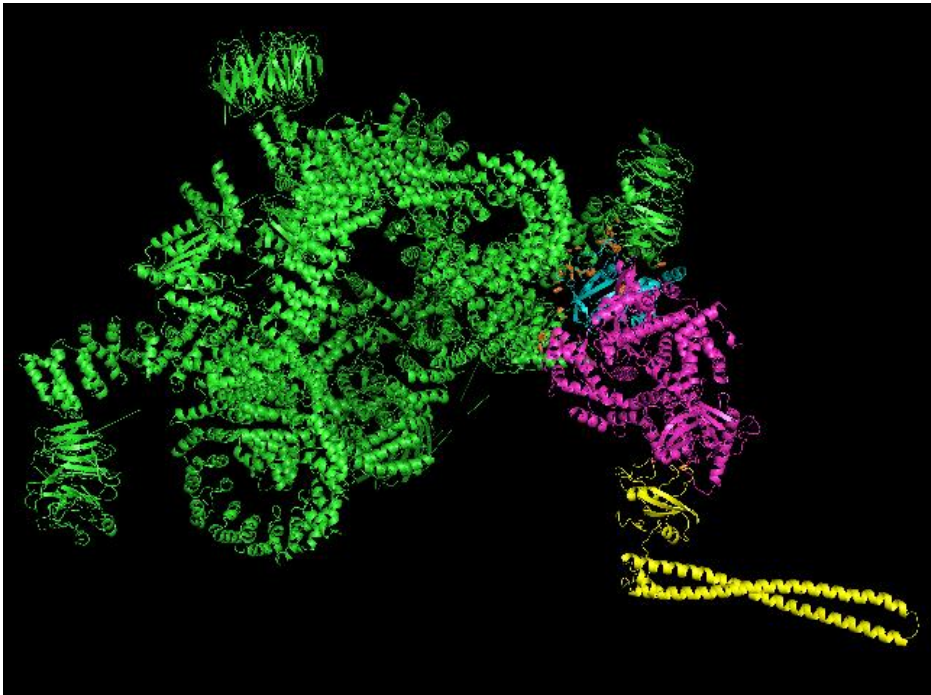


HADDOCK Score: 371.6 +/- 11.5

B.



C.



HADDOCK Score: 2151.9 +/- 40.0

D.

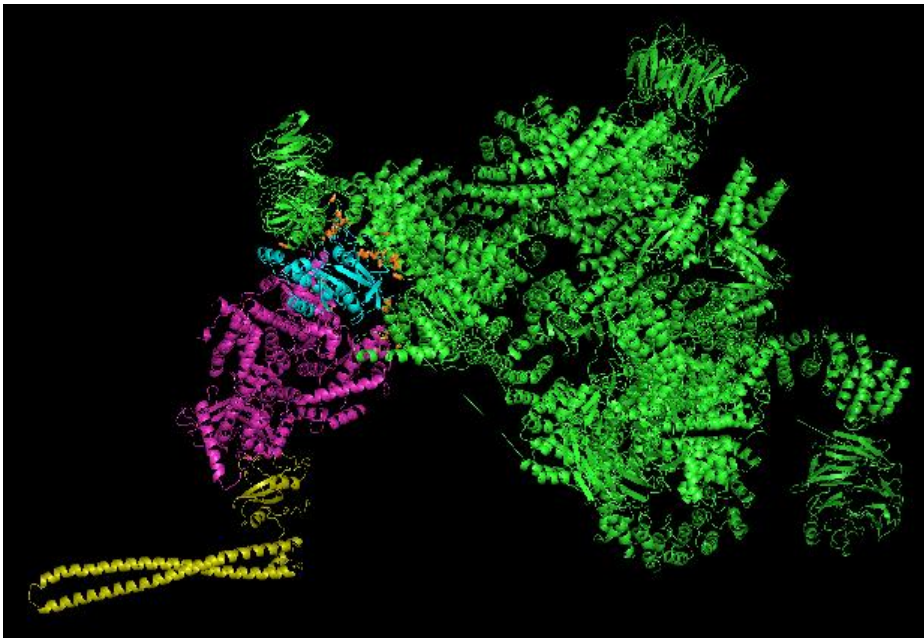


**Figure 4.11** The successful docking runs predicted a possible scaffold function of p110 $\alpha$ .

A and B. Green: mTORC2, Blue: Rac1, Pink: p110 $\alpha$ , Yellow: niSH2 domain of p85 $\alpha$ , Orange: Any contact between chains within 3.0 Å. The binding of p110 $\alpha$  and Rac1 is facilitated on RICTOR. A and B are the same complex, but turned 180° around y axis, showing the back of the same complex. C and D. Green: mTORC1, Blue: Rac1, Pink: p110 $\alpha$ , Yellow: ciSH2 domain of p85 $\alpha$ , Orange: Any contact between chains within 3.0 Å. The binding of p110 $\alpha$  and Rac1 is facilitated on RAPTOR. C and D are the same complex, but turned 180° around y axis, showing the back of the same complex. The images were generated in PyMOL.

It is important to note that p110 $\beta$  had interactions with mTOR. In figure 4.11 parts A and B, p110 $\beta$  is bound by p85 $\alpha$  niSH2 domain, and in parts C and D, it is bound by p85 $\alpha$  ciSH2 domain. As their HADDOCK scores are positive, it indicates the complex was formed without using the defined restraints. In those restraints, we used RAPTOR sites to be involved in binding. When the residues that are involved in interaction were checked, they were on mTOR, not RAPTOR. It shows that there are different residues partaking in interactions that were not noted in the literature yet.

We observed that cSH2 domain of p85 $\alpha$  did not interfere with the binding, but nSH2 domain of p85 $\alpha$  hampered the complex formation. It could be the reason why we observed the scaffolding function to be specific to isoform p110 $\beta$  only. p110 $\alpha$  is stabilized only by p85 $\alpha$  nSH2 domain, and inter region interferes with biologically relevant complex formation, in Table 4.2.<sup>31</sup>

We were able to obtain two docking simulations for p110 $\alpha$ . Because their HADDOCK Scores are also positive, the restraints we used as input were not fitting. In addition, these complexes are not biologically relevant as we didn't observe a retaining signal of phospho-mTOR after catalytically inhibiting p110 $\alpha$  in figure 4.4. Or, the complex is formed in another orientation where other facilitators like RNAs and proteins that we didn't identify are also present, and shaping the interactions in the complexes.

#### **4.5 Genotoxic Stress Sensitivity**

We observed that WT MEFs and MEFs with activated p110 exogenous expression have different patterns of phosphorylated Akt substrates (Figure 4.3). We deduced that the outcome of these phosphorylated substrates could be apoptosis inhibition and increase in

cellular survival, or elevated rate of cycling. These substrates were activated in constitutively activated p110 $\beta$  MEFs. We addressed the possible difference in sensitivity to apoptosis by 2D growth assays, in which the cells were treated with two different genotoxic stressors, doxorubicin and cisplatin.

#### 4.5.1 Doxorubicin – Induced Genotoxic Stress

A.

Cell Line	IC50 ( $\mu$ M)
WT MEFs	43.4281
Myr_ $\alpha$ MEFs	28.8463
Myr_ $\beta$ MEFs	20.0437
Myr_ $\delta$ MEFs	46.7041
Myr_Akt1 MEFs	24.8971

B.

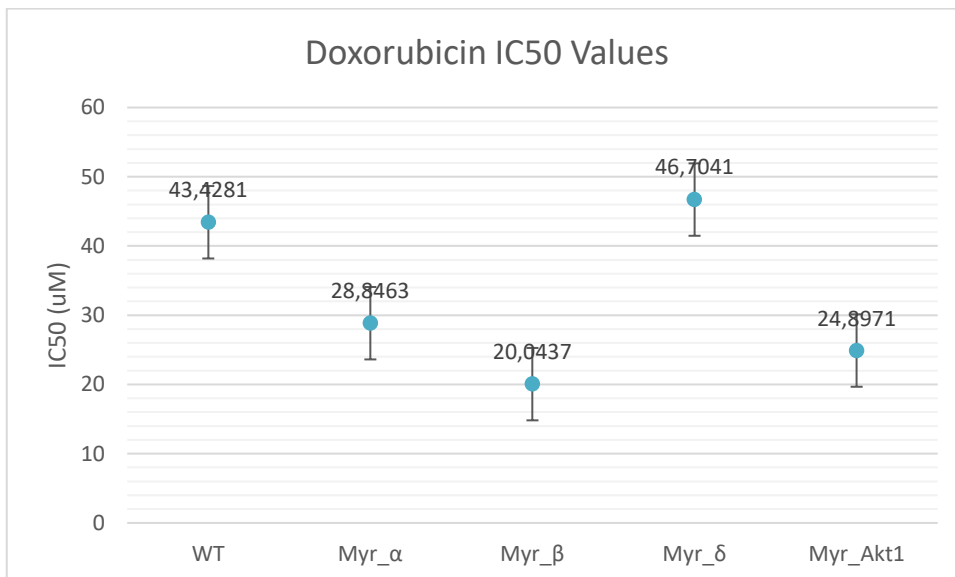


**Figure 4.12 Doxorubicin sensitivities of WT MEFs and MEFs expressing activated p110s exogenously.**

A. IC50 values of each cell line has been calculated from dose – response curves. B. Depiction of IC50 values per cell line. WT MEFs are used as baseline control and myristoylated Akt1 MEFs are used as positive control.

In figure 4.3, we observed increased Akt activity, which could lead to inhibition of apoptosis, cell survival, and progression of cell cycle<sup>34</sup> in myristoylated p110 $\beta$  MEFs. Myristoylated p110 $\beta$  cell line has the lowest IC50, indicating that it is the most sensitive cell line to genotoxic stress induced by Doxorubicin treatment. It is followed by myristoylated Akt1, myristoylated p110 $\alpha$ , and WT cells. Myristoylated p110 $\delta$ , which is the least sensitive cell line to doxorubicin, has an IC50 of 46.70  $\mu$ M, which is more than double of that of myristoylated p110 $\beta$ . These results suggest that putative list including apoptosis inhibition and cell survival proteins in figure 4.3 does not account for the genotoxic sensitivity. The reason of sensitivity for genotoxic stress in myristoylated p110 $\beta$  cells can be explained by increment in Akt activity, as it leads to progression of cell cycle.<sup>34</sup> We reason that increased sensitivity for doxorubicin in myristoylated p110 $\beta$  MEFs is because they cycle more.

#### 4.5.2 Cisplatin – Induced Genotoxic Stress

A.

Cell Line	IC50 ( $\mu$ M)
WT MEFs	0.4594
Myr_ $\alpha$ MEFs	0.3889
Myr_ $\beta$ MEFs	0.2056
Myr_ $\delta$ MEFs	1.4837
Myr_Akt1 MEFs	0.4865

B.

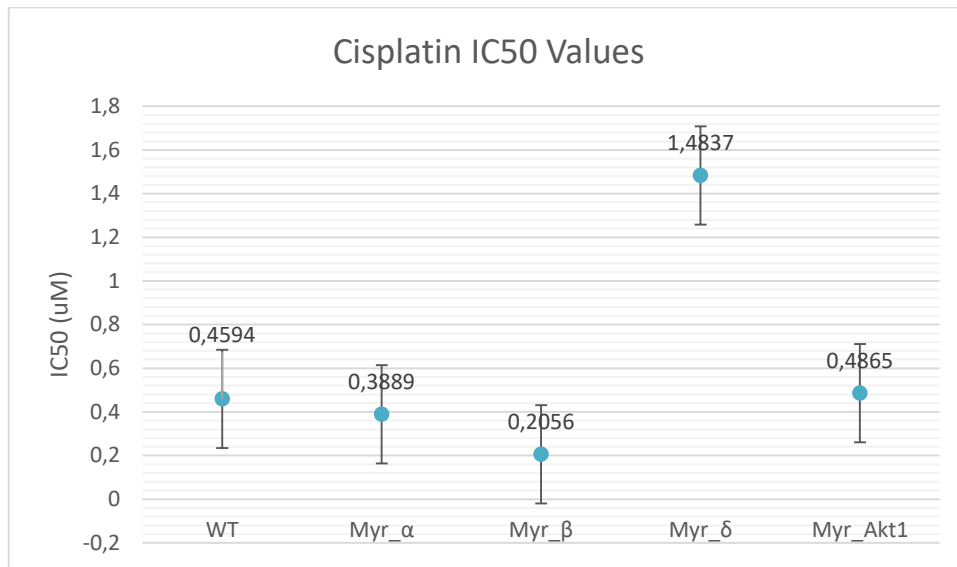


**Figure 4.13 Cisplatin sensitivity of WT MEFs and MEFs expressing activated p110s ectopically.**

A. IC50 values of each cell line has been calculated from dose – response curves. B. Depiction of IC50 values per cell line.

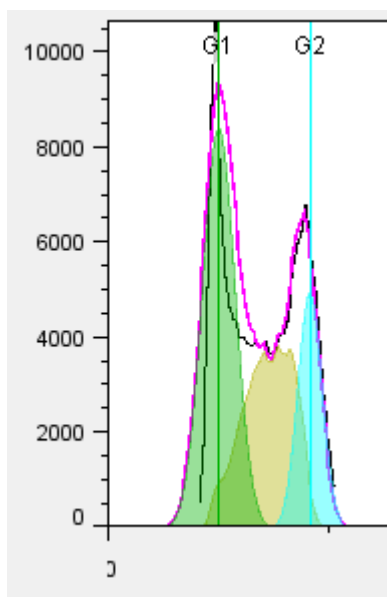
We wanted to investigate the same question as doxorubicin treatments; whether we can hold increased Akt activity in figure 4.3 responsible for resistance to apoptosis or increase in cycling rate by inducing genotoxic stress. Myr\_β cell line has the lowest IC50, which indicates that myristoylated p110β expressing cell line is the most sensitive cell line to genotoxic stress induced with Cisplatin. Myristoylated p110δ has the highest IC50 value that is more than seven times that of myristoylated p110β MEFs. These results are in line with doxorubicin part, which indicate that increase in cell cycle regulatory protein activity in myristoylated p110β MEFs lead to genotoxic sensitivity.

To summarize, in both genotoxic stress conditions, myristoylated p110β MEFs have been observed to be the most sensitive cell line, and myristoylated p110δ MEFs are the least sensitive one. We infer that activated Akt substrates (Gsk3a, Cot, and Chk1) as could be one of the reasons of increase in cycling rate in myristoylated p110β MEFs.

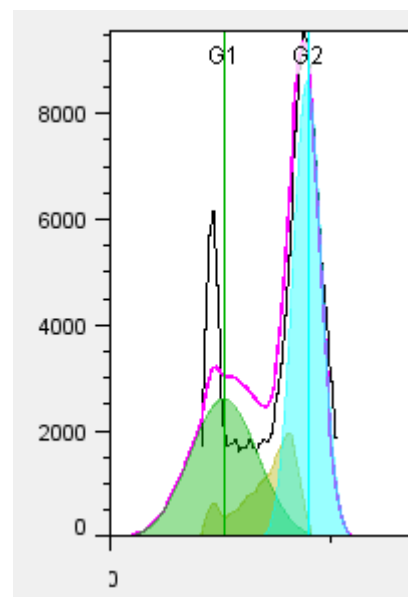
#### 4.6 Cell Cycle Analysis of MEFs Overexpressing p110s

Myristoylated p110 $\beta$  expressing MEFs had the highest level of phosphorylated Akt substrates (Figure 4.3, part A) and they had the highest signal of Ser473 phosphorylated Akt (Figure 4.2). In addition, the same cell line has shown the most sensitivity for genotoxic stress (Figures 4.12 and 4.13). We reasoned the fact that myristoylated p110 $\beta$  MEFs are the most sensitive cell line because they cycle faster than other cell lines. To address that hypothesis, we analysed cell cycle kinetics of  $\alpha,\beta$   $+/+$  Cre HA p110 $\alpha$  (HA Alpha), and  $\alpha,\beta$   $+/+$  Cre HA p110 $\beta$  (HA Beta) MEFs.

A.



B.



C.

	HA Alpha	HA Beta
G1	45.25%	35.33%
S	35.04%	16.36%
G2	19.70%	48.29%

**Figure 4.14 Cell cycle analysis of HA Alpha and HA Beta MEFs exhibits different cell cycle kinetics.**

The cells were fixed with 70% EtOH and stained by PI. A. HA Alpha MEFs, B. HA Beta MEFs. C. Percentage of population in different cell cycle phases derived from panels A and B. In each analysis, more than 60 000 cells were counted. Data analyzed in FlowJo.

We wanted to address our hypothesis that whether myristoylated p110 $\beta$  MEFs are cycling faster than other MEFs. In order to investigate that question, we analyzed cell cycle kinetics of WT, HA Alpha and HA Beta MEFs. We used WT MEFs' gates in other two MEFs. We observed that the cell population in G2-M phase of HA Beta MEFs are the largest. These results indicate that HA Beta MEFs having the largest population of G2-M phase, more mitotic and faster cycling cells might be more prone to genotoxic insults.

#### **4.7 Investigation of Non-Canonical Functions of p110 $\beta$**

Myristoylated p110 $\beta$  MEFs have shown increased Akt phosphorylation on residue Ser473 in comparison to the other cell lines when treated with 4% FBS (Figure 4.2). Phosphorylation on that site was erased when myristoylated p110 $\beta$  MEFs treated with their isoform selective catalytic inhibitor, KIN 193. (Figure 4.4, lane 4). In figure 4.4, lane 4, phosphorylation of residue Ser 2448 of mTOR, which is a marker for pathway activity, was not erased even though myristoylated p110 $\beta$  cells were treated with KIN193. To address a possible scaffold function of p110 $\beta$ , WT and myristoylated p110 $\alpha$  and p110 $\beta$  cells were treated with Rac1 catalytic inhibitor EHT 1864 and mTOR inhibitor Rapamycin.

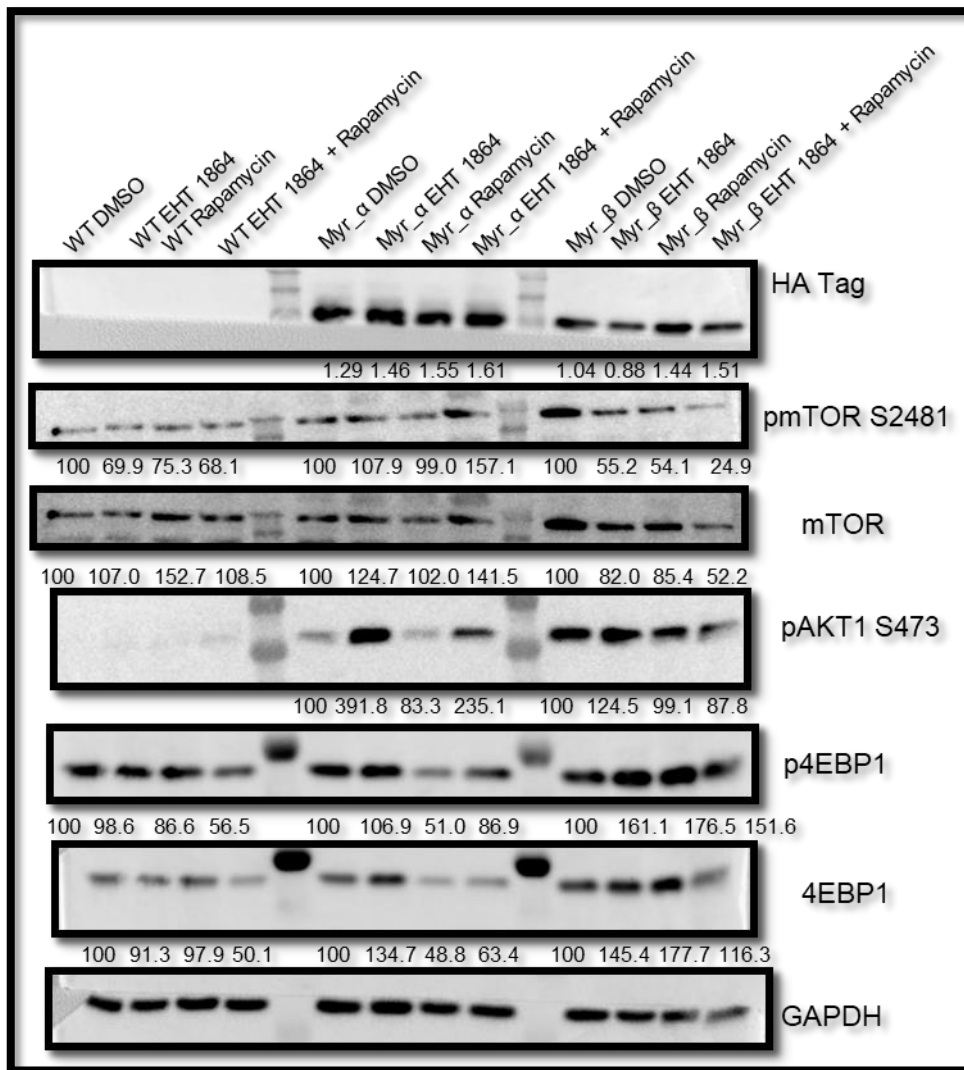


**Figure 4.15 Biochemical investigation of scaffold function of activated p110 $\beta$ .**

Western Blot. HA Tag antibody was used to quantify protein levels of myristoylated p110 constructs that were tagged with HA. The cells were treated with 4% FBS. EHT 1864 was used in 5  $\mu$ M, and Rapamycin was used in 100 nM for 2 hours. Each well was loaded with 30  $\mu$ g protein lysate. The numbers below the blots are normalized signal intensities quantified in ImageJ software. In normalization, DMSO value of each cell line for every antibody was normalized to 100.

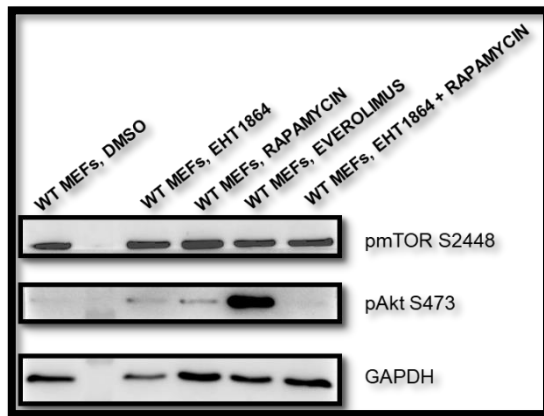
Rapamycin is shown to inhibit mTORC1 in acute treatments (2 hours), and it starts to inhibit mTORC2 in long term treatments (24 hours).<sup>72</sup> So, in this experimental setup, Rapamycin inhibits only mTORC1. As expected, when cells were treated with Rapamycin, phospho-mTOR levels were decreased in comparison to the control

treatments. Phospho-Akt Ser473, which is a target of mTORC2, did not change when mTORC1 was inhibited by Rapamycin, as expected.

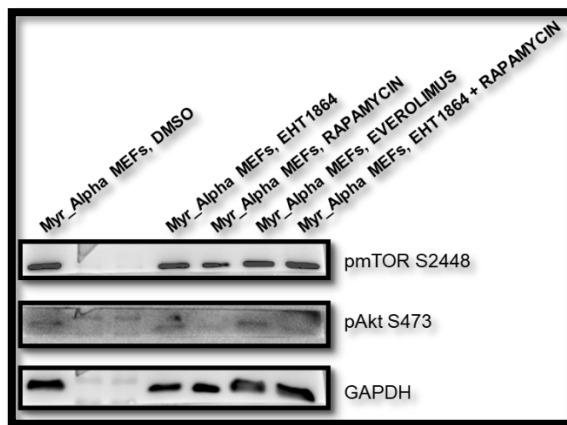
To investigate whether the possible scaffolding function of p110 $\beta$  is mediated via Rac1, WT and myristoylated p110 $\alpha$  and p110 $\beta$  MEFs were treated with the inhibitors above for two hours, and autophosphorylation signals of mTOR (residue Ser 2481) and Ser473 phosphorylation signals of Akt as a output of mTORC2 activity were monitored. EHT 1864 was used to catalytically inhibit Rac1. In myristoylated p110 $\beta$  MEFs, phospho-mTOR signal was higher in concordance with higher phospho-Akt Ser473 levels. Strikingly, catalytic inhibition of Rac1 show decreased phosphorylation of mTOR in myristoylated p110 $\beta$  expressing MEFs, and not in myristoylated p110 $\alpha$  or WT MEFs. In parallel with the hypothesis that p110 $\beta$  facilitating mTOR phosphorylation, it shows that Rac1 facilitates mTORC1 phosphorylation only in the presence of p110beta. mTORC2 was not affected by EHT 1864 treatment in myristoylated p110 $\beta$  MEFs as pAkt Ser473 levels did not decrease upon EHT 1864 treatment. The fact that mTORC2 activity was not decreased upon Rac1 inhibition shows that p110 $\beta$  has a function in autophosphorylation of mTOR in mTORC2. Another interesting point to highlight is the fact that phospho-Akt Ser473 levels increased when myristoylated p110 $\alpha$  MEFs were treated with Rac1 catalytic inhibitor EHT 1864. It might implicate that Rac1 is inhibitory for mTORC2 activity in the absence of an associated p110beta. Thus, p110 $\beta$  could be facilitating a scaffolding function where autophosphorylation of mTORC2 is mediated and tuned by Rac1 activity. Rac1 was also observed to be partaken in mTOR translocation to membrane in order to localize and regulate the activity of mTORC1 and mTORC2.<sup>71</sup>

To investigate whether p110 $\beta$  scaffolding function is also mediating phosphorylation of the residue Ser2481, marking pathway activity, was investigated upon long term treatment with the same inhibitors. To that end, EHT 1864 was utilized to inhibit Rac1, Rapamycin was used to inhibit mTORC1 and 2, and the FDA approved rapalog, Everolimus to inhibit mTORC1 as positive controls.

A.



B.



C.

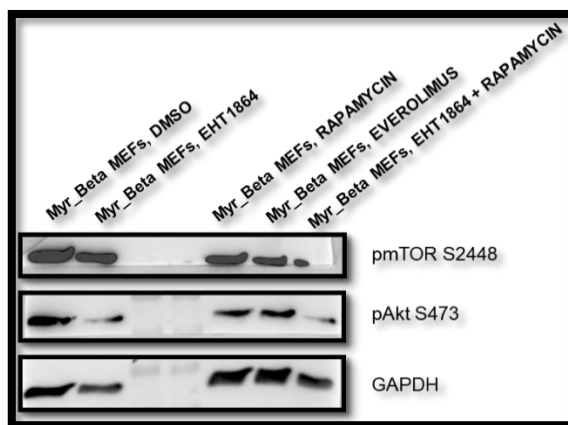


Figure 4.16 Scaffolding function of p110 $\beta$  on mTORC2 activity is tuned by Rac1.

MEFs were treated with 4% FBS. 5  $\mu$ M EHT 1864, 100 nM Rapamycin, and 50 nM Everolimus were used in long term treatments before harvesting cells. Each well contains 30  $\mu$ g protein lysate. A. WT MEFs, B. Myristoylated p110 $\alpha$  MEFs, C. Myristoylated p110 $\beta$  MEFs.

As expected, in WT MEFs and myristoylated p110 $\alpha$  MEFs did not show any change in their phospho-Akt Ser 473 levels when treated with EHT 1864. Phospho-Akt Ser473 levels were significantly decreased in myristoylated p110 $\beta$  MEFs upon upon EHT 1864 treatment. On the other hand, phosphorylation of mTOR was not reduced to the extent of the signal in myr-p110alpha MEFs less upon rapamycin treatments. This could be explained by the participation of p110beta in functional mTOR complexes keeping the the kinase active in response to the allosteric inhibitor rapamycin. Rac1 and mTORC1 inhibitor combination in all experimental samples diminished p-AKT signal considerably, implicating the critical role of Rac1 activity to maintain the competence of mTOR in phosphorylating AKT.

#### **4.8 Migration Kinetics of Activated p110s**

As mTORC2 and Rac1 are known cytoskeleton regulators, the scaffolding function of p110 $\beta$  was investigated on migration.<sup>73</sup> To do that, wound healing assay was performed on WT MEFs, myristoylated p110 $\alpha$  and myristoylated p110 $\beta$  MEFs with different inhibitors.

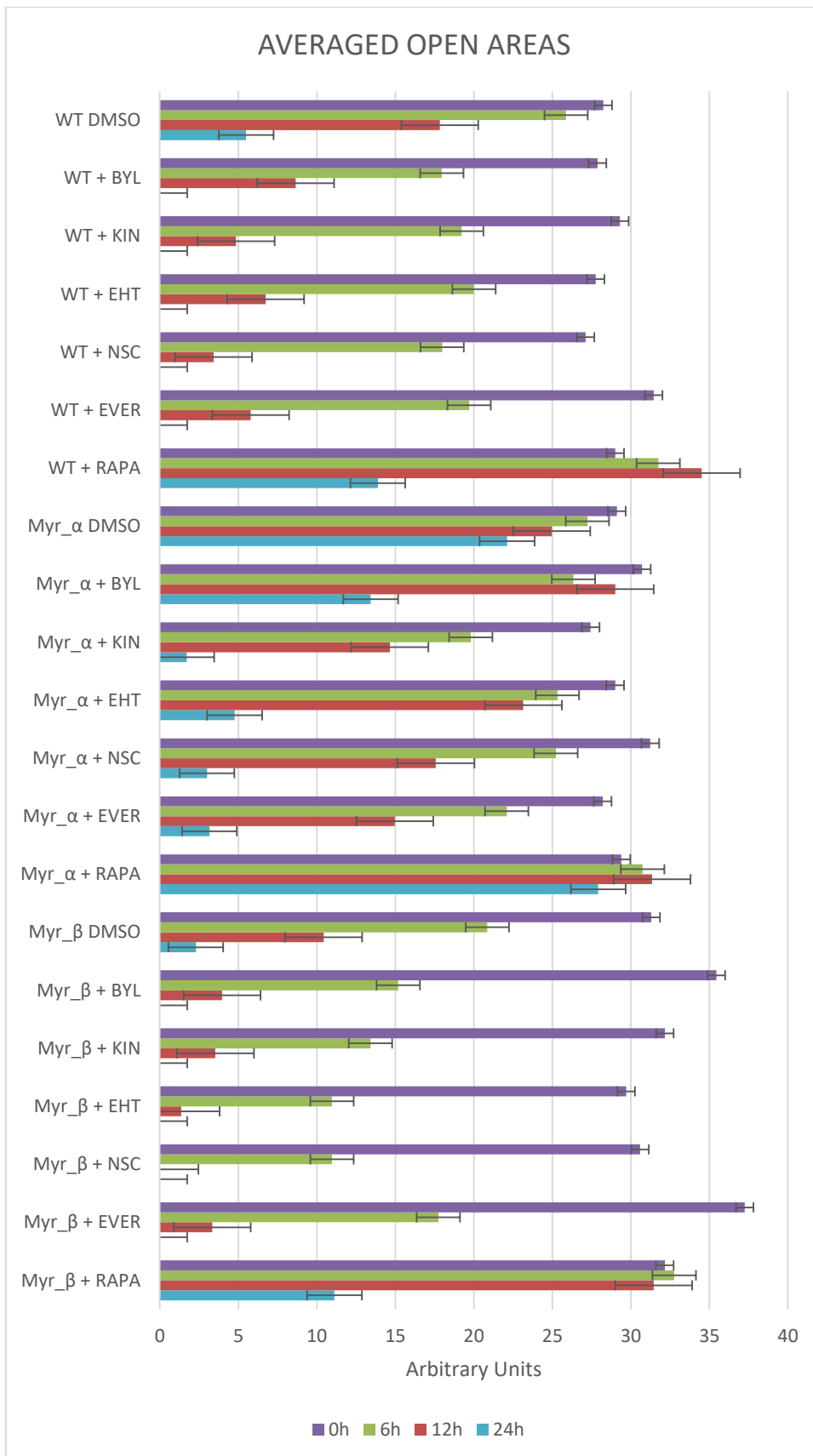


**Figure 4.17 Migration kinetics of WT and constitutively activated p110 $\alpha$  and  $\beta$  MEFs.**

The cells were treated just after scratches with inhibitors. BYL (BYL 719, p110 $\alpha$  inhibitor, 1  $\mu$ M), KIN (KIN 193, p110 $\beta$  inhibitor, 1  $\mu$ M), EHT (EHT 1864, Rac1 catalytic inhibitor, 5  $\mu$ M), NSC (NSC23766, inhibition of Rac1 interaction with its GEFs, 50  $\mu$ M), EVER (Everolimus, mTORC1, 50 nM), RAPA (Rapamycin, mTORC1 and mTORC2, 100 nM). WT MEFs were used as baseline control. The photos were analyzed by TScratch software.

In figure 4.17, in all cell lines, mTORC2 inhibition by rapamycin has blocked migration of cells, meaning that mTORC2 mediates cytoskeleton rearrangements, and the scaffold function of p110 $\beta$  that was previously observed in figure 4.15 does not specifically regulate migration. As shown in recent literature, p110 isoforms are not directly involved in migration.<sup>74</sup> Rather, small G proteins like Rac1 and Cdc42 have been shown to regulate directional migration.<sup>75</sup> On the other hand, at 24 hour timepoint, myristoylated p110 $\alpha$  MEFs had the most open area in EHT 1864 treatment, in comparison to p110 $\beta$  competent cell lines, WT and myristoylated p110 $\beta$  MEFs. That points out the fact that Rac1 catalytic activity is a non-redundant cytoskeleton regulator in myristoylated p110 $\alpha$  MEFs, and p110 $\beta$  competent cells can tolerate Rac1 catalytic inhibition, as mTORC2 and Rac1 have been shown to have redundant effects on cytoskeleton regulation in migration.<sup>76</sup>

## Chapter 5

### 5. Discussion

PI3K signaling induces Akt phosphorylations on T308 and S473 residues.<sup>61</sup> Thus, it is expected to observe increased phospho-Akt S473 phosphorylation in myristoylated p110 MEFs in comparison to WT MEFs. Although p110 $\alpha$  is the major isoform in transducing PI3K signaling,<sup>35</sup> we observed the highest phosphorylation levels in myristoylated p110 $\beta$  MEFs. Although Akt is first phosphorylated on T308, and then S473, S473 site is not always an indicative of fully activated Akt.<sup>61</sup> Instead, those phospho-residues may indicate phosphorylation of different Akt substrates. E.g, Akt T308 phosphorylation has been shown to be enough for glucose uptake through Glut4 receptor in fat and muscle cells upon insulin stimulation, but other cell types may require S473 phosphorylation mediated by mTORC2 for Glut1 recruitment.<sup>77</sup> The fact that p110 $\alpha$  mostly signals downstream of RTKs and p110 $\beta$  is acting downstream of GPCRs, different levels of Akt S473 phosphorylation by p110 $\alpha$  and p110 $\beta$  may point to their different but complementary roles in cellular physiology.<sup>35</sup>

The main mTOR phosphorylation sites we have studied are Ser2448 and Ser 2481. Ser2448 phosphorylation is one of the PI3K pathway activation markers, as Ser2448 phosphorylation is shown to be mediated by p70S6K, and p70S6K1 is activated by Akt. Rapamycin inhibits Ser2448 phosphorylation of mTOR in short term treatment.<sup>78</sup> Ser2481 phosphorylation on the other hand, depicts mTOR autophosphorylation. It is a measure of mTOR catalytic activity.<sup>79</sup> As Ser2481 phosphorylation depends on PI3K activity, Ser2481 phosphorylation is upstream of Ser2448 phosphorylation.<sup>80</sup> In our investigations, we evaluated both phosphorylation sites. In figure 4.14, we observed mTOR Ser2481 phosphorylation decreasing after Rac1 catalytic inhibition by EHT 1864, only in myristoylated p110 $\beta$  MEFs. This suggests that Rac1 and p110 $\beta$  interaction is facilitating the scaffolding function of p110 $\beta$ , and this function maintains mTOR activity. In figure 4.4, we investigated effects of catalytic activity of p110 $\alpha$  and p110 $\beta$  with respect to mTOR Ser 2448 phosphorylation. We observed that p110 $\beta$  exhibits non canonical function promoting Ser2448 phosphorylation of mTOR.. It indicates p110 $\beta$  could be sustaining mTOR activity without a requirement for its catalytic activity. In figure 4.16

part C, we demonstrate the same effect by inhibiting both mTORC1 and mTORC2 by long term Rapamycin treatments, and showing that Akt S473, the mTORC2 phosphorylation site, is still phosphorylated. This indicates that the non-canonical function of p110 $\beta$  may entail scaffolding of the mTOR complex. Followed by S473 phosphorylation, Akt phosphorylates p70S6K1, and p70S6K1 phosphorylates mTOR, and mTORC1 phosphorylates 4EBP1. In figure 4.14, 4EBP1 phosphorylation is retained when myristoylated p110 $\beta$  MEFs are treated with rapamycin for short-term, likewise S473 phosphorylation on Akt, in myristoylated p110 $\beta$  MEFs. This indicates that p110 $\beta$  mediates autophosphorylation of mTOR independent of complex specificity. We were able to simulate a possible complex formation in HADDOCK, in figure 4.10.

We observed Src phosphorylation only in MEFs with intact p110 $\beta$  in figure 4.6. It needs to be investigated whether Src phosphorylation is mediated by p110 $\beta$  catalytic activity by using p110 $\beta$  specific inhibitor KIN 193. In addition to role of p110 $\beta$  facilitating Src phosphorylation by acting as a scaffold,<sup>66</sup> it could be a readout for GPCR internalization,<sup>81</sup> and followed by autophagy.<sup>49</sup> When insulin signaling is activated, Akt phosphorylates  $\beta$ 2-adrenergic receptor on Tyr350. This phosphorylation has been depicted as an anchor for SH2 domain-containing proteins, such as c-Src,<sup>81</sup> and p85.<sup>10,31</sup> p110 $\beta$  is one of the possible actors in Src autophosphorylation through its scaffolding function,<sup>66</sup> and autophosphorylation of Src leads to receptor internalization.<sup>81</sup> It could be another mechanism to keep the glucose, favouring anabolism over catabolism, until the internalized receptor is degraded in autophagy. In addition, in that scenario, it is expected for mTORC1 to be activated to favour anabolic reactions where cellular nutrients are synthesized, and to allow autophagy,<sup>40</sup> which could be facilitated by p110 $\beta$  – mediated Src phosphorylation.

Rac1 binds to mTOR, RAPTOR, and RICTOR by its RKR motif on C – terminal tail.<sup>71</sup> To simulate the p110 $\beta$  scaffolding function, we used HADDOCK to perform protein – protein dockings. To our surprise, we were able to simulate conditions with mTORC1 and p110 $\beta$  only. The input parameters we used included RAPTOR to be bound by Rac1, as in schematic representation in figure 4.9 part B. As we received a positive HADDOCK score, the restrictions we have given have not been used by the system, and the system predicted the binding to be facilitated by mTOR, as in figure 4.9 part A. In addition,

HADDOCK also predicted that p110 $\beta$  could be interacting with mTOR as well. The predicted residues underlies the scaffold generated by p110 $\beta$ .

In scaffolding function of p110 $\beta$ , Rac1 catalytic activity is required as inhibition of Rac1 catalytic activity by EHT 1864 results in decrease in mTOR phosphorylation (figures 4.4, 4.15, and 4.16). In literature, Rac1 binding to mTOR is depicted as independent of Rac1 catalytic activity by using NSC23766.<sup>71</sup> NSC23766 works by blocking the interaction of Rac1 with some of its GEFs.<sup>82</sup> In that paper, the authors have used NSC23766 in 10  $\mu$ M,<sup>71</sup> which is quite low in comparison to the effective dose, being 50  $\mu$ M.<sup>83</sup> We show that Rac1 catalytic activity is required for non-canonical functions of p110 $\beta$  in EHT 1864 treated samples, where Rac1 is induced to release its bound nucleotide.<sup>82</sup>

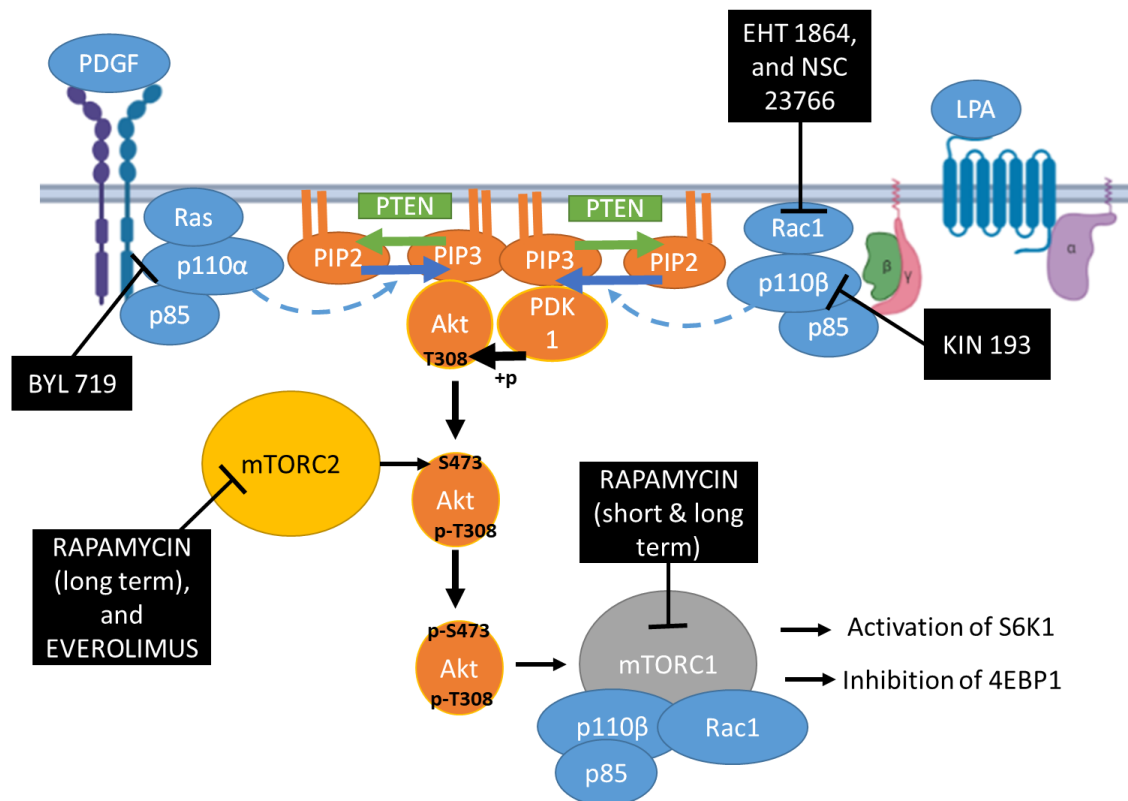
p110 $\beta$  has been reported to have different scaffolding functions in the literature.<sup>78</sup> p110 $\beta$  ablation in mice livers has shown p110 $\beta$  has kinase – independent function in insulin metabolism, as Akt phosphorylation persisted. In addition, p110 $\beta$  kinase – independent function is involved in cellular trafficking and proliferation.<sup>63</sup>

In addition, p110 $\beta$  regulates cell cycle by controlling DNA replication elongation. Prenylated p110 $\beta$  cells were reported to terminate S phase faster than activated p110 $\alpha$  cells,<sup>84</sup> resulting in more prenylated p110 $\beta$  cells in G2 phase. We observed more p110 $\beta$  overexpressing MEFs than p110 $\alpha$  overexpressing MEFs in G2 phase in figure 4.13. In addition, MEFs that overexpress p110 $\alpha$  lack p110 $\beta$ , so more p110 $\alpha$  MEFs are captured in S phase than p110 $\beta$  MEFs. In addition, another mechanism involving mTORC1 and Wnt pathway has been proposed to regulate cell cycle. In this mechanism, mTORC1 inhibition of autophagy results in rescue of Dvl, and Wnt pathway activation. Activated Wnt pathway induces cyclin D1 activity, which results in continuation of cell cycle.<sup>54</sup> As we observed more p110 $\beta$  MEFs in G2 phase in figure 4.14, and p110 $\beta$  having a potential scaffolding function (in figures 4.4, 4.15, and 4.16), in addition to a possible interaction with mTORC1 calculated by HADDOCK (in figure 4.10), the proposed mechanism involving Wnt pathway is physiologically relevant.

We observed very low phospho – Akt signals in myristoylated p110 $\delta$  MEFs in figure 4.2. We showed that the low levels of phospho – Akt is an indicative of low activity by investigating phosphorylation levels of Akt substrates in figure 4.3. In p110 $\delta$ , we

hypothesized that there could be another mechanism involved in survival. To investigate that, we performed a phospho – Tyrosine blot in figure 4.5, depicting a possibility of a JAK protein activated only in myristoylated p110 $\delta$  MEFs. We have found that phospho – STAT3 is phosphorylated the most in myristoylated p110 $\delta$  MEFs in figure 4.7. To address the identity of the JAK protein, we used STRING database. In figure 4.8, the provided networks have shown that only in condition where p110 $\delta$  and STAT3 are input, a whole connectome was able to be formed. In addition, the appeared JAK protein was JAK2, suggesting a possibility of the identity of tyrosine – phosphorylated protein in figure 4.5 to be JAK2. In literature, JAK2 is shown to form a complex with PI3K, Yes, and PP2A,<sup>85</sup> which strengthens our predictions. Still, phospho – JAK2 and immunoprecipitations need to be performed in order to validate these assumptions.

A.



B.

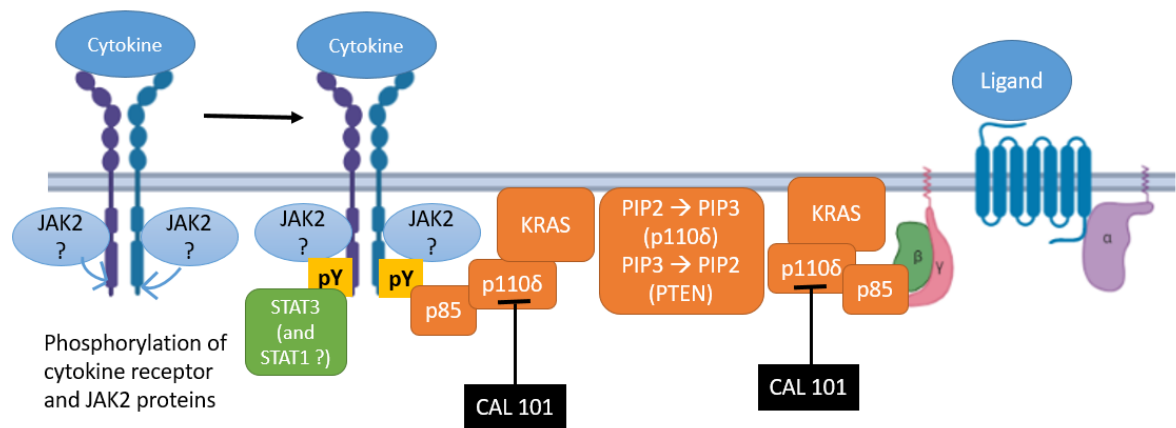


**Figure 5.1 A schematic representation of PI3K pathway and used inhibitors.**

A. PI3K $\alpha$  and PI3K $\beta$ , and B. PI3K $\delta$  signaling mechanisms. In panel A, p110 $\alpha$  is shown to be located downstream of activated RTKs, and p110 $\beta$  is shown to be located downstream of activated GPCRs. In panel B, p110 $\delta$  is shown to be located downstream of activated cytokine receptors and different GPCRs. Black rectangles represent the inhibitors used in this study.

## Chapter 6

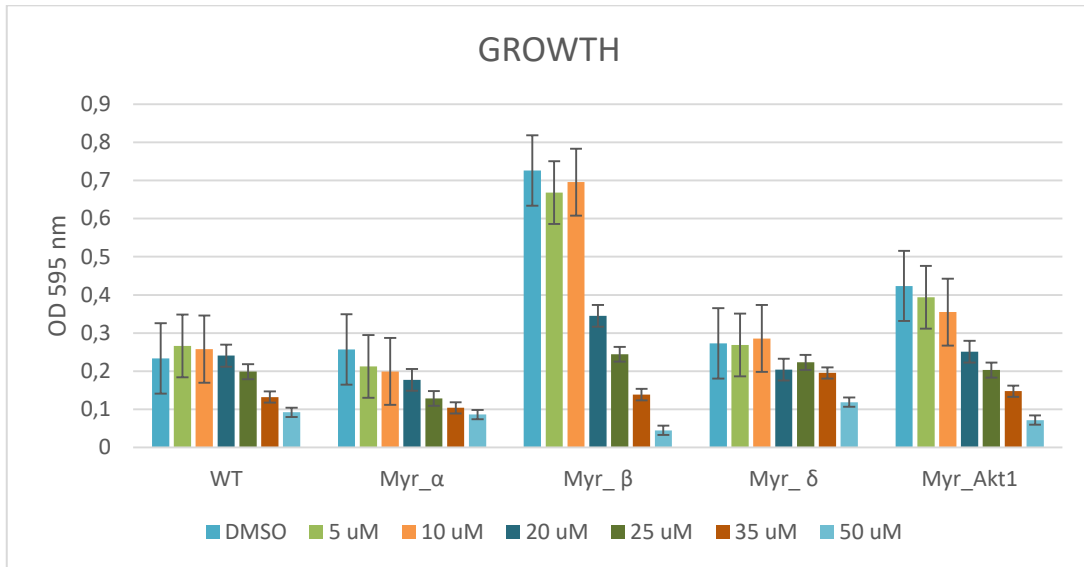
### 6. Conclusion and Future Perspectives

We show that p110 $\alpha$  and p110 $\beta$  has redundant as well as unique functions by exogenously expressing p110 $\alpha$  and p110 $\beta$  on p110 $\alpha$  and p110 $\beta$  knock-out MEF model. We present that p110 $\alpha$ , p110 $\beta$ , and p110 $\delta$  activities distinctly lead to differential Akt Ser473 phosphorylations. As a result, Akt downstream becomes activated with respect to Ser473 levels. As Akt regulates cellular survival, apoptosis, and cell cycle, we investigated which functions of Akt are relevant in our scenario. By using two different chemotherapeutic agents, doxorubicin and cisplatin, we investigated DNA damage – induced apoptosis. The most sensitive cell line is myristoylated p110 $\beta$  MEFs, and myristoylated p110 $\beta$  MEFs had the most activated Akt. As an explanation, we hypothesized that more activated Akt in p110 $\beta$  expressing cells positively effects cell cycle progression. To test that hypothesis, we analysed cell cycles of p110 $\alpha$  and p110 $\beta$  MEFs. We found out that, p110 $\beta$  MEFs have more cells in G2/M population in comparison to p110 $\alpha$  MEFs. Thus, we concluded that genotoxic sensitivity of p110 $\beta$  MEFs is caused by increased cell cycle activity. We discovered a possible p110 $\beta$  kinase – independent function while investigating p110 $\alpha$  and p110 $\beta$  catalytic activities on PI3K downstream effectors. We investigated the components acting in the complex facilitated by p110 $\beta$  scaffold. We found three actors: Rac1, mTOR, and p110 $\beta$ . To investigate the physiological role of that complex, we inhibited p110 $\beta$ , Rac1, and mTOR separately in in vitro wound healing assays. We found that p110 $\beta$  expressing cells can tolerate Rac1 inhibition in migration, but p110 $\alpha$  cannot. This finding shows that myristoylated p110 $\alpha$  MEFs are more dependent on Rac1 activity in migration in comparison to myristoylated p110 $\beta$  MEFs.

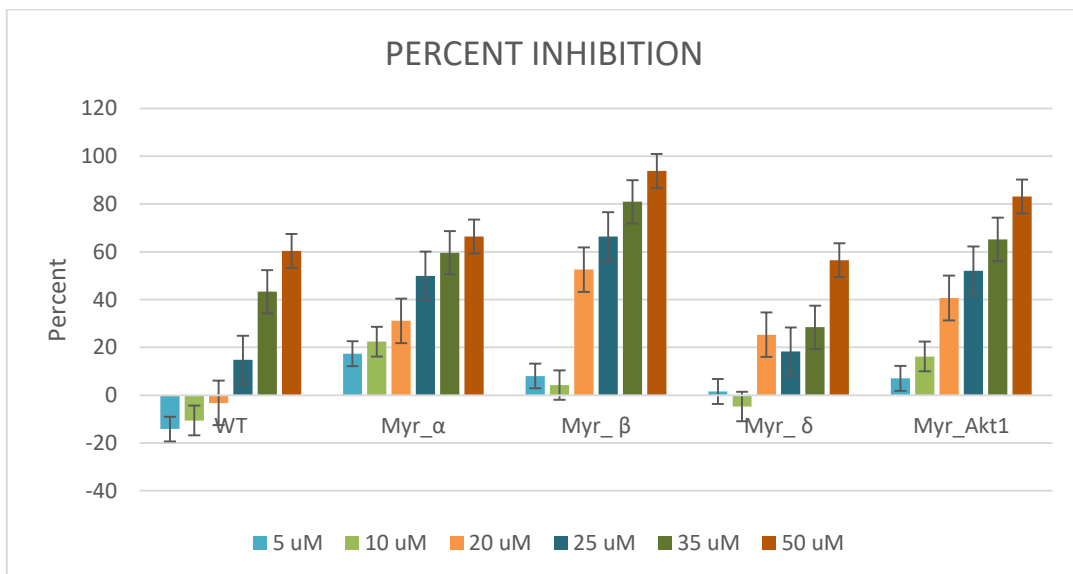
This study exhibits a possible p110 $\beta$  scaffolding function which is not described previously. This function needs to be further addressed by mutational screens followed by immunoprecipitation experiments. In addition, the role of this scaffold needs to be addressed in the context of cellular physiology. The reason why the scaffold forms with p110 $\beta$  rather than p110 $\alpha$  could be studied further by p85 $\alpha$  knock-down experiments followed by immunoprecipitations. Also, it could be further tested whether this complex involving p110 $\beta$ , Rac1, and mTOR is physiologically relevant to other cell types.

## Appendices

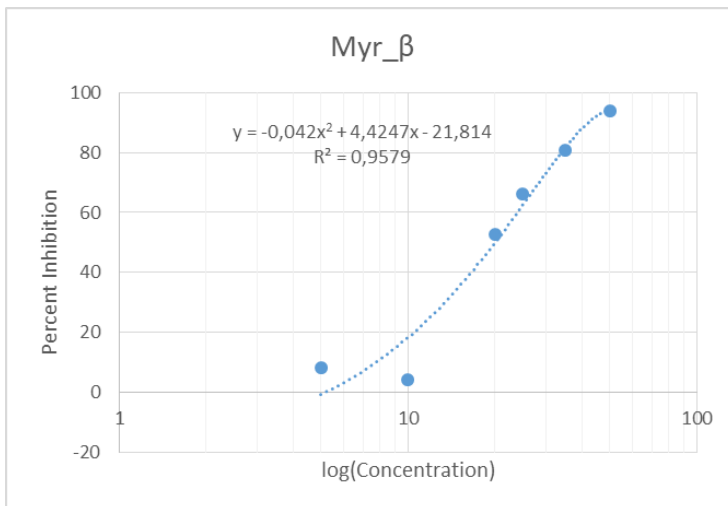
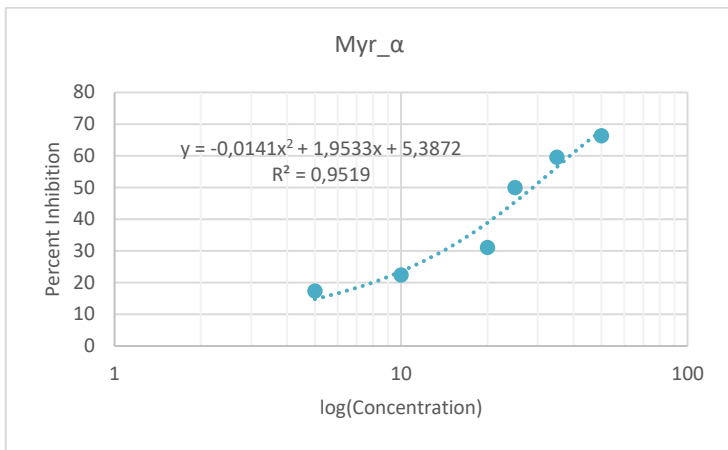
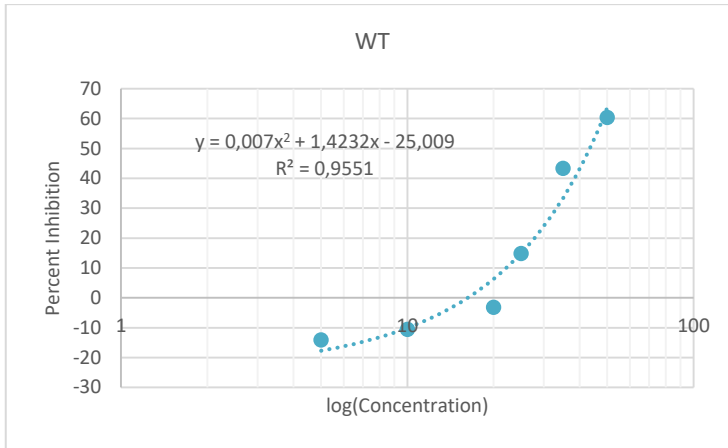
### Appendix A - Doxorubicin – Induced Genotoxic Stress

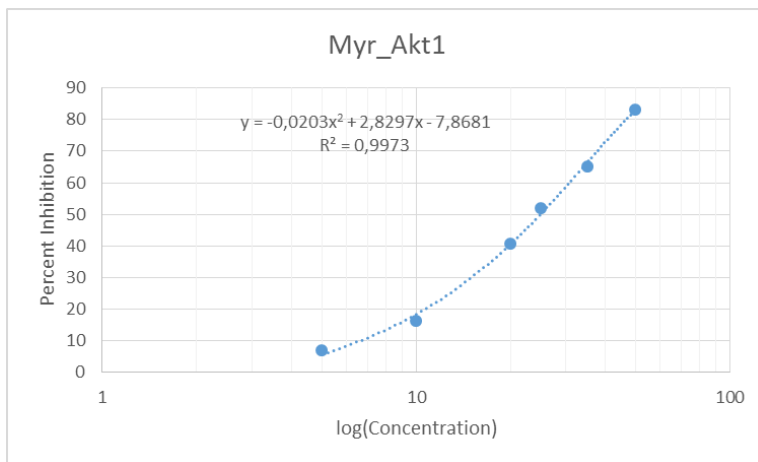
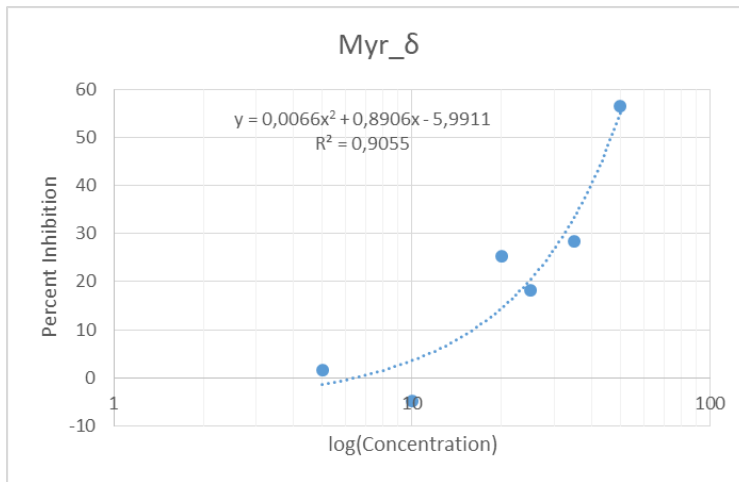


**Figure A.1 Growth levels of MEFs under different Doxorubicin concentration treatments.**



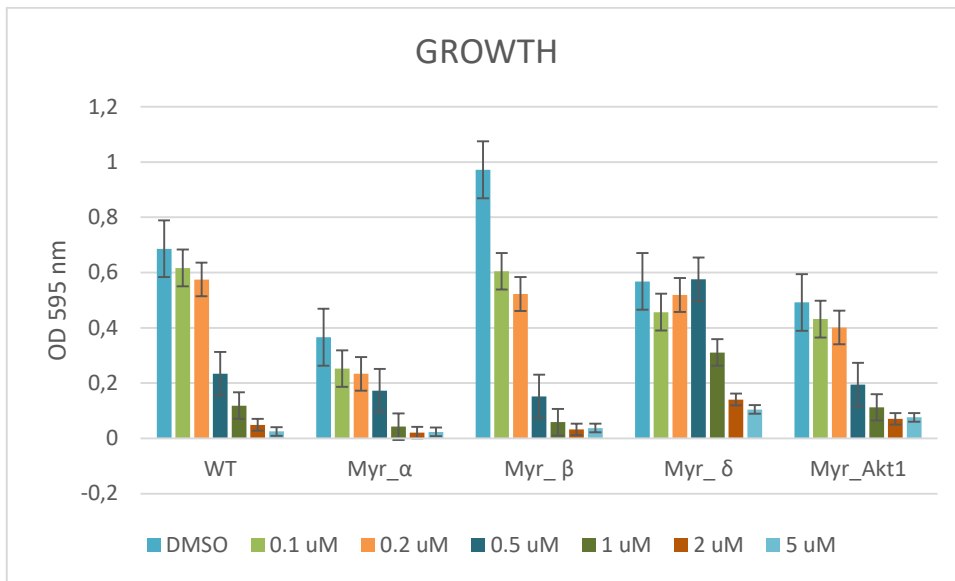
**Figure A.2 Percent inhibition of MEFs that were treated with different concentrations of Doxorubicin. Growth levels were used to draw percent inhibition graph.**



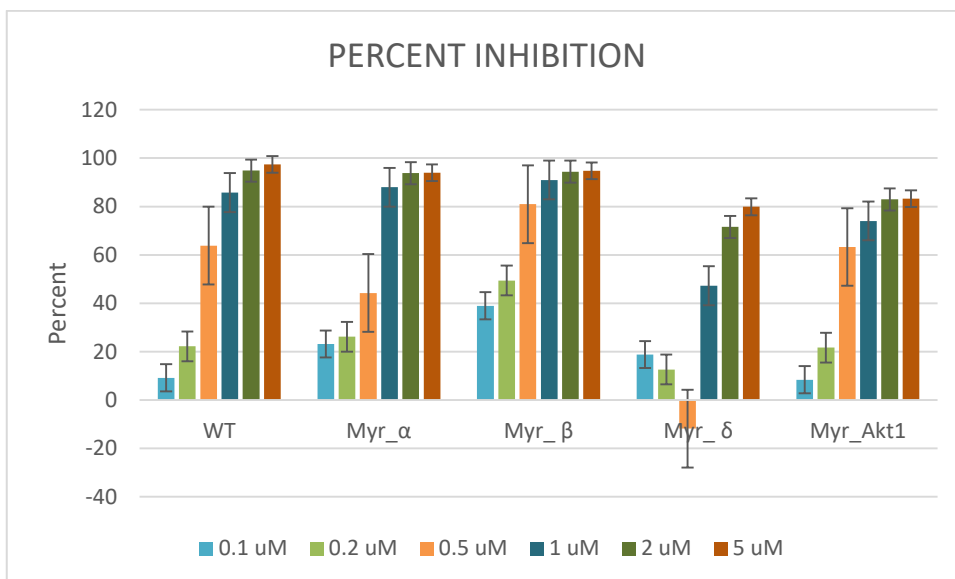


**Figure A.3 Dose – response curves of MEFs treated with Doxorubicin. IC50 values were calculated by using these graph.**

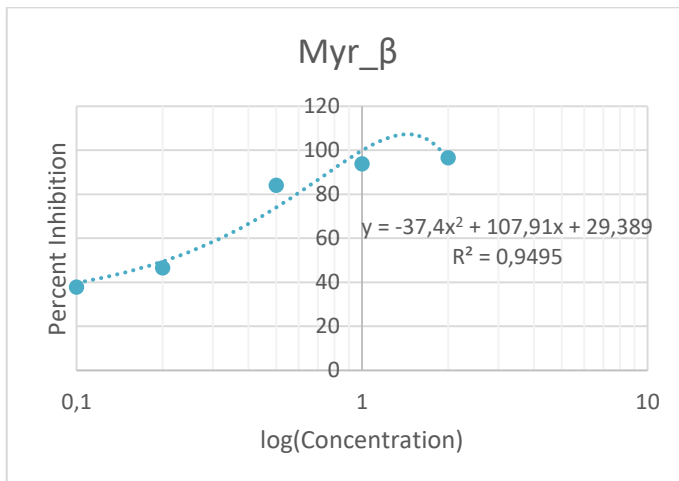
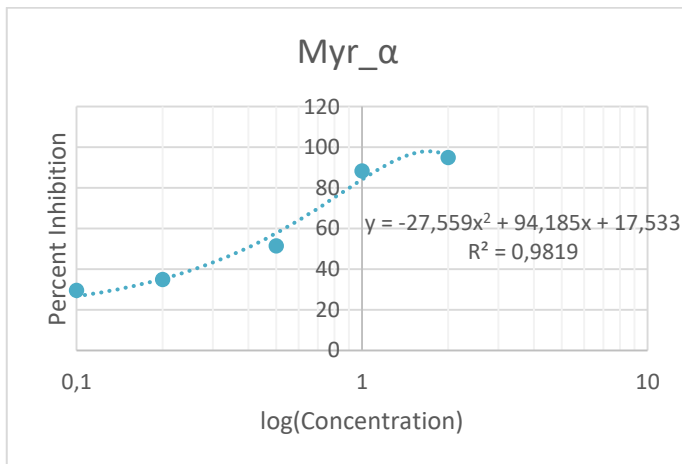
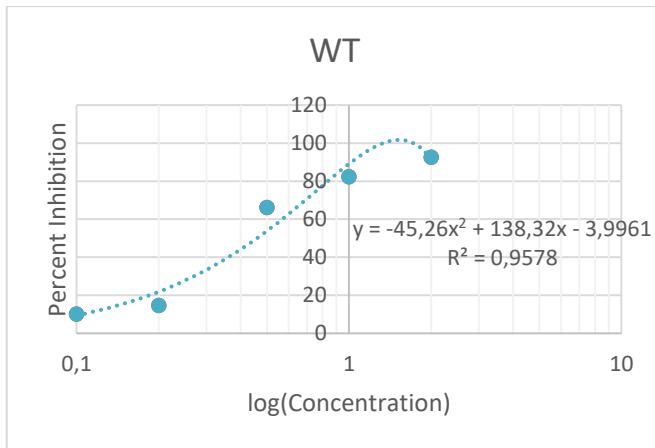
## Appendix B - Cisplatin – Induced Genotoxic Stress



**Figure B.1 Growth levels of MEFs under different Cisplatin concentration treatments.**



**Figure B.2 Percent inhibition of MEFs that were treated with different concentrations of Cisplatin. Growth levels were used to draw percent inhibition graph.**



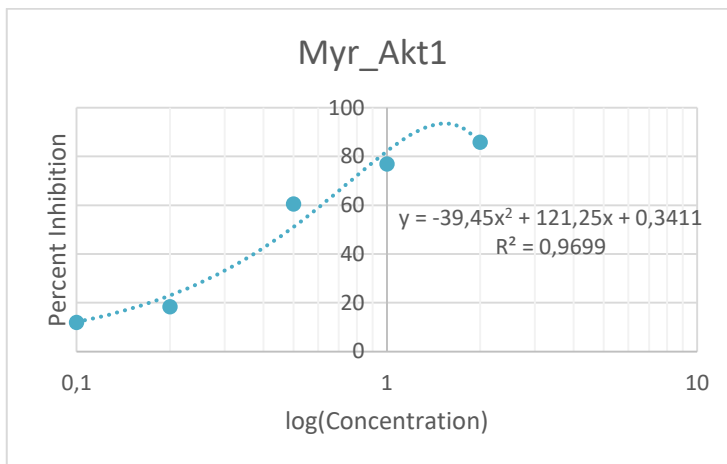
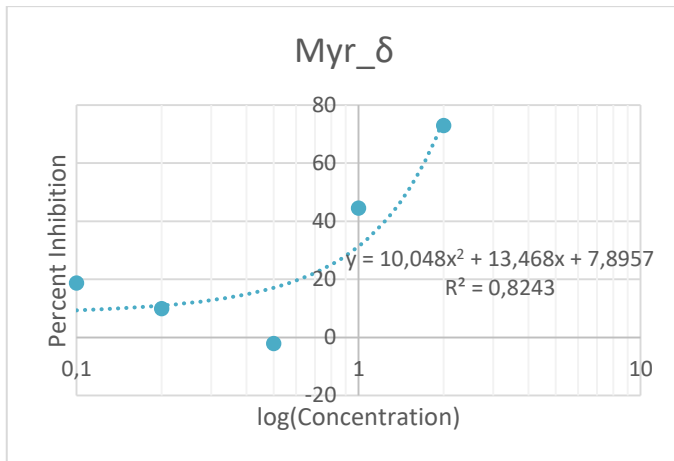


**Figure B.3 Dose – response curves of MEFs treated with Cisplatin.** IC50 values were calculated by using these graph.

## Appendix C – Copyright Permissions

Figure 1.1 : Reprinted with the permission from Ref. [1], John Wiley and Sons

Figure 1.2 : Reprinted with the permission from Ref. [17], John Wiley and Sons

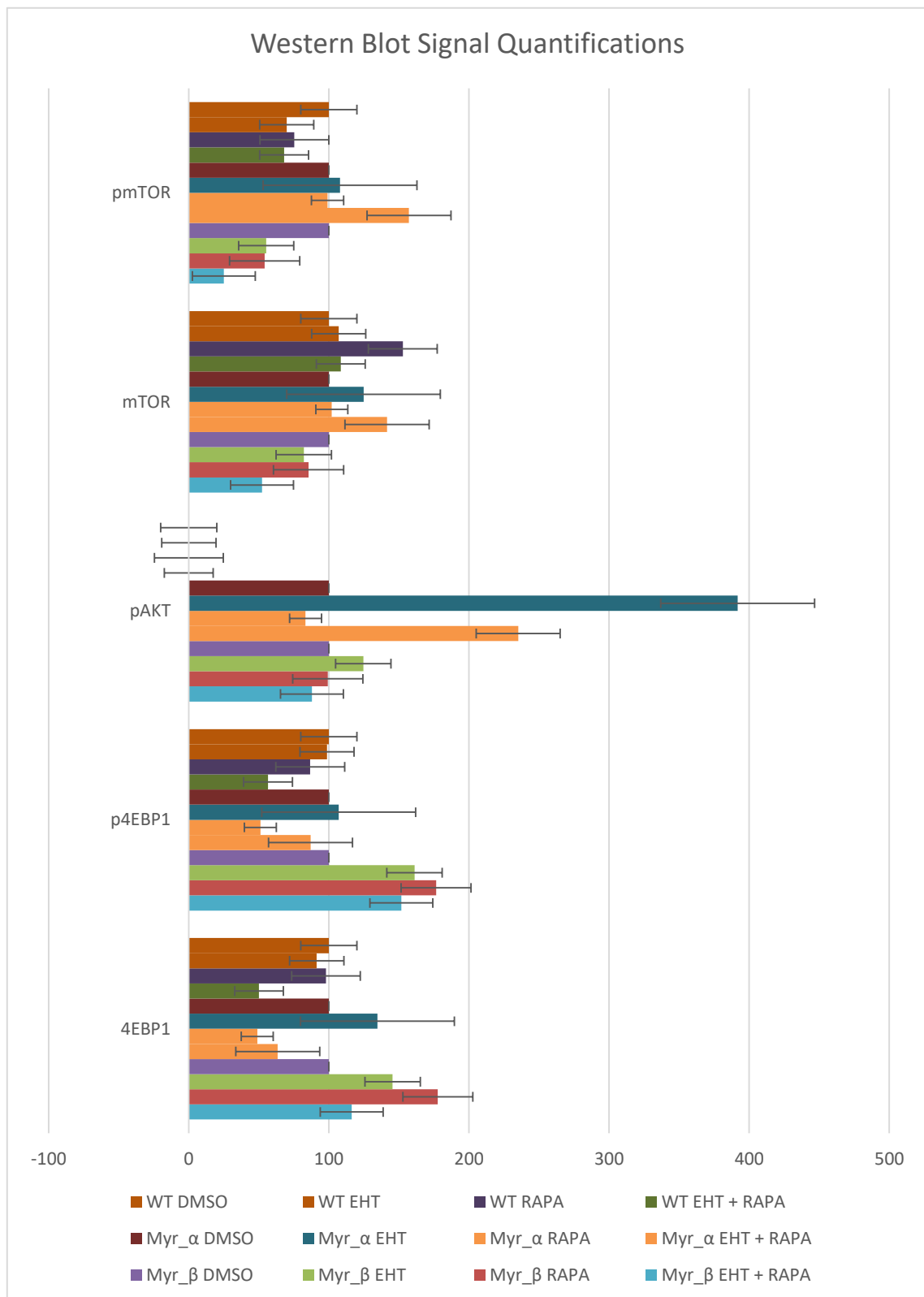
Figure 1.3 : Reprinted with the permission from Ref. [24], Elsevier

Figure 1.4 : Reprinted with the permission from Ref. [31], Elsevier

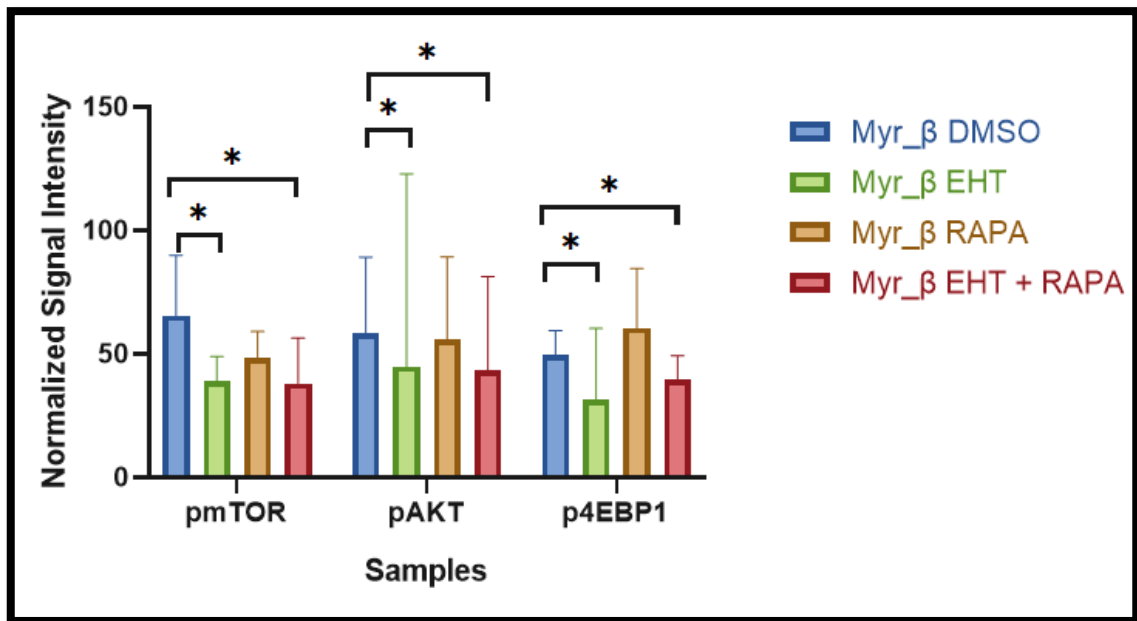
Figure 1.5 : Reprinted with the permission from Ref. [41], Rockefeller University Press

Figure 1.6 : Reprinted with permission from Ref. [50], Elsevier

## Appendix D – Western Blot Quantifications in Chapter 4.7



**Figure D.1** Graphical representation of the blot in figure 4.15.



**Figure D.2** By using two different biological replicates, one – tailed t – test has been performed for the setup in part 4.7, figure 4.15. \*, p value < 0.05.

## Bibliography

1. Bray F, Ferlay J, Soerjomataram I, Siegel RL, Torre LA, Jemal A. Global cancer statistics 2018: GLOBOCAN estimates of incidence and mortality worldwide for 36 cancers in 185 countries. *CA Cancer J Clin.* 2018;68(6):394-424. doi:10.3322/caac.21492
2. Sawyers C. Targeted cancer therapy. *Nature.* 2004;432:294-297.
3. Hanahan D, Weinberg RA. Hallmarks of cancer: The next generation. *Cell.* 2011;144(5):646-674. doi:10.1016/j.cell.2011.02.013
4. Blank O, B VT, Monsef I, Specht L, Engert A, Skoetz N. Chemotherapy alone versus chemotherapy plus radiotherapy for adults with early stage Hodgkin lymphoma ( Review ) SUMMARY OF FINDINGS FOR THE MAIN COMPARISON. 2017;(4). doi:10.1002/14651858.CD007110.pub3.www.cochranelibrary.com
5. Weber GF. *Molecular Therapies of Cancer.*; 2015. doi:10.1007/978-3-319-13278-5\_4
6. Weinberg RA. *The Biology of Cancer.* 2nd ed. Garland Science; 2014.
7. Lodish, A. Berk H. *Molecular Cell Biology.* 6th ed. (Ahr K, Tontono M, Pantages Frost E, Rice E, eds.). New York: W. H. Freeman and Company; 2007.
8. Hunter T, Blume-Jensen P. Oncogenic kinase signalling. *Nature.* 2001;411(6835):355.
9. Ardito F, Giuliani M, Perrone D, Troiano G, Muzio L Lo. The crucial role of protein phosphorylation in cell signaling and its use as targeted therapy (Review). *Int J Mol Med.* 2017;40(2):271-280. doi:10.3892/ijmm.2017.3036
10. Cizmecioglu O, Ni J, Xie S, Zhao JJ, Roberts TM. Rac1-mediated membrane raft localization of PI3K/p110 $\beta$  is required for its activation by GPCRs or PTEN loss. *Elife.* 2016;5:1-21. doi:10.7554/elife.17635
11. Engelman JA. Targeting PI3K signalling in cancer: Opportunities, challenges and limitations. *Nat Rev Cancer.* 2009;9(8):550-562. doi:10.1038/nrc2664

12. Engelman JA, Luo J, Cantley LC. The evolution of phosphatidylinositol 3-kinases as regulators of growth and metabolism. *Nat Rev Genet.* 2006;7(8):606-619. doi:10.1038/nrg1879
13. Fruman DA, Chiu H, Hopkins BD, Bagrodia S, Cantley LC, Abraham RT. The PI3K Pathway in Human Disease. *Cell.* 2017;170(4):605-635. doi:10.1016/j.cell.2017.07.029
14. Rommel C, Vanhaesebroeck B, Vogt PK. *Phosphoinositide 3-Kinase in Health and Disease.* Springer; 2010.
15. Shi F, Zhang J, Liu H, et al. The dual PI3K/mTOR inhibitor dactolisib elicits anti-tumor activity in vitro and in vivo. *Oncotarget.* 2018;9(1):706-717. doi:10.18632/oncotarget.23091
16. Vivanco I, Sawyers CL. The phosphatidylinositol 3-kinase-AKT pathway in humancancer. *Nat Rev Cancer.* 2002;2(7):489-501. doi:10.1038/nrc839
17. Xie J, Erneux C, Pirson I. How does SHIP1/2 balance PtdIns(3,4)P2 and does it signal independently of its phosphatase activity? *BioEssays.* 2013;35(8):733-743. doi:10.1002/bies.201200168
18. Wozniak DJ, Kajdacsy-Balla A, Macias V, et al. PTEN is a protein phosphatase that targets active PTK6 and inhibits PTK6 oncogenic signaling in prostate cancer. *Nat Commun.* 2017;8(1). doi:10.1038/s41467-017-01574-5
19. Ehm P, Nalaskowski MM, Wundenberg T, Jücker M. The tumor suppressor SHIP1 colocalizes in nucleolar cavities with p53 and components of PML nuclear bodies. *Nucleus.* 2015;6(2):154-164. doi:10.1080/19491034.2015.1022701
20. Hoekstra E, Das AM, Willemsen M, et al. Lipid phosphatase SHIP2 functions as oncogene in colorectal cancer by regulating PKB activation. *Oncotarget.* 2016;7(45):73525-73540. doi:10.18632/oncotarget.12321
21. Ye Y, Ge YM, Xiao MM, et al. Suppression of SHIP2 contributes to tumorigenesis and proliferation of gastric cancer cells via activation of Akt. *J Gastroenterol.* 2016;51(3):230-240. doi:10.1007/s00535-015-1101-0

22. Sueta A, Yamamoto Y, Yamamoto-Ibusuki M, et al. An integrative analysis of PIK3CA mutation, PTEN, and INPP4B expression in terms of trastuzumab efficacy in HER2-positive breast cancer. *PLoS One*. 2014;9(12):1-17. doi:10.1371/journal.pone.0116054
23. Fruman DA, Chiu H, Hopkins BD, Bagrodia S, Cantley LC, Abraham RT. The PI3K Pathway in Human Disease. *Cell*. 2017;170(4):605-635. doi:10.1016/j.cell.2017.07.029
24. Wishart MJ, Dixon JE, Dixon JE. PTEN and myotubularin phosphatases: from 3-phosphoinositide dephosphorylation to disease. *Trends Cell Biol*. 2002;12(12):579-585. <http://tcb.trends.com>.
25. Liu P, Cheng H, Roberts TM, Zhao JJ. Targeting the phosphoinositide 3-kinase pathway in cancer. *Nat Rev Drug Discov*. 2009;8(8):627-644. doi:10.1038/nrd2926
26. Harwood FC, Klein Geltink RI, O'Hara BP, et al. ETV7 is an essential component of a rapamycin-insensitive mTOR complex in cancer. *Sci Adv*. 2018;4(9). doi:10.1126/sciadv.aar3938
27. Saxton RA, Sabatini DM. mTOR Signaling in Growth, Metabolism, and Disease. *Cell*. 2017;168(6):960-976. doi:10.1016/j.cell.2017.02.004
28. Mary E. Irwin, Kelly L. Mueller, Natacha Bohin, Yubin Ge and JLB. Lipid raft localization of EGFR alters the response of cancer cells to the EGFR tyrosine kinase inhibitor gefitinib. *J Cell Physiol*. 2011;226(9):2316–2328. doi:10.1038/jid.2014.371
29. Okkenhaug K, Ali K, Vanhaesebroeck B. Antigen receptor signalling: a distinctive role for the p110 $\delta$  isoform of PI3K. *Trends Immunol*. 2007;28(2):80-87. doi:10.1016/j.it.2006.12.007
30. Udenwobele DI, Su RC, Good S V., Ball TB, Shrivastav SV, Shrivastav A. Myristoylation: An important protein modification in the immune response. *Front Immunol*. 2017;8(JUN):1-16. doi:10.3389/fimmu.2017.00751
31. Burke JE, Williams RL. Dynamic steps in receptor tyrosine kinase mediated

- activation of class IA phosphoinositide 3-kinases (PI3K) captured by H/D exchange (HDX-MS). *Adv Biol Regul.* 2013;53(1):97-110.  
doi:10.1016/j.jbior.2012.09.005
32. Zhang X, Vadas O, Perisic O, et al. Structure of Lipid Kinase p110 $\beta$ /p85 $\beta$  Elucidates an Unusual SH2-Domain-Mediated Inhibitory Mechanism. *Mol Cell.* 2011;41(5):567-578. doi:10.1016/j.molcel.2011.01.026
  33. Fritsch R, De Krijger I, Fritsch K, et al. RAS and RHO families of GTPases directly regulate distinct phosphoinositide 3-kinase isoforms. *Cell.* 2013;153(5):1050. doi:10.1016/j.cell.2013.04.031
  34. Sugiyama MG, Fairn GD, Antonescu CN. Akt-ing up just about everywhere: Compartment-specific Akt activation and function in receptor tyrosine kinase signaling. *Front Cell Dev Biol.* 2019;7(APR):1-24. doi:10.3389/fcell.2019.00070
  35. Guillermet-Guibert J, Bjorklof K, Salpekar A, et al. The p110 $\beta$  isoform of phosphoinositide 3-kinase signals downstream of G protein-coupled receptors and is functionally redundant with p110 $\gamma$ . *Proc Natl Acad Sci U S A.* 2008;105(24):8292-8297. doi:10.1073/pnas.0707761105
  36. Yang J, Nie J, Ma X, Wei Y, Peng Y, Wei X. Targeting PI3K in cancer: Mechanisms and advances in clinical trials 06 Biological Sciences 0601 Biochemistry and Cell Biology. *Mol Cancer.* 2019;18(1):1-28.  
doi:10.1186/s12943-019-0954-x
  37. Jia S, Liu Z, Zhang S, et al. Essential roles of PI(3)K-p110 $\beta$  in cell growth, metabolism and tumorigenesis. *Nature.* 2008;454(7205):776-779.  
doi:10.1038/nature07091
  38. Whale AD, Colman L, Lensun L, Rogers HL, Shuttleworth SJ. Functional characterization of a novel somatic oncogenic mutation of PIK3CB. *Signal Transduct Target Ther.* 2017;2(September):1-9. doi:10.1038/sigtrans.2017.63
  39. Condon KJ, Sabatini DM. Nutrient regulation of mTORC1 at a glance. *J Cell Sci.* 2019;132(21):0-2. doi:10.1242/JCS.222570
  40. Liu GY, Sabatini DM. mTOR at the nexus of nutrition, growth, ageing and

- disease. *Nat Rev Mol Cell Biol.* 2020;21(4):183-203. doi:10.1038/s41580-019-0199-y
41. Betz C, Hall MN. Where is mTOR and what is it doing there? *J Cell Biol.* 2013;203(4):563-574. doi:10.1083/jcb.201306041
  42. Wang L, Harris TE, Roth RA, Lawrence JC. PRAS40 regulates mTORC1 kinase activity by functioning as a direct inhibitor of substrate binding. *J Biol Chem.* 2007;282(27):20036-20044. doi:10.1074/jbc.M702376200
  43. Eales KL, Hollinshead KER, Tennant DA. Hypoxia and metabolic adaptation of cancer cells. *Oncogenesis.* 2016;5(1):e190-e190. doi:10.1038/oncsis.2015.50
  44. Rabanal-Ruiz Y, Otten EG, Korolchuk VI. MTORC1 as the main gateway to autophagy. *Essays Biochem.* 2017;61(6):565-584. doi:10.1042/EBC20170027
  45. Jewell JL, Fu V, Hong AW, et al. GPCR signaling inhibits mTORC1 via PKA phosphorylation of raptor. *Elife.* 2019;8:1-26. doi:10.7554/eLife.43038
  46. Polak P, Hall MN. mTORC2 Caught in a SINful Akt. *Dev Cell.* 2006;11(4):433-434. doi:10.1016/j.devcel.2006.09.005
  47. Julien L-A, Carriere A, Moreau J, Roux PP. mTORC1-Activated S6K1 Phosphorylates Rictor on Threonine 1135 and Regulates mTORC2 Signaling. *Mol Cell Biol.* 2010;30(4):908-921. doi:10.1128/mcb.00601-09
  48. Tzivion G, Dobson M, Ramakrishnan G. FoxO transcription factors; Regulation by AKT and 14-3-3 proteins. *Biochim Biophys Acta - Mol Cell Res.* 2011;1813(11):1938-1945. doi:10.1016/j.bbamcr.2011.06.002
  49. Chia-Chen Chen, Sang-Min Jeon, Prashanth T. Bhaskar, Veronique Nogueira, Deepa Sundararajan, Ivana Tonic, Youngkyu Park and NH. FoxOs inhibit mTORC1 and activate Akt by inducing the expression of Sestrin3 and Rictor. *Dev Cell.* 2010;18(4):592-604. doi:10.1161/CIRCULATIONAHA.110.956839
  50. Mendoza MC, Er EE, Blenis J. The Ras-ERK and PI3K-mTOR pathways: Cross-talk and compensation. *Trends Biochem Sci.* 2011;36(6):320-328. doi:10.1016/j.tibs.2011.03.006

51. Sakkab D, Lewitzky M, Posern G, et al. Signaling of hepatocyte growth factor/scatter factor (HGF) to the small GTPase Rap1 via the large docking protein Gab1 and the adapter protein CRKL. *J Biol Chem.* 2000;275(15):10772-10778. doi:10.1074/jbc.275.15.10772
52. Holgado-Madruga M, Emllet DR, Moscatello DK, Godwin AK, Wong AJ. A Grb2-associated docking protein in EGF- and insulin-receptor signalling. *Nature.* 1996;379(6565):560-564. doi:10.1038/379560a0
53. Rocchi S, Tartare-Deckert S, Murdaca J, Holgado-Madruga M, Wong AJ, Van Obberghen E. Determination of Gab1 (Grb2-associated binder-1) interaction with insulin receptor-signaling molecules. *Mol Endocrinol.* 1998;12(7):914-923. doi:10.1210/mend.12.7.0141
54. Vadlakonda L, Pasupuleti M, Pallu R. Role of PI3K-AKT-mTOR and Wnt signaling pathways in transition of G1-S phase of cell cycle in cancer cells. *Front Oncol.* 2013;3 APR(April):1-7. doi:10.3389/fonc.2013.00085
55. Camara AKS, Zhou YF, Wen PC, Tajkhorshid E, Kwok WM. Mitochondrial VDAC1: A key gatekeeper as potential therapeutic target. *Front Physiol.* 2017;8(JUN):1-18. doi:10.3389/fphys.2017.00460
56. Samuels Y, Ericson K. Oncogenic PI3K and its role in cancer. *Curr Opin Oncol.* 2006;18(1):77-82. doi:10.1097/01.cco.0000198021.99347.b9
57. Whale AD, Colman L, Lensun L, Rogers HL, Shuttleworth SJ. Functional characterization of a novel somatic oncogenic mutation of PIK3CB. *Signal Transduct Target Ther.* 2017;2(June):1-9. doi:10.1038/sigtrans.2017.63
58. Buchanan CM, Lee KL, Shepherd PR. For better or worse: The potential for dose limiting the on-target toxicity of PI 3-kinase inhibitors. *Biomolecules.* 2019;9(9):1-26. doi:10.3390/biom9090402
59. Carnero A, Blanco-Aparicio C, Renner O, Link W, Leal J. The PTEN/PI3K/AKT Signalling Pathway in Cancer, Therapeutic Implications. *Curr Cancer Drug Targets.* 2008;8(3):187-198. doi:10.2174/156800908784293659
60. Singh P, Dar MS, Dar MJ. p110 $\alpha$  and p110 $\beta$  isoforms of PI3K signaling: are they

- two sides of the same coin? *FEBS Lett.* 2016;590(18):3071-3082.  
doi:10.1002/1873-3468.12377
61. Manning, Brendan D., Toker A. AKT/PKB Signaling: Navigating the Network. 2017;169(3):381-405. doi:10.1016/j.cell.2017.04.001.AKT/PKB
  62. Merkely B, Gara E, Lendvai Z, et al. Signaling Via PI3K/FOXO1A Pathway Modulates Formation and Survival of Human Embryonic Stem Cell-Derived Endothelial Cells. *Stem Cells Dev.* 2015;24(7):869-878.  
doi:10.1089/scd.2014.0247
  63. Jia S, Liu Z, Zhang S, et al. Kinase-dependent and -independent functions of the p110 $\beta$  phosphoinositide-3-kinase in cell growth, metabolic regulation and oncogenic transformation. *Nature.* 2008;454(7205):776-779.  
doi:10.1038/nature07091.Kinase-dependent
  64. Hunter T. Tyrosine phosphorylation: thirty years and counting. *Curr Opin Cell Biol.* 2009;21(2):140-146. doi:10.1016/j.ceb.2009.01.028
  65. Amata I, Maffei M, Pons M. Phosphorylation of unique domains of Src family kinases. *Front Genet.* 2014;5(JUN):1-6. doi:10.3389/fgene.2014.00181
  66. Zhang J, Gao X, Schmit F, et al. CRKL Mediates p110 $\beta$ -Dependent PI3K Signaling in PTEN-Deficient Cancer Cells. *Cell Rep.* 2017;20(3):549-557.  
doi:10.1016/j.celrep.2017.06.054
  67. Johnston JA, Bacon CM, Finbloom DS, et al. Tyrosine phosphorylation and activation of STAT5, STAT3, and Janus kinases by interleukins 2 and 15. *Proc Natl Acad Sci U S A.* 1995;92(19):8705-8709. doi:10.1073/pnas.92.19.8705
  68. Harrison DA. The JAK / STAT Pathway : Fact Sheet. *Cold Spring Harb Perspect Biol.* 2012;4(a011205):1-3.
  69. Dominguez C, Boelens R, Bonvin AMJJ. HADDOCK: A protein-protein docking approach based on biochemical or biophysical information. *J Am Chem Soc.* 2003;125(7):1731-1737. doi:10.1021/ja026939x
  70. Roel-Touris J, Don CG, Honorato RR, Rodrigues JPGLM, Bonvin AMJJ. Less Is More: Coarse-Grained Integrative Modeling of Large Biomolecular Assemblies

- with HADDOCK. *J Chem Theory Comput.* 2019;15(11):6358-6367.  
doi:10.1021/acs.jctc.9b00310
71. Saci A, Cantley LC, Carpenter CL. Rac1 Regulates the Activity of mTORC1 and mTORC2 and Controls Cellular Size. *Mol Cell.* 2011;42(1):50-61.  
doi:10.1016/j.molcel.2011.03.017
72. Sarbassov DD, Ali SM, Sengupta S, et al. Prolonged Rapamycin Treatment Inhibits mTORC2 Assembly and Akt/PKB. *Mol Cell.* 2006;22(2):159-168.  
doi:10.1016/j.molcel.2006.03.029
73. Aslan JE, McCarty OJT. Regulation of the mTOR-Rac1 axis in platelet function. *Small GTPases.* 2012;3(1):67-70. doi:10.4161/sgtp.19137
74. Hervieu A, Heuss SF, Zhang C, et al. A PI3K- And GTPase-independent Rac1-mTOR mechanism mediates MET-driven anchorage-independent cell growth but not migration. *Sci Signal.* 2020;13(637). doi:10.1126/scisignal.aba8627
75. Rikitake Y, Takai Y. *Directional Cell Migration. Regulation by Small G Proteins, Nectin-like Molecule-5, and Afadin.* Vol 287. 1st ed. Elsevier Inc.; 2011. doi:10.1016/B978-0-12-386043-9.00003-7
76. Morrison Joly M, Williams MM, Hicks DJ, et al. Two distinct mTORC2-dependent pathways converge on Rac1 to drive breast cancer metastasis. *Breast Cancer Res.* 2017;19(1):1-15. doi:10.1186/s13058-017-0868-8
77. Yudushkin I. Getting the akt together: Guiding intracellular akt activity by pi3k. *Biomolecules.* 2019;9(2). doi:10.3390/biom9020067
78. Chiang GG, Abraham RT. Phosphorylation of mammalian target of rapamycin (mTOR) at Ser-2448 is mediated by p70S6 kinase. *J Biol Chem.* 2005;280(27):25485-25490. doi:10.1074/jbc.M501707200
79. Soliman GA, Acosta-Jaquez HA, Dunlop EA, et al. mTOR Ser-2481 autophosphorylation monitors mTORC-specific catalytic activity and clarifies rapamycin mechanism of action. *J Biol Chem.* 2010;285(11):7866-7879.  
doi:10.1074/jbc.M109.096222
80. Peterson RT, Beal PA, Comb MJ, Schreiber SL. FKBP12-rapamycin-associated

- protein (FRAP) autophosphorylates at serine 2481 under translationally repressive conditions. *J Biol Chem.* 2000;275(10):7416-7423.  
doi:10.1074/jbc.275.10.7416
81. Tobin AB. G-protein-coupled receptor phosphorylation: Where, when and by whom. *Br J Pharmacol.* 2008;153(SUPPL. 1):167-176.  
doi:10.1038/sj.bjp.0707662
  82. Shutes A, Onesto C, Picard V, Leblond B, Schweighoffer F, Der CJ. Specificity and mechanism of action of EHT 1864, a novel small molecule inhibitor of Rac family small GTPases. *J Biol Chem.* 2007;282(49):35666-35678.  
doi:10.1074/jbc.M703571200
  83. Akbar H, Cancelas J, Williams DA, Zheng J, Zheng Y. Rational design and applications of a Rac GTPase-specific small molecule inhibitor. *Methods Enzymol.* 2006;406(20):554-565. doi:10.1016/S0076-6879(06)06043-5
  84. Marqués M, Kumar A, Poveda AM, et al. Specific function of phosphoinositide 3-kinase beta in the control of DNA replication. *Proc Natl Acad Sci U S A.* 2009;106(18):7525-7530. doi:10.1073/pnas.0812000106
  85. Fuhrer DK, Yang YC. Complex formation of JAK2 with PP2A, P13K, and Yes in response to the hematopoietic cytokine interleukin-11. *Biochem Biophys Res Commun.* 1996;224(2):289-296. doi:10.1006/bbrc.1996.1023